



January 2017

Novel Approaches In Lignomics Employing Liquid Chromatography And Mass Spectrometry

Anastasia Alekseyevna Andrianova

Follow this and additional works at: <https://commons.und.edu/theses>

Recommended Citation

Andrianova, Anastasia Alekseyevna, "Novel Approaches In Lignomics Employing Liquid Chromatography And Mass Spectrometry" (2017). *Theses and Dissertations*. 2163.
<https://commons.und.edu/theses/2163>

This Dissertation is brought to you for free and open access by the Theses, Dissertations, and Senior Projects at UND Scholarly Commons. It has been accepted for inclusion in Theses and Dissertations by an authorized administrator of UND Scholarly Commons. For more information, please contact zeinebyousif@library.und.edu.

NOVEL APPROACHES IN LIGNOMICS EMPLOYING LIQUID CHROMATOGRAPHY
AND MASS SPECTROMETRY

by

Anastasia A. Andrianova
Specialist (BS, MS) in Science, Lomonosov Moscow State University, 2014

A Dissertation
Submitted to the Graduate Faculty

of the

University of North Dakota

in partial fulfillment of the requirements

for the degree of

Doctor of Philosophy

Grand Forks, North Dakota

December
2017

Copyright 2017 Anastasia A. Andrianova

This dissertation, submitted by Anastasia Andrianova in partial fulfillment of the requirements for the Degree of Doctor of Philosophy from the University of North Dakota, has been read by the Faculty Advisory Committee under whom the work has been done and is hereby approved.



Dr. Alena Kubátová, Chair



Dr. Evguenii Kozliak, Co-chair



Dr. David Pierce



Dr. Julia Zhao



Dr. Yun Ji

This dissertation is being submitted by the appointed advisory committee as having met all of the requirements of the School of Graduate Studies at the University of North Dakota and is hereby approved.



Dr. Grant McGimpsey (Dean of the Graduate School)

December 6, 2017

Date

PERMISSION

Title	Novel approaches in lignomics employing liquid chromatography and mass spectrometry
Department	Chemistry
Degree	Doctor of Philosophy

In presenting this dissertation in partial fulfillment of the requirement for a graduate degree from the University of North Dakota, I agree that the library of this University shall make it freely available for inspection. I further agree that permission for extensive copying for scholarly purposes may be granted by the professor who supervised my dissertation work or, in her absence, by the chairperson of the department or the dean of the graduate school. It is understood that any copying or publication or other use of this dissertation or part thereof for financial gain shall not be allowed without my written permission. It is also understood that due recognition shall be given to me and the University of North Dakota in any scholarly use which may be made of any material in my dissertation.

Anastasia A. Andrianova

12/07/2017

TABLE OF CONTENTS

ABBREVIATIONS	x
LIST OF FIGURES	xii
LIST OF TABLES	xvii
ACKNOWLEDGEMENTS	xix
ABSTRACT	xxi
CHAPTER I. INTRODUCTION	1
I.1. Lignin Composition	1
I.2. Approaches to Qualitative Analysis of Lignin	3
I.2.1. Size Exclusion Chromatography for Lignin MW Elucidation	4
I.2.2. MS in Lignin MW and Structure Elucidation	7
I.3. Lignin Fractionation for Its Comprehensive Characterization	17
I.4. Statement of Purpose	20
CHAPTER II. LIQUID CHROMATOGRAPHY OF LIGNIN	22
II.1. Experimental	22
II.1.1. Materials and Reagents	22
II.1.2. Lignin Sample Preparation and Acetylation	25
II.1.3. Instrumentation	25
II.1.4. SEC Data Handling	28

II.2. Results and Discussion.....	28
II.2.1. SEC Separation of Polymeric Model Compounds.....	28
II.2.2. Unwanted Interactions in SEC Separation of Low-MW Phenolic Standards	32
II.2.3. GPC Effect of the Pore & Particle Size.....	35
II.2.4. SEC of Alkali Lignin.....	36
II.2.5. Lignin MW Determination by MALDI MS.....	39
II.2.6. RP HPLC C18 as a Complementary Method to SEC for Polymer Analysis.....	41
CHAPTER III. ATMOSPHERIC PRESSURE IONIZATION WITH HIGH-RESOLUTION MASS SPECTROMETRY AS A TOOL FOR LIGNOMICS	44
III.1. Experimental.....	44
III.1.1. Materials and Reagents	44
III.1.2. MS Analysis: Ionization	47
III.1.3. MS Characteristics and Data Processing	48
III.2. Results and Discussion	49
III.2.1. Electrolyte Screening: Effect on the Representative Model Compounds in ESI.....	50
III.2.2. Impact of Oxygenated Functional Groups on ESI Ionization.....	53
III.2.3. Ionization of Lignin Model Compounds by APCI TOF MS	56
III.2.4. Lignin ESI: Electrolyte Selection	59
III.2.5. Lignin ESI: Mass Spectrum Deconvolution	62
III.2.6. Lignin MW Determination by ESI HR TOF MS.....	64
III.2.7. Ionization: MALDI HR TOF MS vs. ESI HR TOF MS.....	65

III.2.8. Ion Mobility ESI MS: Confirmation of the Multiply Charged Species Formation	65
CHAPTER IV. LIGNIN FRACTIONATION AND CHARACTERIZATION BY PREPARATIVE SIZE EXCLUSION CHROMATOGRAPHY	68
IV.1. Experimental.....	68
IV.1.1. Lignin Fractionation via Preparative SEC	68
IV.1.2. Analysis of Lignin MW Fractions	69
IV.1.2.1. HP SEC	69
IV.1.2.2. TCA	70
IV.1.2.3. STEM, DLS Analysis and Zeta Potential Measurements.....	70
IV.2. Results and Discussion	71
IV.2.1. Lignin Fractionation on Analytical SEC	71
IV.2.2. Lignin Fractionation on Preparative SEC	73
IV.2.2.1. HP SEC and TCA of the Pre-Eluate	77
IV.2.2.2. HP SEC and TCA of Lignin Fractions	78
IV.2.2.3. Molecular Weight and Molecular Size of Lignin Fractions and the Pre-Eluate.....	80
CHAPTER V. APPLICATION OF THE DEVELOPED METHODS TO SYNTHETIC POLYMERS AND DEGRADED LIGNIN.....	83
V.1. Characterization of Biomodified Lignin Using Liquid Chromatography.....	83
V.1.1. Experimental	83
V.1.2. Results and Discussion.....	84
V.1.2.1. Lignin MW Increase upon Biomodification by SEC.....	84
V.1.2.2. HPLC for Lignin Structural Changes Elucidation upon Biomodification	85

V.2. Lignin MW Decrease upon Thermal Treatment with Hydrogen Peroxide.....	88
V.2.1. Experimental	88
V.2.2. Results and Discussion.....	88
V.3. ESI HR TOF MS for the MW Determination of Synthetic Polymers	91
V.3.1. Experimental	91
V.3.2. Results and Discussion.....	94
V.3.2.1. PPG MW Determination via Direct Infusion.....	94
V.3.2.2. Determination of the MW of a Copolymer via Direct Infusion.....	95
V.3.2.3. PEG MW Determination via Direct Infusion of a Polymer Mixture	96
V.3.2.4. PEG MW Determination via RP HPLC of a Polymer Mixture	98
CONCLUSIONS.....	100
Liquid Chromatography of Lignin.....	100
HR MS as a Tool for Lignomics.....	102
Lignin Fractionation and Characterization by Preparative SEC.....	102
Applications of the Developed Methods	103
APPENDICES	104
Appendix A.....	105
Appendix B.....	114
Appendix C.....	116
Appendix D.....	118

Appendix E	123
Appendix F	124
Appendix G.....	125
Appendix H.....	126
Appendix I	135
Appendix J	136
REFERENCES	140

ABBREVIATIONS

ACN	Acetonitrile
ALC2	4-(1-Hydroxyethyl)-2-methoxyphenyl benzoate
ALK2	(<i>E</i>)-4,4'-(Ethene-1,2-diyl)bis(2-methoxyphenol)
APCI	Atmospheric pressure chemical ionization
APPI	Atmospheric pressure photoionization
<i>C. versicolor</i>	<i>Coriolus versicolor</i>
CHCA	α -cyano-4-hydroxycinnamic acid
D2V	Dehydrodivanillin
DAD	Diode array detector
DCM	Dichloromethane
DHB	2,5-dihydroxybenzoic acid
DLS	Dynamic light scattering
DMSO	Dimethyl sulfoxide
E	Eugenol
ESI	Electrospray ionization
EST2	4-Formyl-2-methoxyphenyl benzoate
ET2	1,2-Dimethoxy-4-[(2-methoxyphenoxy)methyl]benzene
ET3-1	4-[2-(3,4-Dimethoxybenzyl)-4,5-dimethoxybenzyl]-2-methoxyphenol
ET3-2	1-(3,4-dimethoxybenzyl)-4,5-dimethoxy-2-[(2-methoxyphenoxy)methyl]benzene
FIA	Flow injection analysis
FID	Flame ionization detector
FTIR	Fourier transform infrared spectroscopy
G	Guaiacol
GC	Gas chromatography
GDVB	Glucose rings bonded to a pure divinylbenzene
GFC	Gel filtration chromatography
GPC	Gel permeation chromatography
G- β -2	Guaiacylglycerol- β -guaiacyl ether

HA	Homovanillyl alcohol
HP SEC	High performance size exclusion chromatography
HPMA	Hydroxylated polymethacrylate
IM	Ion mobility
k	Retention factor
LC	Liquid chromatography
LDI	Laser desorption/ionization
<i>m/z</i>	Mass-to-charge
MALDI	Matrix-assisted laser desorption/ionization
M_n	Number-average molecular weight
M_p	Peak maximum molecular weight
MS	Mass spectrometry
MW	Molecular weight
M_w	Weight-average molecular weight
M_z	Z-average molecular weight
P2	Pinoresinol
PDI	Polydispersity index
PEG	Polyethylene glycol
PMMA	Poly(methyl methacrylate)
PS	Polystyrene
PSDVB	Polystyrene/divinylbenzene
PSS Na	Sodium polystyrene sulfonate
Pyr-GC	Pyrolysis - gas chromatography
S	Syringol
SA	Syringaldehyde
SEC	Size exclusion chromatography
SIMS	Secondary ion MS
STEM	Scanning transmission electron microscopy
TCA	Thermal carbon analysis
THF	Tetrahydrofuran
TIC	Total ion current
t_r	Retention time
V	Vanillin
VA	Vanillic acid
VER	Veratrole

LIST OF FIGURES

Figure	Page
Figure 1. Lignin structural motifs and relative percentage of eight linkages, such as dibenzodioxin, spirodienone, β - β , 4-O-5, β -1, β -5, 5-5, and β -O-4 found in lignin. ¹⁰	2
Figure 2. Retention factor (k) of polymeric standards, i.e., PS and PMMA, vs. log MW in SEC utilizing various stationary phases: a) HPMA; b) GDVB; c) PSDVB.	31
Figure 3. Relationship between the retention factor (k) of low-MW lignin model compounds in SEC on various stationary phases and a) log MW on HPMA; b) the pK _a on HPMA; c) the log MW on GDVB; d) the pK _a on GDVB; e) the log MW on PSDVB; f) the pK _a on PSDVB.	33
Figure 4. Retention factor (k) of low-MW lignin model compounds and polymeric standards as a function of log MW in GPC utilizing the columns with various stationary phase: a) GDVB, and b) PSDVB.	34
Figure 5. Intact and acetylated alkali lignin elution profiles utilizing various stationary phases: (a) PSDVB; (b) GDVB.	37
Figure 6. LDI (no matrix) HR TOF mass spectrum of alkali lignin. The insert shows a zoomed in part of the spectrum in the range 2800–8000 <i>m/z</i>	41
Figure 7. Correlation between the retention factor (k) of a) PEG standards and log MW; b) low-MW lignin structure model compounds and log MW; c) low-MW lignin structure model compounds and the pK _a in RP HPLC utilizing C ₁₈ column.	42
Figure 8. ESI TOF MS response obtained in the presence of different electrolytes via a direct infusion for two representative dimers (a) G- β -2; (b) ET2 in the positive and negative ionization modes. For most of the electrolytes used, the response for [M+Na] ⁺ and deprotonated molecular ions is shown, except for LiCl and	

LiOH whose application resulted in the formation of $[M+Li]^+$. The electrolyte concentration was $1.0 \text{ mmol}\cdot\text{L}^{-1}$ unless specified otherwise.	51
Figure 9. Positive ESI TOF mass spectra of 5 ppm G- β -2 ($[M+Na]^+$ 343.1152 m/z) in the presence of $1.0 \text{ mmol}\cdot\text{L}^{-1}$ of a) ammonium acetate (mass accuracy error 5 ppm); b) acetic acid (mass accuracy error 7 ppm); and c) sodium hydroxide (mass accuracy error 6.7 ppm).	52
Figure 10. Ionization efficiency of lignin model compounds by APCI TOF MS.	56
Figure 11. Comparison of mass spectra recorded upon utilizing a) ESI and b) APCI ionization sources in the negative mode.	58
Figure 12. The highest mass-to-charge (m/z) values of the ions detected in the mass spectrum of (a) 15–90 ppm intact alkali lignin and (c) 15 ppm acetylated alkali lignin dissolved in ACN-water 1:1 in the positive and negative ionization modes while using different electrolytes; MW (Da) obtained after spectrum deconvolution of (b) 15–90 ppm intact alkali lignin and (d) 15 ppm acetylated alkali lignin. An electrolyte concentration was $1.0 \text{ mmol}\cdot\text{L}^{-1}$ unless specified otherwise.	60
Figure 13. Positive ESI HR TOF mass spectra of an 80 ppm solution of intact lignin in ACN-water (1:1) with $100 \text{ mmol}\cdot\text{L}^{-1}$ formic acid: a), c) and e) zoomed and full original mass spectra; b), d) and f) zoomed and full mass spectra after deconvolution.	63
Figure 14. a) Ion mobility image of a 100 ppm solution of intact lignin in ACN-water (1:1) with $100 \text{ mmol}\cdot\text{L}^{-1}$ formic acid, recorded in the positive ESI mode. b) Original and deconvoluted mass spectra of a 100 ppm solution of intact lignin in ACN-water (1:1) with $100 \text{ mmol}\cdot\text{L}^{-1}$ formic acid recorded in the positive ESI mode. The blank spectrum was subtracted before deconvolution. An accurate deconvolution algorithm is described in equation 3.	66
Figure 15. The validation of lignin fractionation conditions employing analytical SEC column: a) HP SEC elution profiles of the fractions; b) TCA profiles of lignin fractions.	73
Figure 16. a) HP SEC and b) TCA profiles of lignin fractions (initial SEC fractionation) when the pre-eluate and fraction 1 were collected jointly.	74
Figure 17. a) Lignin elution profile in the preparative SEC with the corresponding fraction areas and their relative carbon content determined by TCA; b) HP SEC and b)	

TCA profiles of lignin fractions when fraction 1 and the pre-eluate were collected separately.....	76
Figure 18. a) Average hydrodynamic diameter and b) zeta-potential of the particles in the solution of lignin MW fractions and the pre-eluate determined by DLS.....	82
Figure 19. SEC elution profiles of the intact untreated and <i>C. versicolor</i> -treated lignin after subtracting the chromatogram of the control sample.....	84
Figure 20. The RP HPLC-DAD contour plots of the original lignin and its fungal biotransformation product a) without and b) in the presence of DMSO.....	86
Figure 21. The extracted wavelength RP HPLC-DAD chromatograms (15–25 min) at 290 nm and 540 nm of the original lignin and its fungal biotransformation product a, c) without and b,d) in the presence of DMSO	87
Figure 22. SEC elution profiles of the water-soluble portion of lignin autoclaved in the presence of 0%, 5% and 10% of H ₂ O ₂ (v/v) a) in a 100% aqueous system; b) in an aqueous system containing 25% of methanol.	89
Scheme 1. The ring-opening copolymerization of styrene oxide with maleic anhydride using zinc complex.....	92
Figure 23. Deconvoluted ESI mass spectrum of a copolymer of styrene oxide and maleic anhydride analyzed by DI ESI HR TOF MS.	95
Figure 24. Deconvoluted ESI mass spectrum of PEG standard mixtures a) 1 and b) 2 analyzed by DI ESI HR TOF MS.	97
Figure A1. Overlaid DAD chromatograms of lignin structure model compounds and polymeric standards on various stationary phases: a) HPMA; b) GDVB; c) PSDVB.....	110
Figure A2. Overlaid DAD chromatograms of PS standards (580–19760 Da) analyzed on (a) the PLgel 500 Å and (b) the PLgel 1000 Å columns.....	112
Figure A3. Alkali and Indulin AT lignin elution profiles on the PSDVB stationary phase (the PLgel 1000 Å column).....	113
Figure B1. MALDI mass spectrum of alkali lignin with various matrices: a) without a matrix; b) 2-(4-hydroxyphenylazo)benzoic acid (ration with lignin 1:1); c) 2-(4-	

hydroxyphenylazo)benzoic acid (10-times excess compared to lignin); d) 2-(4-hydroxyphenylazo)benzoic acid (5-times excess compared to lignin); e) α -cyano-4-hydroxycinnamic acid (5-times excess compared to lignin).....	114
Figure C1. a) TIC chromatogram of PEG standards (26100, 6400, 1400 and 320 Da) and b) overlaid DAD chromatograms of low MW lignin model compounds analyzed on GFC Ultrahydrogel 120 Å column.....	116
Figure C2. a) TIC chromatogram of PEG standards (26100, 6400, 1400 and 320 Da) and b) overlaid DAD chromatograms of low MW lignin model compounds analyzed on Zorbax Eclipse Plus C18 column with pore size 95 Å.....	117
Figure F1. Molecular weight of (CsI) _n clusters and calculated masses of the corresponding [(CsI) _n +Cs] ⁺ ion clusters and their ESI positive mass spectra: Full scale (50–7,500 <i>m/z</i>); zoomed in (2,500–7,000 <i>m/z</i>) and 5,000–7,200 <i>m/z</i>	124
Figure G1. Positive ESI mass spectra of (a, b) a 90 ppm solution of intact lignin in THF-water (1:1) with 100 mmol·L ⁻¹ formic acid and (c) the same solution without lignin, i.e., blank. a) Raw alkali lignin spectrum after blank subtraction; b) deconvoluted lignin spectrum after blank subtraction; and c) deconvoluted spectrum of the blank.	125
Figure H1. Overlaid DAD chromatograms of PS standards (580–19,760 Da) and pinoresinol analyzed on the preparative PLgel 1000 Å SEC column.....	126
Figure H2. a) Retention factor (<i>k</i>) of PS, PMMA and pinoresinol vs. log MW in preparative SEC; b) log MW vs. retention time of PS, PMMA and pinoresinol	127
Figure H3. Fractionation experiments performed utilizing a) an analytical SEC 1000 Å PLgel column and b-e) preparative PLgel 1000 Å SEC column with fraction collected in the various retention time windows.....	128
Figure H4. TCA profiles normalized per each lignin MW fraction obtained by fractionation employing the preparative SEC for a)fresh sample; b) aged over 3 month sample.	131
Figure H5. TCA profile of levoglucosan.	132
Figure H6. STEM images of the dried lignin fraction samples and the pre-eluate (magnification 60k): a) fraction 1, b) fraction 2; c) fraction 3; d) fraction 4; e) fraction 5.	133

Figure H7. STEM images of the dried lignin fraction samples and the pre-eluate (magnification 8k): a) the pre-eluate; b) fraction 1, c) fraction 2; d) fraction 3; e) fraction 4; f) fraction 5.	134
Figure I1. Log MW of PS standarrds plotted vs. t_r in analytical SEC utilizing analytical PLgel 1000 Å used for column calibration.	135
Figure J1. ESI mass spectra of PPG standards shown before and after deconvolution: PPG-1000 (a and b), PPG-2000 (c and d), PPG-2700 (e and f), PPG-3500 (g and h).	136
Figure J2. ESI mass spectra of PPG-2700. Features an ion carrying a charge of +4.	137
Figure J3. RP HPLC-ESI MS chromatogram of the narrow MW PEG standard mixture 3.....	138
Figure J4. ESI mass spectra of PEG standards shown before and after deconvolution corresponding to the PEG standards with the M_n values of 269 Da (a, d), 1,380 Da (b, e) and 5,610 Da (c, f).	139

LIST OF TABLES

Table	Page
Table 1. Indulin AT lignin molecular weight determined by SEC reported in literature.	5
Table 2. Comprehensive overview of the MS approaches employed for the analysis of intact lignin and high MW standards	9
Table 3. Low MW species representing lignin used for the evaluation of the column separation performance.	24
Table 4. SEC (GFC and GPC) columns evaluated in this study.....	27
Table 5. Resolution of two PS standard peaks in SEC utilizing the columns with the PSDVB stationary phase, various particle and pore size.	35
Table 6. Lignin model compounds employed in ESI HR MS optimization.	45
Table 7. ESI TOF MS response with acids (either formic or acetic) and ammonium acetate as ESI electrolytes for representative lignin mono- to trimeric structure model compounds in both positive and negative ionization modes ^a	55
Table 8. Number-average, weight-average and z-average molecular weight of lignin determined by ESI HR TOF MS, GPC and MALDI HR TOF MS.	64
Table 9. MW, average hydrodynamic diameter and zeta-potential of the particles in lignin fractions and the pre-eluate determined by SEC and DLS.	80
Table 10. Molecular weight of the water-soluble portion of lignin autoclaved in the presence of 0%, 5% and 10% of H ₂ O ₂ (v/v) in 100% water and in the aqueous system containing 25% of methanol.	90

Table 11. Optimized conditions for DI-MS and HPLC-MS analysis of the selected synthetic polymers.	93
Table 12. Number-average molecular weight for PPG standards determined by ESI HR TOF MS and claimed by the supplier.	94
Table 13. Molecular weight (Da) of copolymer of styrene oxide and maleic anhydride determined by GPC and ESI HR TOF MS.	96
Table 14. Molecular weight (M_n / M_w , Da) of PEG narrow MW distribution standards analyzed in a mixture by ESI HR TOF MS and claimed by the supplier.	98
Table 15. Molecular weight (M_n / M_w , Da) of PEG narrow MW distribution standards (mixture 3) analyzed in a mixture by ESI HR TOF MS and claimed by the supplier.	99
Table A1. Low MW species representing lignin with their structures used for the evaluation of the column separation performance.	105
Table D1. Lignin model compounds and theirs structures employed in ESI HR MS optimization.	118
Table E1. The response (peak area) for target ion $[M+H]^+$ ($155.070 \pm 0.030 m/z$) via FIA of 5 ppm syringol in MeOH/Water (1:1) analyzed in the positive ionization mode.	123

ACKNOWLEDGEMENTS

I am very grateful to my advisor and co-advisor Drs. Alena Kubátová and Evgenii Kozliak for their unwavering support, training, guidance, motivation and encouragement throughout my Doctoral Studies at the University of North Dakota. I greatly appreciate the contribution of Drs. Yun Ji and Irina Smoliakova to my technical training and professional growth as well as the continuous support of my other committee members, Drs. Julia Zhao and David Pierce.

I am extremely appreciative of Thomas DiProspero, Sam Lilak, Clayton Geib, Natallia Yeudakimenka, Shelly Lu and Sarah Reagen who were directly involved in my research projects. I am thankful to current and former members of Dr. Kubátová's and Dr. Kozliak's research group (Honza, Keith, Jana, Brett, Josh S., Josh H., Klára, Audrey, and Rich) for their help and consistent support. I would also like to thank the collaborators from outside UND Chemistry Department, particularly Drs. Angel Ugrinov and Mukund Sibi (North Dakota State University), Dr. Alevtina Smirnova (South Dakota School of Mines and Technology), Dr. Cheng Zhang (South Dakota State University) and Bill Johnson (Agilent Technologies).

I would like to thank the University of North Dakota, UND Chemistry Department, and UND Graduate School for accepting me to the program and supporting me financially. I appreciate the financial support from the following funding agencies: The North Dakota EPSCoR Programs (Dakota BioCon tracks I and II, CSMS, and Doctoral Dissertation Award), UND Graduate School, Dr. Ernest & Jennie Coon teaching award and Dr. Roland Severson research award, ACS and

ASMS for travel stipends as well as CAS for accepting me to the SciFinder Future Leaders in Chemistry program.

Finally, I would like to thank my family and friends (particularly Dmitry Andrianov, Elena Alieva, Evgeniya Suvorova, Antonia Forbes, Duminda Liyanage Aleksandrova, Ivana Brzoňová, Chris Buelke, Rahul Shahni, Asina Sodsuchin, Eric Timian and Megan Goltz) for their love, consistent support and encouragement to pursue my Doctoral degree.

To my parents Svetlana Artemyeva and Aleksei Artemyev

ABSTRACT

Characterization of lignin and its degradation products, more specifically determination of their molecular weight (MW) distribution, is essential for assessment and applications of these potentially renewable phenolics. In this dissertation a suite of lignomics approaches allowing for comprehensive and accurate characterization of lignin focusing on the low and high MW species was developed. These methods may be used either in combination or independently. The methods were validated and applied to characterizing lignin and the products of its transformation.

Several size exclusion chromatography (SEC) systems were previously deemed to be suitable for MW-based separations and thus are frequently used for lignin analysis, however the nature of secondary non-SEC interactions remains unclear. In this dissertation, several representative gel filtration and gel permeation systems were assessed. This work confirmed that undesired secondary non-SEC interactions may be detrimental and need to be carefully evaluated. From the evaluated SEC columns, only the stationary phase with highly cross-linked porous polystyrene/divinylbenzene provided the most effective separation by MW for both low and high MW model compounds. It was shown that polystyrene and poly(methyl methacrylate) standards may be reliably used for the SEC column calibration if an appropriate stationary phase was utilized. Notably, the column with a higher pore and lower particle size provided a better resolution towards polymeric standards, even though the particle size effect was downplayed in the earlier SEC studies of lignin. It was demonstrated that for several evaluated SEC systems, the separation was

strongly affected by functionalities of the analytes and correlated with the compounds' pK_a rather than MW. The separation on the stationary phases featuring polar hydroxyl groups was shown to lead to specific column-analyte secondary interactions, perhaps based on their hydrogen bonding with lignin. A novel approach for lignin mean MW calculation based on mass spectrometry data was implemented. The determined number-average MW corroborated the SEC results.

Furthermore, an electrospray ionization high-resolution time-of-flight mass spectrometry lignomics was developed as a method to expand the lignomics toolkit while targeting the simultaneous detection of low and high molecular weight lignin species. The effect of a broad range of electrolytes and various ionization conditions on ion formation and ionization effectiveness was studied using a suite of mono-, di- and triarene lignin model compounds as well as intact lignin. Contrary to the expectations based on literature, the positive ionization mode was found to be more effective for methoxy-substituted arenes and polyphenols, i.e., species of a broadly varied MW structurally similar to the native lignin. For the first time, an effective formation of multiply charged species of lignin with the subsequent mass spectrum deconvolution was reported. The obtained MW values were in good agreement with those determined by SEC and LDI.

To minimize heterogeneity of lignin, which hinders its characterization by the spectral and thermal methods, narrow MW lignin fractions were obtained by preparative SEC considering the most suitable chromatographic conditions. Characterization of these fractions was performed with a suite of methods while using traditional chemistry approaches as well as nanoparticle characterization. Commercially available alkali lignin was shown to contain the impurities that were structurally different from lignin. The results of thermal carbon analysis suggested that these impurities may have a carbohydrate-like nature.

Furthermore, the developed chromatography and mass spectrometry methods may be widely applied in a challenging field of both natural and synthetic polymer characterization. In this dissertation, the application of the newly developed approaches to characterizing the lignin-derived products and synthetic polymers was shown.

CHAPTER I. INTRODUCTION

I.1. Lignin Composition

Lignin, one of the most abundant biopolymers, occurs in plant cell walls¹ and contributes up to 20 and 30% of the dry weight of hardwood and softwood, respectively.² Three types of phenylpropanoid monomer units, namely *p*-coumaryl, coniferyl and sinapyl, which are seemingly randomly linked by C-O and C-C bonds (Fig. 1), define the structure of heterogeneous polymeric lignin.²⁻⁵ The difference in chemical composition of various types of lignin is in the prevalence of certain aromatic units in their polymer structure. Lignin from hardwood contains almost equal amounts of coniferyl and sinapyl units and a lower content of *p*-coumaryl units, while softwood lignin consists mainly of coniferyl units, with small amounts of *p*-coumaryl units.^{6,7} Various types of the linkages are prevalent depending on the type of lignin, e.g., the β -O-4 bonds found in both softwood (45–50%) and hardwood (60–62%) lignin. Also, other less frequent linkages (1–27%) such as 5-5, β -5, β -1, 4-O-5, β - β , dibenzodioxocin, and spirodienone were identified in the lignin structure (Fig. 1).^{8,9}

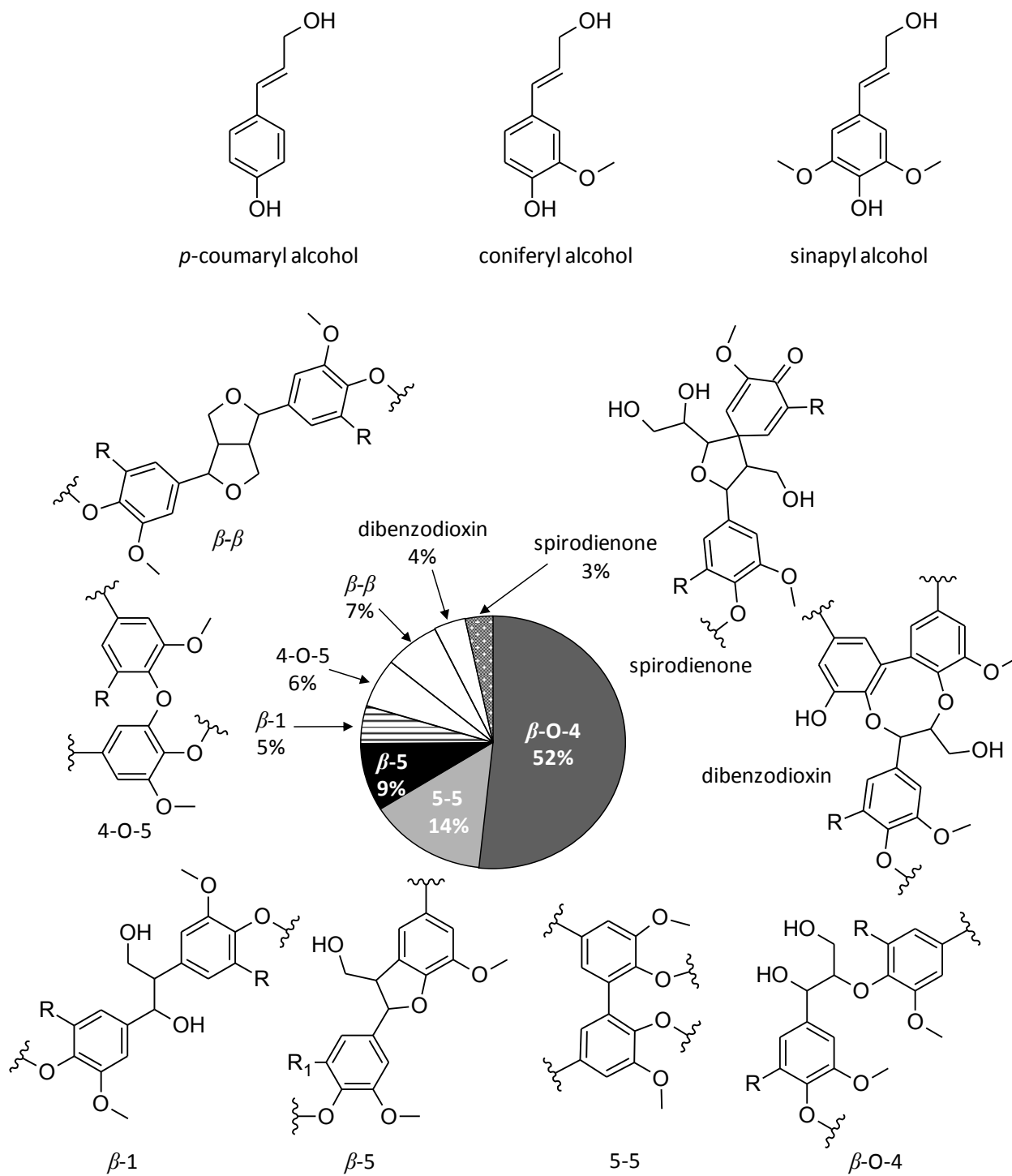


Figure 1. Lignin structural motifs and relative percentage of eight linkages, such as dibenzodioxin, spirodienone, β - β , 4-O-5, β -1, β -5, 5-5, and β -O-4 found in lignin.¹⁰

Being a renewable material, lignin is a potential source of liquid fuel and value-added phenolic chemicals.¹¹ Its extensive production by paper and pulp industries as a by-product, which exceeds 70 million tons annually, has stimulated investigations into value-added utilization of lignin.¹²⁻¹⁴ However, despite significant efforts over several decades, the commercial use of lignin has not exceeded 2% of its annual production.¹² The highly heterogeneous nature of lignin hinders a thorough understanding of its structure and, thus, its value-added utilization.¹⁵ To transform lignin into commercially beneficial substances, various thermal, catalytic and biological degradation processes are being tested.¹⁰ An elaborate and diverse suite of analytical methods is required for the assessment of the initial lignin feedstock as well as the evaluation of the degradation process efficiency and selectivity.¹⁰ Significant efforts in the area of lignin characterization have been pursued recently, yet the task remains challenging.¹⁶

I.2. Approaches to Qualitative Analysis of Lignin

The efficiency of a degradation process is typically evaluated through quantification of low molecular weight (MW) species (<400 Da) present in the mixture of decomposition products by one or two-dimensional gas chromatography (GC or GC×GC) with either flame ionization (FID) or mass spectrometry (MS) detection, or by liquid chromatography with electrospray ionization MS (LC-ESI MS).¹⁰ This analysis allows for a detailed characterization, but it is limited to 20% of the product mass, which is extractable by organic solvents and called bio-oil.¹⁰ Only tentative characterization is reported for the significant portion of lignin degradation products that cannot be characterized by GC. This portion consists of phenolic oligomers and a so-called “coke” solid soot-like residue. For a comprehensive assessment of the degradation efficiency and understanding

of decomposition pathways, a thorough characterization of intact lignin in the form of a native polymer including the determination of MW distribution is essential, yet extremely challenging.

1.2.1. Size Exclusion Chromatography for Lignin MW Elucidation

Currently, the most common method for lignin MW determination is size exclusion chromatography (SEC) with either organic (gel permeation chromatography, GPC) or aqueous (gel filtration chromatography, GFC) mobile phases.^{7, 10, 17} Several studies pointed out that the observed MW values strongly depended on the SEC analysis setup, lignin pretreatment and data handling.^{18, 19} The uncertainty in the reported MW values (see Table 1 for Indulin AT lignin),²⁰⁻²⁶ with reported number average (M_n) and weight average (M_w) values varying within a range of 530–2,600 Da and 3,500–6,549 Da, respectively, stresses the challenge in lignin MW characterization. Some studies determined a high polydispersity index (PDI) defined as a M_w/M_n ratio being as high as 8 or even 10, while the supplier provided the values of 1,900 Da and 6,900 Da for M_n and M_w , respectively, resulting in a lower PDI of 3.6 (Table 1). In contrast, the other application of GFC with an aqueous-based mobile phase suggested a low heterogeneity of Indulin AT lignin with a PDI of 2.1.²¹ One of the pioneering studies that characterized Indulin AT lignin using vapor pressure osmometry and sedimentation equilibrium reported values of 1,600 Da and 3,500 Da for M_n and M_w , respectively.²⁶

Table 1. Indulin AT lignin molecular weight determined by SEC reported in literature.

M _n	M _w	PDI	Method			Reference
			Stationary Phase	Mobile Phase	Standards	
GFC						
530	4,290	8.1	Hydroxylated methacrylate (TSKgel GMPWxl)	Aqueous sol. 0.5 M NaOH	PSS Na ^a	2016 ²²
1,900	6,900	3.6	NR ^b	Aqueous-based	PSS Na	2013 ^c
2,600	5,500	2.1	Sulfonated styrene- divinylbenzene copolymer- network	Aqueous sol. 0.1 M NaOH	PSS Na	2014 ²¹
GPC						
656	6,549	10.0	Cross-linked styrene- divinylbenzene copolymer (Styragel)	Tetrahydrofuran	PS ^d	2016 ²³
1,580	6,060	3.8	NR ^b	Lithium chloride/dimethylacetamide	Pullulan	2011 ²⁰

^a PSS Na stands for sodium polystyrene sulfonate.

^b Analysis details were not reported.

^c MeadWestvaco Indulin AT lignin used in this study. Its properties were provided by the supplier.

^d PS stands for polystyrene.

The main uncertainty of SEC when analyzing lignin and its decomposition products is that the separation is not driven exclusively by size exclusion but also by other interactions occurring due to lignin's heteropolymer nature and variety of its functional groups.^{7, 27, 28} This problem may be amplified when polymeric standards different from the lignin chemical structure are used, e.g., polystyrenes (PS). Such standards cannot emulate the non-size-specific interactions and thus may result in a misleading SEC calibration.

To minimize the uncertainty of SEC when analyzing lignin, it is essential to elucidate the nature of unwanted secondary interactions. This elucidation would lead to a proper selection of

analysis conditions that selectively promote the size-driven separation mechanism and reliable calibration. While the non-SEC interactions were studied for proteins²⁹ and polysaccharides,³⁰ similar studies were not reported for lignin. Lambrecht et al. discussed the impact of co-solvents in extraction media when separating proteins and suggested an optimal medium for analysis of various protein mixtures, avoiding any non-SEC effects.²⁹ He et al. stressed the effects of stationary phase material and pore size on the efficiency of size-based separation of polysaccharides in RP HPLC.³⁰

Unlike for regular polymer analytes, a well-defined series of standards is not available for lignin. Lignin's highly heteropolymeric matrix features a rather different suite of unwanted secondary column interactions, whose detailed analysis is yet to be provided. Additionally, to the best of our knowledge, the influence of pore and particle size on SEC of lignin has not been explored. Yet, two conflicting effects, i.e., thermodynamic and kinetic, may lead to opposite trends in separation as it was previously shown for polystyrene standards.³¹

One of the approaches to overcome the uncertainty in SEC results was the application of a multi-angle laser light scattering detector in combination with SEC to verify MW,³²⁻³⁷ however, the resulting MW values might be skewed by polymer association and interference due to lignin's fluorescence.^{38, 39} Another problem is the low lignin solubility in a vast majority of solvents typically used in GPC or GFC. To address this limitation and also to limit the contribution of various functionalities, lignin is often acetylated.¹⁹ While addressing the issue of limited solubility, lignin acetylation may contribute to the undesired polymer MW increase, which depends on the number of hydroxyl groups subjected to acetylation, and can vary from one lignin sample to another.³⁹ Lange et al. suggested introducing an additional abundance-weighted direct correction factors to account for the system-inherent bias.³⁹ This factor accounted for both the sample type

and derivatization characteristics and resulted in lower MW values. The precision and accuracy of this corrected GPC-based determination of acetylated and acetobrominated lignin M_n was assessed with an independent NMR-based M_n determination.³⁹

1.2.2. MS in Lignin MW and Structure Elucidation

While mass spectrometry is often the method of choice, Table 1 demonstrates the limitations of various MS approaches and unresolved issues reported for intact lignin characterization alone,²⁷ or in combination with pyrolysis (Pyr) GC.⁴⁰⁻⁵⁰ Pyr-GC is traditionally used to determine the type of lignin or lignocellulose, however it neither provides any MW information nor allows for a differentiation of small and large MW species.¹⁰ The application of Pyr-GC-MS typically targets the speciation of syringol and guaiacol within lignin structural units.⁴⁹

Matrix-assisted laser desorption/ionization (MALDI) MS is currently considered the only suitable MS approach⁵¹ for determination of MW distribution in synthetic polymers, proteins and polysaccharides.⁵¹ However, MALDI provides only limited structural information⁵²⁻⁵⁴ due to partial fragmentation, which makes it impossible to distinguish small and large molecules.⁵²⁻⁵⁴ This issue could be addressed by coupling MS to LC; however, MALDI cannot be used as an online detector due to the required sample preparation procedure, which includes the analyte co-crystallization in a mixture with a matrix. Moreover, sample co-crystallization leads to undesirable association effects.⁵⁵ MALDI ionization also results in the predominant formation of single charged species, thus suppressing the ionization of high MW species and promoting the formation of ions featuring low m/z ratios.⁵³ Additionally, the analyte MW is typically limited to the mass

analyzer operation range.⁵⁶ These limitations result in a noisy lignin spectrum lacking resolved peaks, particularly on the higher end of the m/z scale.^{51, 54, 56, 57}

Intact lignin has also been investigated using MS with ESI and atmospheric pressure chemical ionization (APCI). However these studies focused only on a limited m/z range (up to 1,000 m/z ⁵⁸⁻⁶⁴ and 1,500 m/z ^{59, 65-68}) aiming to evaluate lignin degradation products (Table 1).^{27, 69} The significance of these studies was in the successful elucidation of the structural patterns and common linkages in various types of lignin, yet the MW was left undetermined,⁵⁸⁻⁶⁸ as well as a potential formation of multiply charged species characteristic for ESI, which is widely used in proteomics,⁷⁰ yet has not been reported to our knowledge for lignin. Several research groups utilized ESI with an extended m/z range (up to 3,500 m/z ⁷¹ and 7,000 m/z ⁵⁵), however the reported spectra showed a low signal-to-noise ratio and low intensity above 1,000 m/z , possibly due to the use of ionization conditions targeting low MW species. To the best of our knowledge, a thorough optimization of ionization conditions and mass analyzer parameters within an extended m/z range aiming for a greater peak resolution and higher signal-to-noise ratio has not been reported.

Table 2. Comprehensive overview of the MS approaches employed for the analysis of intact lignin and high MW standards

Ionization Mode	Mass Analyzer	Analyte	Solvent	Electrolyte/ MALDI Matrix	MW or m/z Range Detected	Ref
APPI						
–	Q-orbitrap	Dioxane lignin	Acetone–water mixture (9:1)	0.1% NH ₄ OH	300–1800 m/z	64
+	HR Q-TOF-MS	Wheat straw lignin	Dioxane (100%) or	NR ^a	Positive mode:	58
–	HR Q-TOF-MS	Wheat straw lignin	Dioxane/MeOH/CHCl ₃		300–1,120 m/z	
+/-	HR Q-TOF-MS/MS	Oligomeric species in lignin	(1:1:1)		Negative mode: 200–700 m/z	
APCI						
–	Q-orbitrap	Dioxane lignin	Acetone–water mixture (9:1)	0.1% NH ₄ OH	300–1800 m/z	64
–	Ion trap	Synthesized oligomeric standards	H ₂ O/MeOH (50:50);	0.1% acetate	100–1,000 m/z	59
–	Single quadrupole	Lignin partially depolymerized under acetic conditions	H ₂ O/MeOH	NR	150–650 m/z	60

Table 2. cont.

Ionization Mode	Mass Analyzer	Analyte	Solvent	Electrolyte/ MALDI Matrix	MW or <i>m/z</i> Range Detected	Ref
+/-	Quadrupole– hexapole–quadrupole	Wheat straw intact and acetylated lignin	CHCl ₃ /MeOH (2:1)	A mixture of formic and acetic acid	100–550 <i>m/z</i>	⁶¹
ESI						
–	Q-orbitrap	Dioxane lignin	Acetone–water mixture (9:1)	0.1% NH ₄ OH	300–1800 <i>m/z</i>	⁶⁴
–	Q-TOF	Dried sorghum feedstock, corn stover hydrolysate, xylobiose and xylotetraose	H ₂ O/traces of MeOH	None or traces of H ₂ SO ₄	50–2,000 <i>m/z</i>	⁶⁸
+	Linear trap quadrupole – Fourier transform hybrid linear trap/7-T Fourier transform – ion cyclotron resonance MS	Bagasse lignin (100–100,000 g·mol ⁻¹ ¹ with a maximum at 2·10 ³ g·mol ⁻¹ according to GPC); steam explosion lignin	DMSO/MeOH (9:1)	NR	150–2,000 <i>m/z</i>	⁶⁵

Table 2. cont.

Ionization Mode	Mass Analyzer	Analyte	Solvent	Electrolyte/ MALDI Matrix	MW or <i>m/z</i> Range Detected	Ref
–	Magnetic sector	Spruce and eucalyptus dioxane lignin, eucalyptus kraft -organosolv and oxygen spruce lignin	MeOH/H ₂ O (1:1)/2.5% NH ₃ or dioxane/H ₂ O (7:3)	2.5% NH ₄ OH ^b	100–7,000 <i>m/z</i> (unresolved at higher <i>m/z</i>)	55
–	Q-TOF	Low-molecular-weight fraction of E. globulus dioxane lignin	MeOH/H ₂ O (1:1)/0.25% NH ₃	0.25% NH ₄ OH ^b	50–1,500 <i>m/z</i>	66
+	Triple Q	Oligolignols (3–8 aromatic rings) synthesized from coniferyl alcohol with horseradish peroxidase	ACN/H ₂ O	Cetyltrimethylammonium sulfate	200–1,500 <i>m/z</i>	67
–	Magnetic sector-quadrupole	Wood and residual lignin from kraft pulps, black liquor lignin	MeOH/H ₂ O (1:1)	0.25% NH ₄ OH ^b	300–3,500 <i>m/z</i>	71
–	Triple-quadrupole	Synthetic lignin and soluble lignin extracted from sugar cane	ACN/H ₂ O	0.1% formic acid	100–850 <i>m/z</i>	62
– (nano-mate spray)	Linear trap quadrupole Fourier transform	Isolated oligolignols	ACN/H ₂ O (eluent Collected from RP LC)	0.1% acetic acid	120–1,400 <i>m/z</i>	59

Table 2. cont.

Ionization Mode	Mass Analyzer	Analyte	Solvent	Electrolyte/ MALDI Matrix	MW or m/z Range Detected	Ref
MALDI						
–	Quadrupole-ion-trap analyzing system (linear trap quadrupole-XL)	Hand-cut sections of stems of two <i>Eucalyptus</i> species	NA	Matrix was substituted with thin layer chromatography grade silica	100–1,000 m/z	⁷²
+	TOF	Organosolv lignin and glyoxalated lignin resin	NA	DHB ^c	200–700 m/z	⁷³
+	TOF	Bagasse lignin (100–100,000 $\text{g}\cdot\text{mol}^{-1}$ ¹ with a maximum at $2\cdot 10^3$ $\text{g}\cdot\text{mol}^{-1}$ according to GPC); steam explosion lignin	NA	DHB	Mass distribution with a maximum around m/z 360; no signal above 2000 m/z	⁶⁵
+/-	TOF	Lignin fractions extracted from <i>Miscanthus x giganteus</i> under alkali or acid conditions	NA	CHCA ^d / α -cyclodextrin	100–800 Da	⁵²

Table 2. cont.

Ionization Mode	Mass Analyzer	Analyte	Solvent	Electrolyte/ MALDI Matrix	MW or <i>m/z</i> Range Detected	Ref
+/-	TOF	Softwood kraft lignin, mixed hardwood organosolv lignin, acid hydrolysis lignin from bagasse, and steam explosion lignin from aspen (acetylated sample)	NA	DHB or all- <i>trans</i> -retinoic acid	50–14,000 <i>m/z</i> (unresolved at higher <i>m/z</i>); 50–14,000 Da (singly charged ions are almost exclusively generated)	⁵⁶
+	TOF	Milled wood lignin, alkali lignin and a synthetic lignin (G-type) obtained by enzymic polymerization of coniferyl alcohol	NA	DHB, 2-aminobenzoic acid or sinapinic acid (Sinapinic acid was preferred.)	200–1,700 Da	⁷⁴

Table 2. cont.

Ionization Mode	Mass Analyzer	Analyte	Solvent	Electrolyte/ MALDI Matrix	MW or m/z Range Detected	Ref
+/-	Quadrupole ion trap TOF (QIT-TOF)	Dioxane lignin	NA	<i>N-tert</i> -butyl- <i>N</i> -isopropyl- <i>N</i> -methylammonium α -cyano-4-hydroxycinnamate ionic liquid or no matrix. The latter provided poor spectral data.	50–2,000 Da (unresolved) and 2000–6000 Da (unresolved)	⁵¹
+	TOF	Milled wood lignin and synthetic lignin (polymerisation of coniferyl alcohol with peroxidase)	NA	DHB	400–2,600 Da	⁵³
+	TOF	Pyrolytic lignin and its SEC fractions	NA	DHB or no matrix	50–4,000 Da (unresolved)	⁵⁷
NA	TOF	Soda hardwood lignin (Eucalyptus) and softwood kraft lignin	NA	DHB	70–700 Da	⁷⁵
+	TOF	Native and degraded birch wood lignin	NA	DHB	1,000–2,000 m/z	⁵⁴

Table 2. cont.

Ionization Mode	Mass Analyzer	Analyte	Solvent	Electrolyte/ MALDI Matrix	MW or <i>m/z</i> Range Detected	Ref
Secondary Ion MS (SIMS)						
+	TOF	Milled wood lignin, birch kraft lignin, isolated	DCM/EtOH (2:1) or DMSO prior to deposition on silver disk	None	10–1,200 <i>m/z</i>	⁷⁶

^a NR denotes not reported.

^b The w/v concentration was provided in respect to NH₃.

^c DHB stands for 2,5-dihydroxybenzoic acid.

^d CHCA stands for α -cyano-4-hydroxycinnamic acid.

The intermediate products of lignin degradation, i.e., lignin mono- to oligomeric standards, appear to be suitable model compounds for understanding the ionization mechanism of intact and degraded lignin.^{59, 62-64} An extensive optimization of ESI and APCI conditions toward the analysis of monomeric and several dimeric lignin model compounds was reported, to our best knowledge, only in the study by Hauptert et al. while utilizing a linear quadrupole ion trap MS.⁷⁷ Kosyakov et al. assessed ESI, APCI and APPI as ionization techniques focusing on specific additives for analysis of lignin and its model compounds using a quadrupole-orbitrap MS.⁶⁴ The limitation of APCI and APPI is their applicability only to a relatively low MW range, below 1,800 Da, and the predominant formation of singly-charged ions. In addition, APCI was shown to suffer from excessive fragmentation of lignin model compounds thus making this method inappropriate for both analysis of complex degradation mixtures^{60, 77} and determination of intact lignin MW.⁶¹ Thus, APPI and APCI may be preferred for studying oligomeric species and structural patterns in lignin. However, these ionization techniques cannot be applied for detection of high MW species in lignin.

Proposed in 2010⁵⁹ the MS-based sequencing of lignin oligomers as an identification tool allowed for coining the term “lignomics”.⁶³ Oligomeric model compounds and isolated oligolignols (up to 650 m/z) were efficiently ionized with APCI and ESI in the negative mode; furthermore, the fragmentation pathways of the major bonding structures in the gas phase were elucidated.^{59, 63} All of these approaches laid the foundation for the development of an MS-based sequencing algorithm, yet they proposed different ionization conditions and were limited by their focus on relatively low m/z values (<900). Thus, detection of high MW species, which are essential components of lignin, remains challenging and prevents lignin MW elucidation with the currently available MS toolkit.

I.3. Lignin Fractionation for Its Comprehensive Characterization

The highly heterogeneous nature of lignin hinders a thorough elucidation of its structure and thus limits its value-added utilization.¹⁵ This problem, however, could be addressed by lignin fractionation by molecular size and weight, which allows for characterization of samples less complex than native lignin, presumably more homogenous, i.e., featuring narrower molecular size distribution, MW or similar in chemical structure.¹⁴ Then, narrow MW well-characterized fractions may be utilized either directly or after their selective processing.^{14, 15} Characterization of the fractionated lignin may also be streamlined, as the fraction's homogeneity may minimize the unwanted side effects of analysis. Currently, there are three main methods that have been used for lignin fractionation, either alone or in combination,⁷⁸⁻⁸¹ i.e., selective solvent fractionation,^{14, 15, 82-96} differential precipitation^{80, 97-106} and membrane ultra- and nanofiltration.¹⁰⁷⁻¹¹⁷

Selective solvent extraction is based on partial solubility of lignin fractions in various solvents such as methanol, ethanol, isopropanol, acetone, diethyl ether, ethyl acetate, dioxane, tetrahydrofuran (THF), butanone, hexane, propyleneglycolmonomethyl ether, and dichloromethane (DCM).^{14, 15, 82-96} A major advantage of this method is the application of relatively inexpensive instrumentation and a moderately easy process scale up. On the other hand, the solubility of certain fractions depends on a variety of factors, with MW being one of the solubility-determining parameters but not the only one.¹¹⁸ Diverse lignin functionalities may significantly affect the composition of the fraction extracted into a certain solvent¹¹⁹ since polymer solubility is known to be affected by the chain chemistry, compositional and stereochemistry.¹¹⁸ The MW of each fraction is difficult to control and manipulate because of a high variability in lignin structure obtained from different sources by different methods.¹¹³ Similar issues are encountered when

selective precipitation of dissolved lignin is applied. Furthermore, a non-desired additional chemical alteration of lignin may take place.¹²⁰

Membrane filtration allows for a direct fractionation of black liquor and has the advantage of a controlled separation by the MW through variation of the membrane pore size cut-off.¹⁰⁷⁻¹¹⁷ However, this process is frequently unable to effectively separate low MW species mono-, di- and i.e., triarene phenolic compounds obtaining even the lowest MW fraction with the MW cut-off as high as 5000,¹¹⁶ 1000¹¹² or the lowest of 500 Da. Additionally, membranes tend to foul and the filtration process is not easily scalable to satisfy industrial needs.⁹¹

Kirk et al. employed a preparative fractionation of lignin by GPC as an effective approach for collecting lignin fractions solely based on the molecular size and presumably featuring narrow MW distribution.¹²⁰ An apparent advantage is that the molecular size cut-offs are easy to control by varying the retention time windows when GPC is applied for lignin fractionation. Furthermore, as a type of SEC, GPC is known to be a scalable technique.^{121, 122}

A successful GPC application for obtaining lignin fractions with a desired MW, i.e., separation of nineteen fractions with the number-average MW ranging from 340 to 1250 Da, was reported by Botaro et al.¹²³ They showed that the collected fractions exhibited low polydispersity, with the polydispersity factor near unity for some of the fractions. Fourier transform infrared spectroscopy (FTIR) was utilized for the elucidation of fractions' structural difference and high performance SEC (HP SEC) demonstrated the difference in the distribution across MW from 340 to 2770 Da (M_n) of the collected fractions.¹²³ However, in the study by Botaro et al.¹²³ the preparative-scale SEC was performed with hydroxypropylated cross-linked dextran as a stationary phase, which may have contributed to lignin fractionation not exclusively by its MW.¹⁶

Furthermore, the undesired non-SEC interactions, which tend to skew the MW-based separation, may be amplified when a hydroxylated stationary phase is used.¹⁶

I.4. Statement of Purpose

The aim of this work was to develop a suite of lignomics approaches, which may be used either in combination or independently, to characterize lignin MW distribution, including the understanding of SEC mechanistic aspects and approaches to overcome the issues frequently encountered in lignin analysis by chromatography and MS.

First, the separation on various GPC and GFC systems was evaluated using a broad range of standards of high and low MW including those featuring lignin functionalities. The GPC application to lignin was assessed and approaches to minimize undesired secondary non-SEC interactions were investigated. A methodology to evaluate the applicability of a size exclusion chromatographic system to lignin MW determination was proposed. A novel approach for lignin mean MW calculation based on MS data was implemented and used for the validation of GPC results.

In the area of mass spectrometry, the goal was to develop a protocol for extending the lignomics toolkit through detection of high-MW lignin components as well as low-MW phenolics. To achieve this goal, the effect of a broad range of electrolytes on ESI of two representative lignin-like dimers was investigated. This was followed by narrowing the range of electrolytes while assessing the ionization of eleven mono-, di- and triarene lignin model compounds featuring different oxygenated functional groups and linkages typical for lignin and then expanded the method to native lignin. This investigation led to the development of a protocol for successful ionization of high MW lignin species with a focus on multiply charged ion formation. It was also postulated and confirmed that higher MS resolution led to an improved detection of high MW species when an ion mobility (IM) feature was employed with HRMS. The determined average MW values of lignin were compared to those obtained by LDI MS and GPC.

The developed SEC and MS methods allowed for overall lignin characterization, yet its heteropolymeric nature and non-uniform structure complicated the results interpretation. To address this issue, lignin was fractionated based on its molecular size by translating the developed GPC method to a preparative-scale SEC. Narrow MW lignin fractions were obtained by this preparative-scale SEC and characterization was performed with a suite of methods that included traditional chemistry approaches as well as nanoparticle techniques. Specifically, an optimized high performance SEC was used for MW elucidation, a newly developed thermal carbon analysis was used for thermal fractionation and mass balance closure, and scanning transmission electron microscopy (STEM) along with dynamic light scattering (DLS) were employed for evaluating the particle size and correlating it with the MW values.

CHAPTER II. LIQUID CHROMATOGRAPHY OF LIGNIN

II.1. Experimental

II.1.1. Materials and Reagents

All standards used in this study as lignin model compounds for evaluating the columns are listed in Table 3, along with their acronyms, additional details including structures are provided in Appendix A, Table A1. Dehydrodivanillin^{124, 125} and guaiacylglycerol- β -guaiacyl ether¹²⁶ were synthesized according to the literature procedures published earlier. A detailed description of the synthetic procedures can be found elsewhere.¹²⁷ For GFC and RP HPLC column calibration, two sets of narrow polymeric standards were used, i.e., a polyethylene glycol (PEG) standard set with the standards' MW at the peak maximum (M_p) of 349–21,600 purchased from Fluka (Stenheim, Germany) and sodium polystyrene sulfonate (PSS Na) standards M_p of 1,600–15,650 obtained from American Polymer Standards Corporation (Mentor, OH, USA). PS narrow standards of M_p of 580–19,760 purchased from Varian (Amherst, MA, USA) and poly(methyl methacrylate) (PMMA) narrow standards with M_p of 550–26,080 purchased from Agilent Technologies (Santa Clara, CA, USA) were used for the GPC column calibration. 2-Chloroacetophenone (Sigma-Aldrich) was used as an internal standard in RP HPLC analysis.

Indulin AT lignin was purchased from MeadWestvaco (Richmond, VA, USA). Alkali lignin and ammonium acetate ($\geq 99\%$), were purchased from Sigma-Aldrich (St. Louis, MO, USA). HPLC-MS grade acetonitrile (ACN) and unstabilized THF containing no preservatives were

obtained from Fisher Scientific (Fair Lawn, NJ, USA) to eliminate interferences from butylated hydroxytoluene used as a common stabilizer system. Deionized water was obtained using a Direct-Q® 3 system, Millipore, Billerica, MA, USA.

Table 3. Low MW species representing lignin used for the evaluation of the column separation performance.

	Compounds	Class of methoxyphenols (extra functional groups)	Molecular Formula	MW (g·mol ⁻¹)	pK _a	Supplier/Synthesized	Purity
1	Guaiacol	G	C ₇ H ₈ O ₂	124.24	9.93	Acros Organics ^a	≥99%
2	<i>p</i> -Guaiacol	G	C ₇ H ₈ O ₂	124.24	9.90	Pfaltz and Bauer ^b	99%
3	Creosol	Alkyl-G	C ₈ H ₁₀ O ₂	138.16	10.34	Sigma-Aldrich ^c	≥98%
4	Veratrole	–	C ₈ H ₁₀ O ₂	138.16	~40	Sigma-Aldrich	99%
5	Vanillin	Carbonyl-G	C ₈ H ₈ O ₃	152.15	7.38	Sigma-Aldrich	99%
6	Syringol	Methoxy-G	C ₈ H ₁₀ O ₃	154.16	9.98	Acros Organics	99%
7	Eugenol	Alkenyl-G	C ₁₀ H ₁₂ O ₂	164.20	10.19	Acros Organics	99%
8	Isoeugenol	Alkenyl-G	C ₁₀ H ₁₂ O ₂	164.20	9.89	Sigma-Aldrich	98.8%
9	4'-Hydroxy-3'-methoxyacetophenone	Carbonyl-G	C ₉ H ₁₀ O ₃	166.17	7.81	Sigma-Aldrich	98%
10	4-Propylguaiacol	Alkyl-G	C ₁₀ H ₁₄ O ₂	166.22	10.29	Sigma-Aldrich	≥99%
11	Vanillic acid	Carboxyl-G	C ₈ H ₈ O ₄	168.15	4.45	Fluka ^d	97%
12	Veratrole alcohol	–	C ₉ H ₁₂ O ₃	168.19	>16	Sigma-Aldrich	96%
13	Homovanillic acid	Carboxyl-G	C ₉ H ₁₀ O ₄	182.15	4.41	Acros Organics	98%
14	Syringaldehyde	Carbonyl-G	C ₉ H ₁₀ O ₄	182.17	7.8	Sigma-Aldrich	98%
15	Dehydrodivanillin	Carbonyl-G	C ₁₆ H ₁₄ O ₆	302.07	7.04	In-house synthesis based on refs. ^{124, 128}	≥95%
16	Guaiacylglycerol- β -guaiacyl ether	≥2 hydroxy-G	C ₁₇ H ₂₀ O ₆	320.34	9.88	In-house synthesis based on ref. ¹²⁶	≥95%
17	Pinoresinol	≥2 hydroxy-G	C ₂₀ H ₂₂ O ₆	358.38	9.76	Sigma-Aldrich	≥95%

^a Acros Organics (Morris Plains, NJ, USA).

^b Pfaltz and Bauer (Waterbury, CT, USA).

^c Sigma-Aldrich (St. Louis, MO, USA).

^d Fluka (Steinheim, Germany).

II.1.2. Lignin Sample Preparation and Acetylation

In this study, we successfully addressed the lignin solubility issue through its complete dissolution in a 1:1 v/v THF-water system at a high concentration (up to 50 mg/mL) for GPC (organic mobile phase). The original concentrated solution was further diluted with 100% THF to obtain the samples with a desired lignin concentration, thus minimizing the water content to 10% or less. No precipitation occurred even if the water content was decreased to 1%.

We also evaluated the effect of acetylation, which is typically used to address the solubility issue in THF (a common GPC solvent).¹⁹ For GFC experiments, lignin was completely dissolved in a 1:1 v/v ACN-water system (up to 10 mg/mL). Acetylation of lignin samples was performed using a conventional method.¹²⁹ Briefly, about 50 mg of the sample was completely dissolved in 500 μ L of dry pyridine and reacted with 500 μ L of acetic anhydride. The reaction mixture was stirred for 12 h at room temperature. Then 200 μ L of methanol was added to the reaction mixture to terminate the reaction. Solvents were evaporated under a stream of nitrogen and the residue was dried in a vacuum oven at 30 °C overnight. Acetylated lignin was completely dissolved in 5.5 mL of THF resulting in a 1% w/v solution. The concentration of acetylated lignin was assessed with respect to the initial intact lignin mass before acetylation.

II.1.3. Instrumentation

SEC analyses were performed on an Agilent 1100 Series HPLC system equipped with a DAD and 6210 TOF MS with ESI detection (Agilent Technologies, Santa Clara, CA, USA).

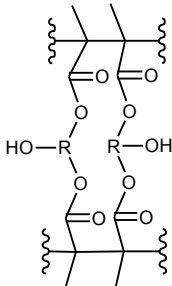
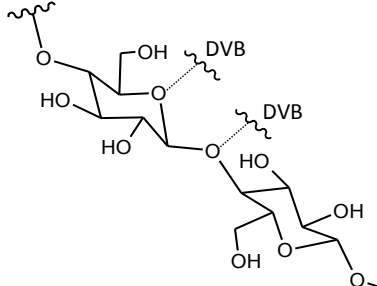
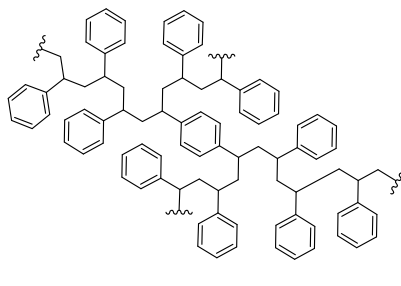
For the GFC assay, 1) an Ultrahydrogel with hydroxylated polymethacrylate-based gel (HPMA) stationary phase was utilized (see Table 4 for technical specifications). A mixture of ACN and water (1:4, v/v) with the addition of 0.5 mmol·L⁻¹ NH₄OAc was used as a mobile phase

at a flow rate of 0.6 mL/min. A typical concentration of standards was 100 ppm (w/v) dissolved in the same solvent system as the mobile phase, with an injection volume of 100 μ L.

HPLC Zorbax Eclipse Plus C18 column (pore size 95 Å), 3.5 μ m particle size, 2.1 \times 150 mm with a guard column, 2.1 \times 12.5 mm was used for evaluating HPLC for polymer separation. The column was thermostated at 30 °C. The mobile phase consisted of 10 mmol·L⁻¹ NH₄OAc in water (solvent A), and 10 mmol·L⁻¹ NH₄OAc in ACN (solvent B). The gradient program used for analysis started with an isocratic elution at 5% B for 10 min, followed by a linear gradient to 80% B from 10 to 20 min with 2 min hold and then linear gradient to 95% B from 22 to 23 min and hold for 1 min. The last step was 24 to 27 minutes to 5% B followed by a 10 min hold. The flow rate was set to 0.3 mL/min. The samples were filtered prior to the analysis. The injection volume was 5 μ L. The DAD detection was performed in a range of 190 to 700 nm with a step of 2 nm.

The GPC separation was tested on three columns (see Table 4 for specs): 2) Jordi Gel GBR with glucose rings bonded to a pure divinylbenzene-based (GDVB) stationary phase, 3) PLgel 1000 Å with a highly cross-linked porous polystyrene/divinylbenzene matrix-based (PSDVB) stationary phase, and 4) PLgel 500 Å also with the PSDVB stationary phase. Unstabilized THF was used as a mobile phase at a flow rate of 1.0 mL/min in all GPC experiments. A typical concentration of standards and lignin was between 0.1 and 1.0% dissolved in THF and THF-water 9:1 v/v, respectively, with an injection volume of 100 μ L.

Table 4. SEC (GFC and GPC) columns evaluated in this study.

	GFC		GPC	
	Ultrahydrogel 120	Jordi Gel GBR 100-GPC	PLgel 1000 Å	PLgel 500 Å
Stationary phase	<p>HPMA</p> 	<p>GDVB</p> 	<p>PSDVB</p> 	
Particle size	6 μm	5 μm	5 μm	10 μm
Pore size	120 Å	100 Å	1000 Å	500 Å
Column dimensions	7.8 × 300 mm	10 × 250 mm	7.5 × 300 mm	7.5 × 300 mm
Separation range	100–5,000 Da	50–5,000 Da	500–60,000 Da	500–25,000 Da
Guard column	Ultrahydrogel (6 mm × 40 mm)	Jordi Gel GBR 500 (10 mm × 50 mm)	PLgel (7.5 mm × 50 mm)	PLgel (7.5 mm × 50 mm)
Column manufacturer	Waters, Milford, MA, USA	Jordi Associates, Bellingham, MA, USA	Agilent Technologies	

A MALDI SYNAPT G2-Si MS System (Waters, Milford, MA, USA) with CryLaS FTS355-Q laser (a repetition rate of 2.5 kHz, wavelength 355 nm) was employed to acquire MALDI MS spectra in the range 50–8000 *m/z*. The system was manually calibrated with red phosphorus and the experiments were performed in positive resolution mode (20,000 Da). The laser energy was set to 350 arbitrary intensity units. Typically, 2,5-dihydroxy benzoic,^{53, 54, 56, 57, 65, 73-75} α -cyano-4-hydroxycinnamic,^{51, 52} retinoic or sinapinic acids were used as matrices for lignin analysis. Contradicting results were reported on the analysis with no matrix used (LDI), so

a few studies claimed successful ionization while the others reported it to be ineffective.⁵¹ In this study, we evaluated lignin ionization with α -cyano-4-hydroxycinnamic acid, 2-(4-hydroxyphenylazo)benzoic acid used as matrices and without any matrix. The best ionization effectiveness was achieved when no matrix was used.

II.1.4. SEC Data Handling

To calculate the number average (M_n) and weight average (M_w) MW of lignin samples, the total absorbance (in au) was used within a wavelength range of 220–750 nm (A_i). The absorbance at measurement point i had to exceed the baseline noise at least 3 times to be considered an analytical signal. M_n and M_w were calculated in MS Excel using the standard SEC equations, 1–2:

$$M_n = \frac{\sum A_i M_i}{\sum A_i} \quad (1)$$

$$M_w = \frac{\sum A_i M_i^2}{\sum A_i M_i} \quad (2).^{130}$$

To calculate the sample MW (M_i) at measurement point i , a linear equation derived from the standards' MW plotted vs. retention time was used.

II.2. Results and Discussion

II.2.1. SEC Separation of Polymeric Model Compounds

In the present study, we assessed several representative gel filtration and gel permeation systems focusing on undesired secondary non-SEC interactions. To differentiate those interactions and size exclusion effects, we used four sets of commercially available polymeric standards as well as low-MW lignin model compounds of varied chemical nature including several phenolic

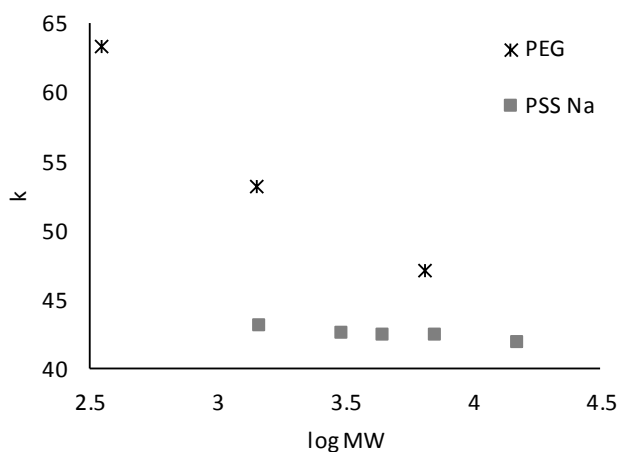
dimers synthesized in-house. We evaluated the GPC application to lignin with a focus on undesired secondary non-SEC interactions, then demonstrated the feasibility of size-based separation and accurate MW determination using the standards of different chemical structure. The determined average MW of lignin utilizing the optimal separation system was compared to that obtained by LDI MS. Furthermore, we investigated the effect of acetylation on lignin MW and its elution profile on the GFC and GPC stationary phases.

The SEC separation was evaluated using three systems (Fig. 2): GFC with a Waters Ultrahydrogel column (HPMA stationary phase) and two GPC columns, Jordi Gel GBR (GDVB stationary phase) and Agilent PLgel (PSDVB stationary phase). The elution profile appeared to be consistent with the size exclusion-based separation only for the last of them (Fig. 2c). HPMA stationary phase allowed for the MW-based separation of both PSS Na and PEG standards (Fig. 2a). However, the standards with the same MW but different structure were retained differently. A stronger retention of PEG standards suggests a contribution of other interactions such as hydrogen bonding occurring on the HPMA stationary phase (Fig. 2a).

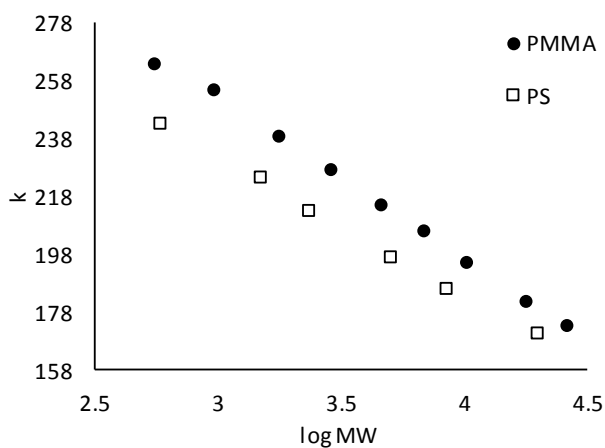
For SEC utilizing the GDVB stationary phase, separation on the basis of size exclusion mechanism was observed, with a similar retention for two different polymeric standards (Fig. 2b). However, PMMA standards had somewhat longer retention times compared to those of PS standards with a similar MW (Fig. 2b). It is of note that the two systems, HPMA GFC and GCDB GPC, for which the retention mechanism was affected beyond that of size exclusion, consisted of stationary phases with an abundance of hydroxyl groups (one with hydroxylated polymethacrylate and the other with glucose). Considering that lignin is also highly hydroxylated, hydrogen bonding may be contributing to the separation mechanism.

By contrast, when using the column with a fairly nonpolar PSDVB stationary phase (Agilent PLgel column), the type of polymeric standard used did not affect the retention, and the application of two different standard sets yielded a single linear calibration curve (Fig. 2c).

a) HPMA (Ultrahydrogel)



b) GDVB (Jordi Gel GBR)



c) PSDVB (Agilent PLgel)

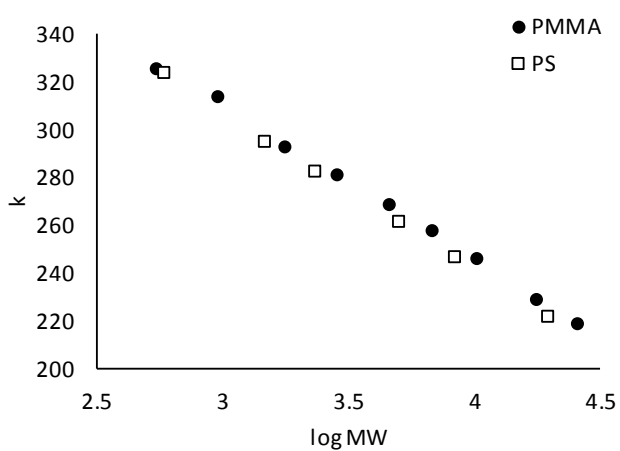


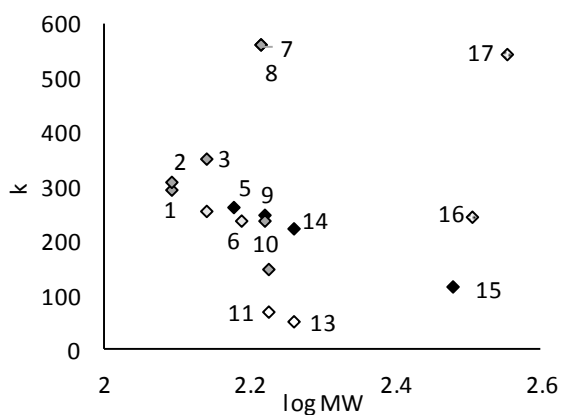
Figure 2. Retention factor (k) of polymeric standards, i.e., PS and PMMA, vs. log MW in SEC utilizing various stationary phases: a) HPMA; b) GDVB; c) PSDVB.

II.2.2. Unwanted Interactions in SEC Separation of Low-MW Phenolic Standards

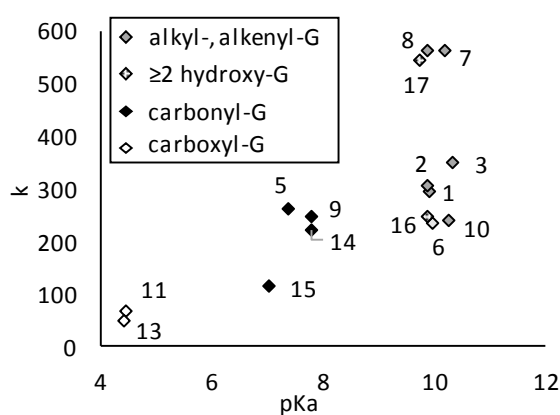
The separation of low-MW lignin model compounds was evaluated to further elucidate the analyte interactions with SEC stationary phases as well as to assess the suitability of these columns for lignin and its degradation products' separation (Fig. 3, for chromatograms see Appendix A, Fig. A1). The elution profiles of low-MW lignin model compounds confirmed the suitability of the PSDVB stationary phase: The retention factor depended exclusively on the MW (Fig. 3e). Notably, a size-based separation was achieved for the species with the MW equal or higher than 150 Da. This threshold corresponded to the mass of monomeric phenolpropanoid units, thus the size-based separation was achieved over the entire desired MW range. Furthermore, we observed that the retention factors, i.e., additional unwanted interactions correlated with the standards' pK_a values on all the stationary phases except for PSDVB (Figs. 3b, d, f).

As expected, this relationship was particularly strong for the GFC system with a polar highly hydroxylated stationary phase where hydrogen bonding may be more pronounced (Figs. 3a, b; for chromatograms see Appendix C, Fig. C1). Perhaps, hydrogen bonding would be observed in the GFC arrays with any stationary phase to a varied extent suggesting that GPC (using an organic-based mobile phase) is more suitable for lignin MW determination. For the GDVB stationary phase, standards' retention could not be related to either their MW or pK_a (Fig. 3d, c), thus suggesting that other chemical factors, besides pK_a, contributed to the unwanted interactions on this column.

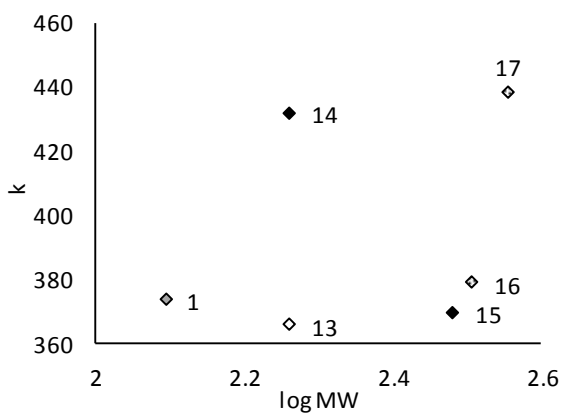
a) HPMA (Ultrahydrogel)



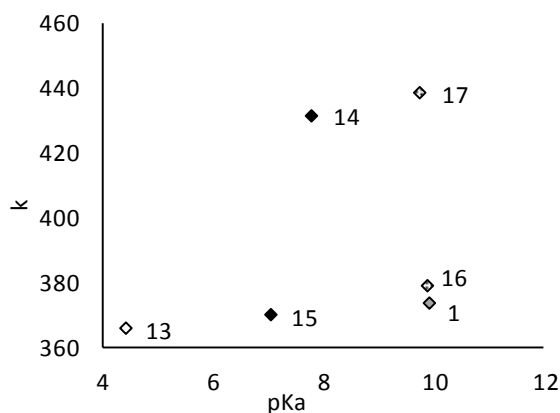
b) HPMA (Ultrahydrogel)



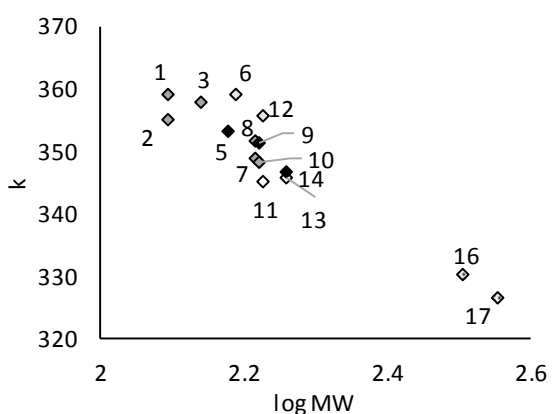
c) GDVB (Jordi Gel GBR)



d) GDVB (Jordi Gel GBR)



e) PSDVB (Agilent PLgel)



f) PSDVB (Agilent PLgel)

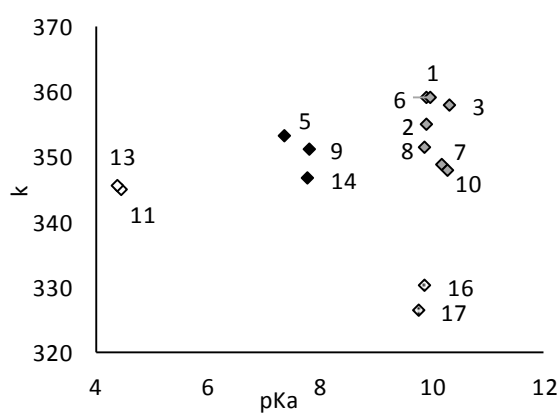


Figure 3. Relationship between the retention factor (k) of low-MW lignin model compounds in SEC on various stationary phases and a) the log MW on HPMA; b) the pK_a on HPMA; c) the log MW on GDVB; d) the pK_a on GDVB; e) the log MW on PSDVB; f) the pK_a on PSDVB.

Combined MW calibration curves obtained with both polymeric standards and low-MW lignin model compounds (Fig. 4) further support the suggestion made earlier that only the separation on the PSDVB stationary phase was not affected by secondary size-exclusion effects (Fig. 4b). Thus, this column was selected for lignin characterization. Furthermore, we have shown that despite the lack of the structurally similar polymer standards, both PS and PMMA standards may be used for accurate SEC column calibration and for validation of the suitability of the stationary phase.

Unexpectedly, all lignin model compounds were strongly retained on the GDVB phase beyond the size exclusion effect (Fig. 4a) even though the manufacturer specification suggests the application of this column for compounds with MW >50 Da. This observation corroborates the occurrence of other unwanted interactions.

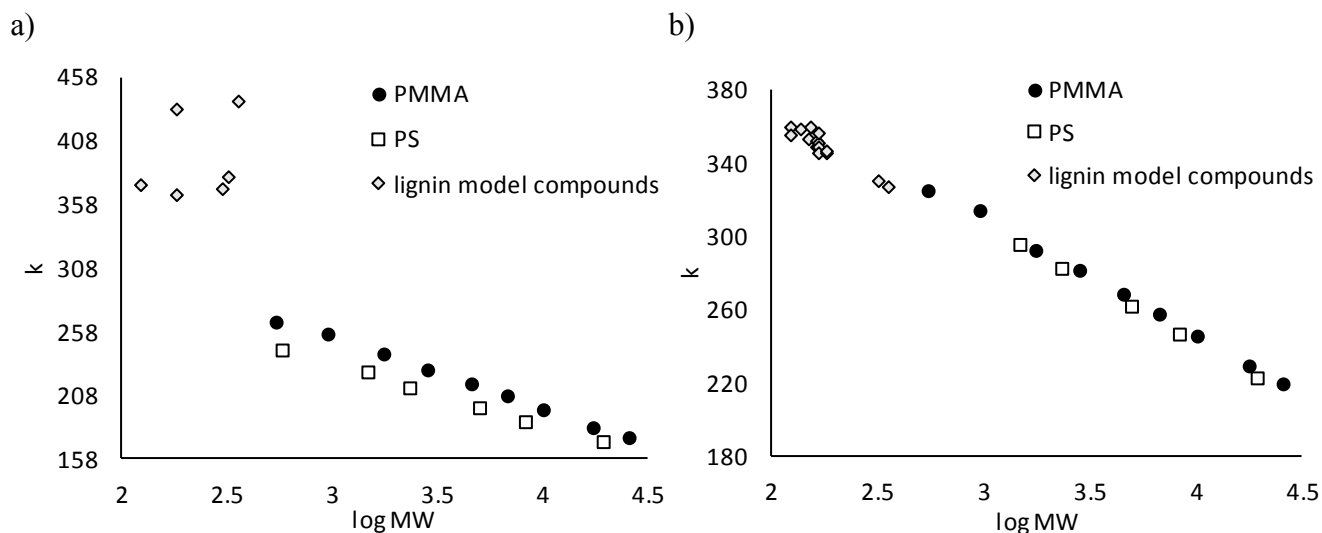


Figure 4. Retention factor (k) of low-MW lignin model compounds and polymeric standards as a function of $\log MW$ in GPC utilizing the columns with various stationary phase: a) GDVB, and b) PSDVB.

II.2.3. GPC Effect of the Pore & Particle Size

Further, we evaluated the effect of the stationary phase pore and particle size on the polymer separation with a focus on a narrower mass range, thus improving separation. Two commercially available columns with a PSDVB stationary phase were evaluated towards the separation of PS standards (Table 5 and Appendix A, Fig. A2): 1) The PLgel 1000 Å column (the separation range 500–60,000 Da) with 5 μm particle size; 2) The PLgel 500 Å column (the separation range 500–25,000 Da) with 10 μm particle size. The columns with a pore size of 500 and 1000 Å were selected, so the size exclusion separation range would encompass the anticipated lignin MW without exceeding it significantly, to avoid the loss of resolution.

In SEC, a smaller pore size would be expected to improve the separation in the given low MW range;^{31, 131} however the particle size might also affect the column performance, even though its effect had been downplayed in the prior SEC studies on lignin. It is apparent that the smaller particle size improved the resolution to a greater extent than the concomitant decrease of the pore size (Table 5). Presumably, the use of smaller particles contributed to a better and more homogeneous column packing resulting in faster diffusion kinetics, which overcame the thermodynamic limitations and provided a superior column performance.

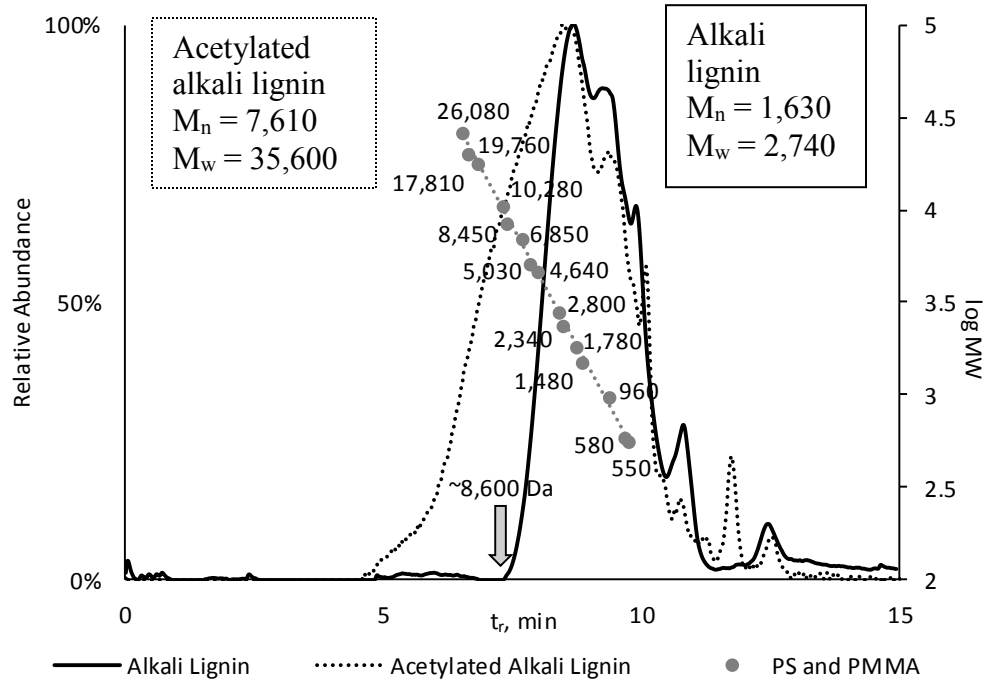
Table 5. Resolution of two PS standard peaks in SEC utilizing the columns with the PSDVB stationary phase, various particle and pore size.

MW of PS standards		Resolution	
Peak A	Peak B	10 μm , 500 Å (500–25,000 Da)	5 μm , 1000 Å (500–60,000 Da)
19,760	8,450	0.3	0.8
8,450	5,030	0.2	0.5
5,030	2,340	0.3	0.6
2,340	1,480	0.2	0.3
1,480	580	0.4	0.6

II.2.4. SEC of Alkali Lignin

Similarly to lignin model compounds and polymer standards, the PSDVB stationary phase appeared to be more suitable for characterization of alkali lignin (Fig. 5a). Based on the polymer standard calibration for this column, the elution profiles suggested an alkali lignin mass range between 100 and 8,600 Da (Fig. 5a) with an M_n of 1,630. A similar elution profile was observed for Indulin AT lignin (Appendix A, Fig. A3) with the determined M_n of 1,900, which is similar to the value reported by the manufacturer (Table 1). This is in contrast with the other evaluated stationary phase (GDVB), on which the alkali lignin sample eluted only after the last PS standard with an MW of 580 Da (Fig. 5b) incorrectly inferring the MW under 580 Da, which is a gross underestimate for intact lignin. This observation confirms the dependence of the GDVB-based separation on other interactions than those based on the size-exclusion effect, which is characteristic for standards (cf. Fig. 3c, d).

a) PSDVB stationary phase



b) GDVB stationary phase

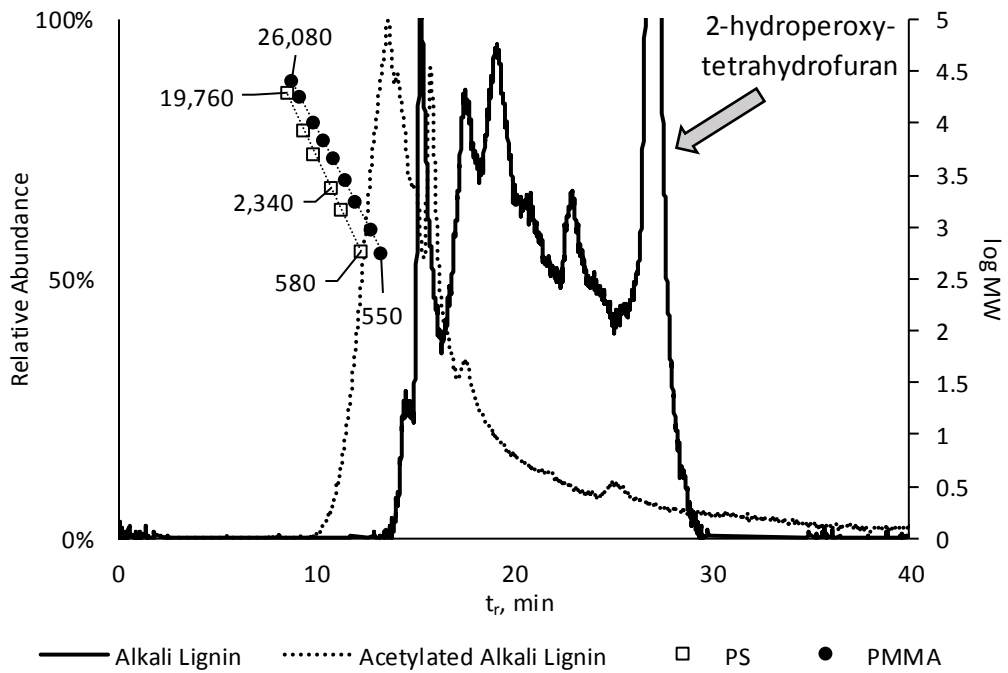


Figure 5. Intact and acetylated alkali lignin elution profiles utilizing various stationary phases: (a) PSDVB; (b) GDVB.

We also investigated the suitability of acetylation, which is frequently used to minimize possible analyte-column interaction through converting the polymer's interacting hydroxyl groups into more chemically inert acetoxy groups. Acetylation also allows for dissolving lignin in organic solvents, i.e., THF or DMF, if it was insoluble prior to the modification.¹⁹ While the acetylation resulted in earlier elution, the increase in retention times was not commensurate with the correct MW for all tested columns (Fig. 5).

Nevertheless, for the GDVB stationary phase (Fig. 5b), even the acetylated lignin eluted only with the PS and PMMA standards of the lowest MW (500–4,000 Da). Most probably the acetoxy and methoxy groups still affected the separation through their interaction with the stationary phase, perhaps, via hydrogen bonding, which is more likely to occur on the GDVB stationary phase due to the glucose rings bound to its surface than on the nonpolar PSDVB stationary phase.

For the GPC column with the PSDVB stationary phase (Agilent PLgel 1000 Å column), the acetylated lignin yielded the apparent masses over 26,000 Da, i.e., significantly higher than expected based on the reported data (*cf.* Table 1). In addition, an incomplete acetylation due to a different accessibility of hydroxyl groups resulted in a PDI increase from 1.7 to 4.7, thus suggesting a higher degree of heterogeneity for the acetylated polymer compared to intact lignin. This observation suggests that acetylation may complicate the determination of lignin MW or even skew the results since it strongly depends on the sample and leads to an unrealistic MW increase whose magnitude may be hard to predict.

To avoid the increase in lignin polydispersity and streamline the chromatographic analysis, our approach for dissolving lignin in THF-water solvents described in Section 2.2 appears to be a viable alternative eliminating the need for acetylation.

The calculated M_n and M_w values typically used for polymer characterization were determined for Indulin AT lignins. While the M_n value for Indulin AT lignin (1,900 Da) was similar to the value provided by the supplier (Table 1), the M_w was altered (3,060 Da vs. 6,900 Da), leading to the necessity of using other techniques such as MS for mass confirmation (shown in the next section). The M_w value provided by the manufacturer was determined utilizing a GFC system with an aqueous-based mobile phase, which might be affected by the undesired interactions with the column material, e.g., hydrogen bonding.

The obtained higher M_w of ~6,000 Da agrees with other recent studies including that observed with a lithium chloride/dimethylacetamide mobile phase, which corroborates the results reported by Sjöholm et al.¹³² A high PDI (10.0) was also recently reported for Indulin AT lignin by Hu et al.²³ using the SEC setup similar to that used in this study, i.e., PSDVB and THF as a stationary and mobile phases, respectively. Two GPC columns with lengths of 30 mm each were used in the study of Hu et al.,²³ whereas we utilized one 300 mm-long column with a 50 mm-long guard column. Thus the difference in PDI may arise from the batch-to-batch variation as well as the variation in the experimental setup: Increasing the column length enhances resolution.¹³¹ Although the M_w determined in this study was lower than suggested in several reports, it was similar to the M_w value for Indulin AT lignin determined by sedimentation equilibrium (3,500 Da)²⁶ The determined M_n value also matched that determined with vapor pressure osmometry (1,600 Da).²⁶

II.2.5. Lignin MW Determination by MALDI MS

To further evaluate the effectiveness of our GPC system for determining the lignin MW distribution, we employed MALDI MS as a reference technique, which was used earlier for

polymer MW determination.^{27, 51, 56, 57, 133-135} First, we evaluated the ionization efficiency with α -cyano-4-hydroxycinnamic acid and 2-(4-hydroxyphenylazo)benzoic acid used as matrices, and without a matrix (Appendix B, Fig. B1). The mass spectrum recorded with no matrix was of a higher clarity and showed well resolved peaks of higher intensity above 2500 m/z suggesting that the matrix structurally similar to lignin increases the background and complexity of spectra, perhaps, due to the undesirable association effects occurring during the sample co-crystallization with a matrix.⁵⁵ The recorded LDI mass spectrum (i.e., without a matrix) demonstrated several local maxima at 500, 1000, 2900, 4500 and 6200 m/z (Fig. 6). The signal decreased to the noise level at m/z values of 7000.

To be able to compare the MS data to SEC results, we adopted and simplified the approach toward a quantitative determination of the molecular mass distribution of synthetic polymers.¹³⁶ We calculated the M_n and M_w for alkali and Indulin AT lignin from LDI MS results using equations 1 and 2, where A_i was an ion abundance and M_i was the m/z value considering the predominant formation of single-charged species in MALDI. The obtained values were 830 and 840 Da and 1,250 and 1,220 Da for M_n and M_w , for alkali and Indulin AT lignin, respectively. Even though this calculation is not intended for evaluation of MS results, the LDI MS data agreed with the results obtained with GPC with a PSDVB stationary phase (Agilent PLgel 1000 Å), suggesting a lower lignin polydispersity and M_w values than those reported in literature.^{20, 21, 23} Some shift towards lower M_w for LDI MS compared to our SEC measurement may be due to suppression of ionization of larger species.

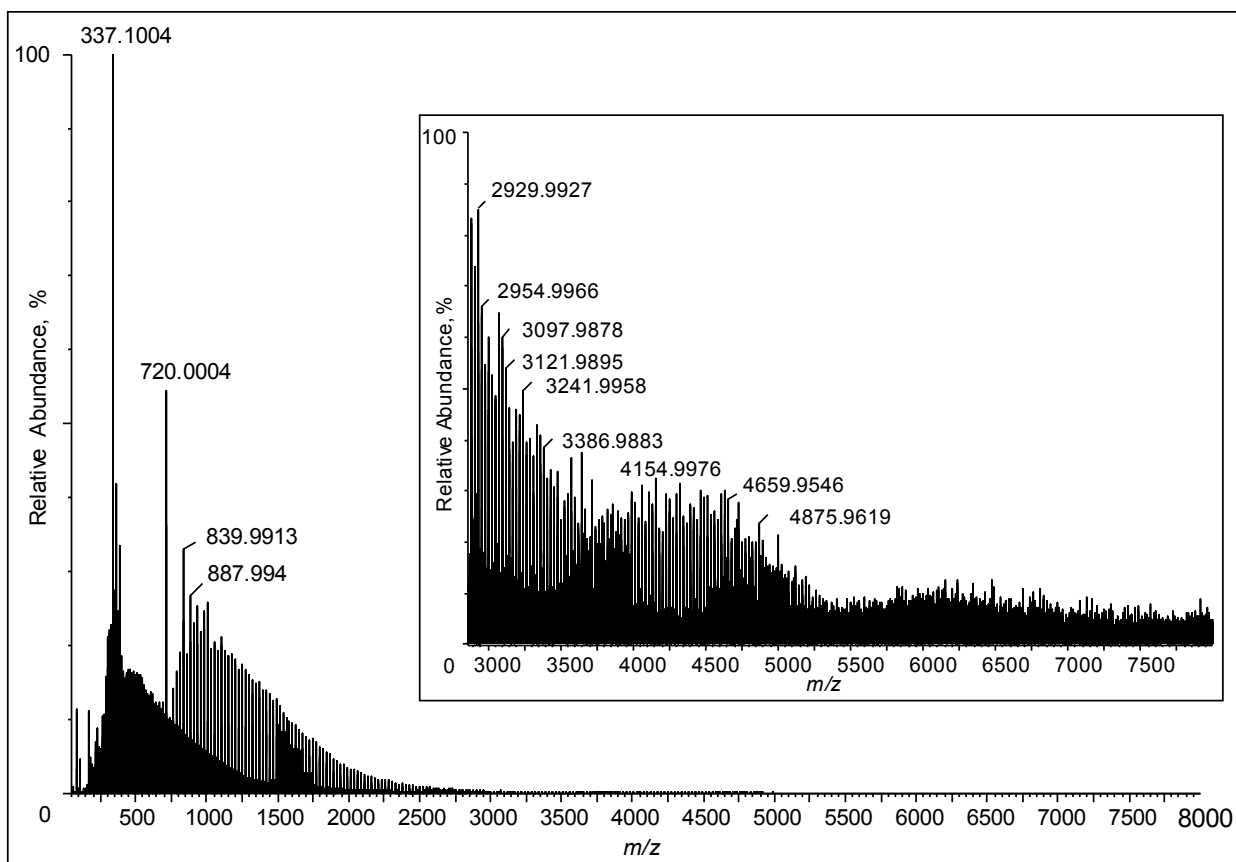


Figure 6. LDI (no matrix) HR TOF mass spectrum of alkali lignin. The insert shows a zoomed in part of the spectrum in the range 2800–8000 m/z .

II.2.6. RP HPLC C18 as a Complementary Method to SEC for Polymer Analysis

We have demonstrated that SEC could be strongly affected by the analyte's functionalities, which skewed the expected MW-based separation. To eliminate one of two interaction types, which occur simultaneously, i.e., the polarity-based and the size-based, we investigated a potential of RP HPLC separation. This project showed that the C18 column could be used for separating polymeric and low-MW model compounds based solely on their polarity (Appendix C, Fig. C2). Typically in SEC, polymers with a higher MW elute earlier. By contrast, in RP HPLC these polymers eluted later than the lower MW polymeric species because those with higher MW were less polar (Fig. 7a). We performed a successful separation of PEG standards with the MW up to

8,100 Da. This MW range was chosen based on the elution profile of alkali lignin and its MW values determined in the previous section.

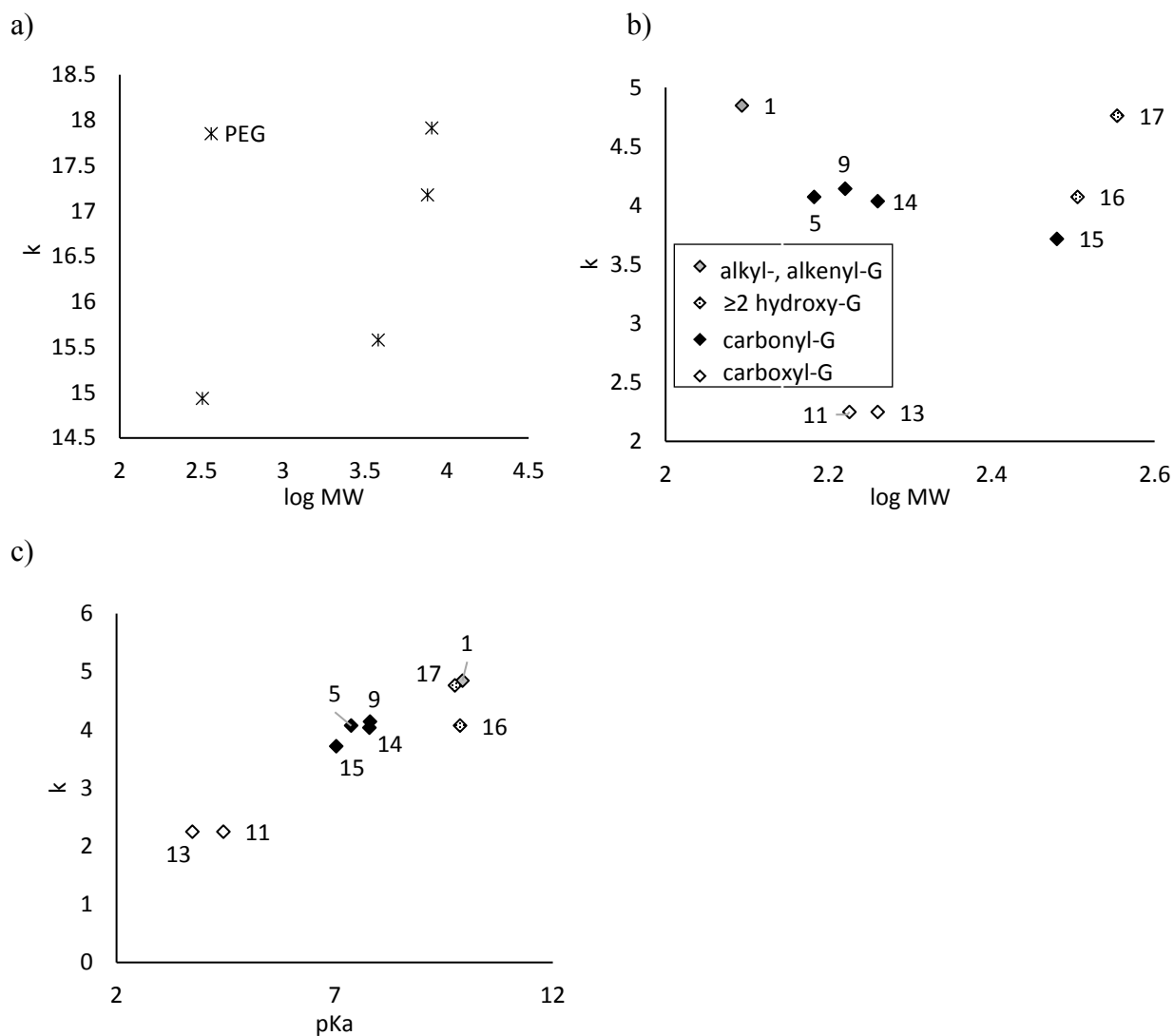


Figure 7. Correlation between the retention factor (k') of a) PEG standards and $\log MW$; b) low-MW lignin structure model compounds and $\log MW$; c) low-MW lignin structure model compounds and the pK_a in RP HPLC utilizing C_{18} column.

The retention of lignin structure model compounds in RP HPLC was not affected by the standards' MW, but was affected by their polarity (Fig. 7b, c). The elution order of the lignin standards depended on the pK_a values, i.e., polar compounds eluted first followed by less polar

standards as it was expected in RP chromatography (Fig. 7c). Thus, we tested the HPLC applicability for polymer analysis as a complement to SEC allowing one to obtain additional information on sample's polarity for a more comprehensive characterization. Application of RP HPLC for the assessment of lignin structural changes upon biomodification is shown in section V.1.2.2.

CHAPTER III. ATMOSPHERIC PRESSURE IONIZATION WITH HIGH-RESOLUTION MASS SPECTROMETRY AS A TOOL FOR LIGNOMICS

III.1. Experimental

III.1.1. Materials and Reagents

All standards used in this study as lignin model compounds are listed in Table 6, along with their acronyms, while details are provided in Appendix D, Table D1. Alkali lignin (CAS Number: 8068-05-1), cesium iodide (99.999%), ammonium acetate ($\geq 99\%$), sodium iodide (99.999%), lithium chloride (99.999%), lithium hydroxide (99.998%) and sodium hydroxide ($\geq 98\%$) were purchased from Sigma-Aldrich (St. Louis, Mo, USA). Ammonium hydroxide, trifluoroacetic, acetic and formic acids (puriss p.a., eluent additive for LC-MS) were obtained from Fluka.

MALDI matrices, i.e., 2-(4'-hydroxybenzeneazo)benzoic acid (HABA, $\geq 99.5\%$) and α -cyano-4-hydroxycinnamic acid (CHCA, $\geq 99\%$), were purchased from Sigma-Aldrich. HPLC-MS grade water, acetonitrile (ACN), unstabilized tetrahydrofuran (THF) and methanol (MeOH) were obtained from Fisher Scientific (Fair Lawn, NJ, USA). All chemicals were used as received, without further purification. Deionized water was obtained using a Direct-Q® 3 system, Millipore, Billerica, MA, USA.

Table 6. Lignin model compounds employed in ESI HR MS optimization.

Compounds	Acronym	Characteristic functionality ^a	MW (g·mol ⁻¹)	Supplier/Synthesized	Purity
Vanillin	V	Carbonyl	152.15	Sigma-Aldrich ^b	99%
Guaiacol	G	—	124.24	Sigma-Aldrich	98%
Eugenol	E	Alkenyl	164.20	Acros Organics ^c	99%
Vanillic acid	VA	Carboxyl	168.15	Fluka ^d	97%
Syringol	S	Methoxy	154.16	Acros Organics	99%
Homovanillyl alcohol	HA	Aliphatic hydroxyl	168.19	Sigma-Aldrich	99%
Veratrole	VER	—	138.16	Sigma-Aldrich	99%
Syringaldehyde	SA	Carbonyl	182.17	Sigma-Aldrich	98%
Pinoresinol	P2	Hydroxyl, methoxy	358.38	Sigma-Aldrich	≥95%
Guaiacylglycerol- β -guaiacyl ether	G- β -2	Aliphatic hydroxyl, methoxy, β -O-4	320.34	In-house synthesis based on ref. ^{126e}	≥95%
1,2-Dimethoxy-4-[(2-methoxyphenoxy)methyl]benzene	ET2	Methoxy, ether dimer	274.12	In-house synthesis based on ref. ¹³⁷	≥95%
4-(1-Hydroxyethyl)-2-methoxyphenyl benzoate	ALC2	Aliphatic hydroxyl dimer, ester	272.1	In-house synthesis based on ref. ¹³⁷	≥95%
4-Formyl-2-methoxyphenyl benzoate	EST2	Carbonyl, ester dimer	256.07	In-house synthesis based on ref. ¹³⁷	≥95%
(<i>E</i>)-4,4'-(Ethene-1,2-diyl)bis(2-methoxyphenol)	ALK2	Hydroxyl, methoxy, alkene dimer	272.10	In-house synthesis based on ref. ¹³⁷	≥95%
Dehydrodivanillin	D2V	Carbonyl, hydroxyl, methoxy, 5-5 dimer	302.07	In-house synthesis based on refs. ^{124, 125}	≥95%
4-[2-(3,4-Dimethoxybenzyl)-4,5-dimethoxybenzyl]-2-methoxyphenol and 1-(3,4-dimethoxybenzyl)-4,5-dimethoxy-2-[(2-methoxyphenoxy)methyl]benzene	ET3-1 ET3-2	Methoxy, ether trimer	424.19	In-house synthesis based on ref. ¹³⁷	≥95%

^a Functional groups and linkages (for oligomers) featured in the studied methoxyphenols compared to guaiacol

^b Sigma-Aldrich (St. Louis, MO, USA)

^c Acros Organics (Morris Plains, NJ, USA)

^d Fluka (Steinheim, Germany)

^e A detailed description of the synthetic procedures can be found elsewhere. ¹²⁷

Several dimeric lignin model compounds, i.e., D2V,^{124, 125} G- β -2,¹²⁶ ET2,¹³⁷ EST2,¹³⁷ ALC2,¹³⁷ ALK2,¹³⁷ and ET3¹³⁷ featuring different functional groups and linkages (Table 6) were synthesized according to the procedures published earlier, with an addition of column chromatography and recrystallization purification steps. A detailed description of the synthetic procedures can be found elsewhere.¹²⁷ These compounds were characterized by ¹H NMR, GC-MS and direct infusion ESI HR TOF MS.

Stock solutions of lignin mono-, di-, and trimeric standards were prepared in 50% MeOH/water with a final concentration of 100 ppm w/v. For intact lignin analysis, it was essential to dissolve the polymer while avoiding the use of aggressive solvents such as dimethyl sulfoxide or *N,N*-dimethylformamide. We have shown that alkali lignin may be completely dissolved in ACN-water (1:1) or THF-water (1:1) mixtures, with concentrations up to 10,000 ppm and 50,000 ppm (w/v), respectively. It is of note that neither pure organic solvents (ACN, THF) nor water dissolved any amounts of lignin to form a true solution. For direct infusion analysis of lignin, alkali lignin was completely dissolved in either water/ACN (1:1) or water/THF (1:1) at a final concentration of 100 or 1000 ppm, respectively. The solutions were diluted to a final lignin concentration of 80 or 90 ppm prior to the analysis. Neither of the utilized electrolytes caused lignin precipitation. All samples and stock solutions were stored in a refrigerator at 4 °C prior to analysis.

To address the solubility issue in THF, the effect of acetylation was evaluated.¹⁹ Acetylation of lignin samples was performed by a conventional method.¹²⁹ In brief, about 50 mg of the sample was completely dissolved in 500 μ L of dry pyridine and reacted with 500 μ L of acetic anhydride. The reaction mixture was stirred for 12 h at room temperature. Then, 200 μ L of methanol was added to the reaction mixture to terminate the reaction. Solvents were evaporated

under a stream of nitrogen and the residue was dried in a vacuum oven at 30 °C overnight. Acetylated lignin was completely dissolved in 5.5 mL of THF resulting in a 10,000 ppm w/v solution, which was further diluted with water/ACN (1:1) or water/THF (1:1) mixtures for the ESI TOF MS analysis.

III.1.2. MS Analysis: Ionization

An Agilent 6210 ESI HR TOF-MS system was used throughout the study for method development and parameter optimization. An initial optimization of MS conditions included selection of the ionization polarity, electrospray (e.g., capillary) and collision-induced dissociation (e.g., fragmentor) potentials, nebulization temperature, nebulizing gas flow rate and nebulization pressure. Samples were introduced via a direct infusion with a syringe pump at a flow of 5 $\mu\text{L}\cdot\text{min}^{-1}$ for the initial optimization. ESI potentials were optimized between 2000 and 5000 V. Nebulization pressure, gas flow and vaporizer temperature were varied between 18–40 psi, 4–12 $\text{L}\cdot\text{min}^{-1}$, and 250–400 °C, respectively. The full range of electrolytes specified in the Materials and Reagents section was evaluated. In the experiments involving THF, all PEEK tubings were replaced with stainless steel.

To optimize the electrolyte concentration, a flow injection analysis (FIA) was performed employing an Agilent 1100 Series HPLC. An aliquot (20 μL) of the prepared solution was injected into a mobile phase consisting of 50% ACN or MeOH in water at a flow rate of 0.2–1.0 $\text{mL}\cdot\text{min}^{-1}$ and delivered directly to the TOF-MS system (no LC column was installed). In this study, we optimized the electrolyte concentration in the mobile phase by doping it only into the sample as we did previously in our work.¹³⁸ We experimentally confirmed that the final electrolyte concentration in the mobile phase after the injection of an electrolyte-doped sample remained the same (Appendix E, Table E1).

The TOF-MS system was calibrated with an ESI (50–3500 m/z) tuning mixture purchased from Agilent. For higher m/z measurements (i.e., analysis of intact lignin in a range of 150–10,000 m/z), the calibration was performed in the positive mode while using $[(\text{CsI})_n + \text{Cs}]^+$ clusters formed by an introduction of cesium iodide [30 mmol·L⁻¹ solution in ACN/water 1:1 (v/v)] via direct infusion at a flow rate of 5 $\mu\text{L}\cdot\text{min}^{-1}$ (Appendix F, Fig. F1). Agilent 6560 IM Q-TOF system equipped with an ESI source was used to acquire IM mass spectra under the optimized conditions determined with 6210 TOF MS system.

A MALDI SYNAPT G2-Si MS System was employed to acquire MALDI MS spectra in the range 50–8000 m/z . The best ionization effectiveness was achieved when no matrix was used. More details on the ionization conditions are provided in section II.2.5.

III.1.3. MS Characteristics and Data Processing

The 6210 HR TOF-MS system with a mass resolution of $>13,000$ (at m/z 2,722) and mass accuracy <2 ppm (m/z 609.2807) was utilized. A 6560 IM Q-TOF MS system used for IM mass imaging had a resolution of $>42,000$ (at m/z 2,722) and mass accuracy <2 ppm. The resolving power of SYNAPT G2-Si MS system was 50,000 and the mass accuracy was under 1 ppm.

Mass Hunter software packages, B.02.00 and B.07.00, were used for data processing. The spectra of intact lignin recorded in the positive mode, which included multiply charged ions, were deconvoluted using a built-in tool utilizing an unbiased isotope model with a peak spacing tolerance of 0.0025 m/z . The maximal assigned charge state was not limited. Both hydrogen and sodium were considered as the charge carriers. The peaks selected for deconvolution were filtered based on their absolute height (≥ 100 counts) and the relative height of the largest peak, which was set to $\geq 0.1\%$ of the largest peak unless otherwise stated. The maximum number of peaks was not specified.

Equation 3 was used for the MW (M) calculation of the multiply charged species:

$$\frac{m}{z} \cdot z - [(atomic\ mass\ of\ charge\ carrier\ (H^1\ or\ Na^{23}) - electron\ rest\ mass) \cdot z] = M, Da \quad (3)$$

An open source alternative software for mass spectrometric data analysis *mMass* Data Miner¹³⁹ was used for MALDI data processing.

To qualitatively assess the MW distribution of lignin utilizing the MS data, we applied an approach used in our previous work for MALDI MS data interpretation.¹⁶ To calculate the number average (M_n), weight average (M_w) and z-average (M_z) MW of lignin samples, equations 4–6, where I_i is the absolute abundance of the deconvoluted species of a given MW (M_i), were used.

$$M_n = \frac{\sum I_i M_i}{\sum I_i} \quad (4)$$

$$M_w = \frac{\sum I_i M_i^2}{\sum I_i M_i} \quad (5)$$

$$M_z = \frac{\sum I_i M_i^3}{\sum I_i M_i^2} \quad (6).^{130}$$

III.2. Results and Discussion

The intermediate products of lignin degradation, i.e., lignin mono- to oligomeric standards, appear to be suitable model compounds for understanding the ionization mechanism of intact and degraded lignin.⁶² Based on the information on electrolyte selection obtained in previous studies,^{59, 62, 66, 67, 77} we first investigated the effect of a broader range of electrolytes and optimized the ESI and APCI TOF MS ionization conditions. This was followed by narrowing the range of electrolytes while assessing the ionization of eleven mono-, di- and triarene lignin model compounds featuring different oxygenated functional groups and linkages typical for lignin and then expanded the method to native lignin.

III.2.1. Electrolyte Screening: Effect on the Representative Model Compounds in ESI

We optimized the ESI TOF MS ionization targeting a broad range of electrolytes using two representative dimers as model compounds (Fig. 8). Two dimers, G- β -2 and ET2, were selected for this initial screening, the former featuring both aromatic and aliphatic hydroxyl groups, while the latter does not have any hydroxyl groups. Both of these standards exhibited the most efficient ionization while forming sodium adducts in the positive mode in the presence of formic or acetic acids at $\leq 10 \text{ mmol}\cdot\text{L}^{-1}$ concentration (Fig. 8).

A preferable ionization of ET2 in the positive ESI mode was expected, due to the lack of hydroxyl groups in its structure. For the hydroxylated compound G- β -2, contrary to expectations, the ionization efficiency improved in the positive ESI mode resulting in an abundant sodium adduct ion (Fig. 8a). The formation of sodium adduct ions even when sodium was not purposely added to the samples is known to occur because of traces of sodium leaching from glassware.¹⁴⁰

An effective ionization was also observed with no electrolyte present (Fig. 8a), the feature frequently observed in ESI TOF MS.¹⁴¹ However, these conditions were deemed to be non-optimal as the lack of a buffer could result in pH instability and consequently cause the dependence of ionization on the sample composition and, as a result, irreproducible data.¹⁴¹

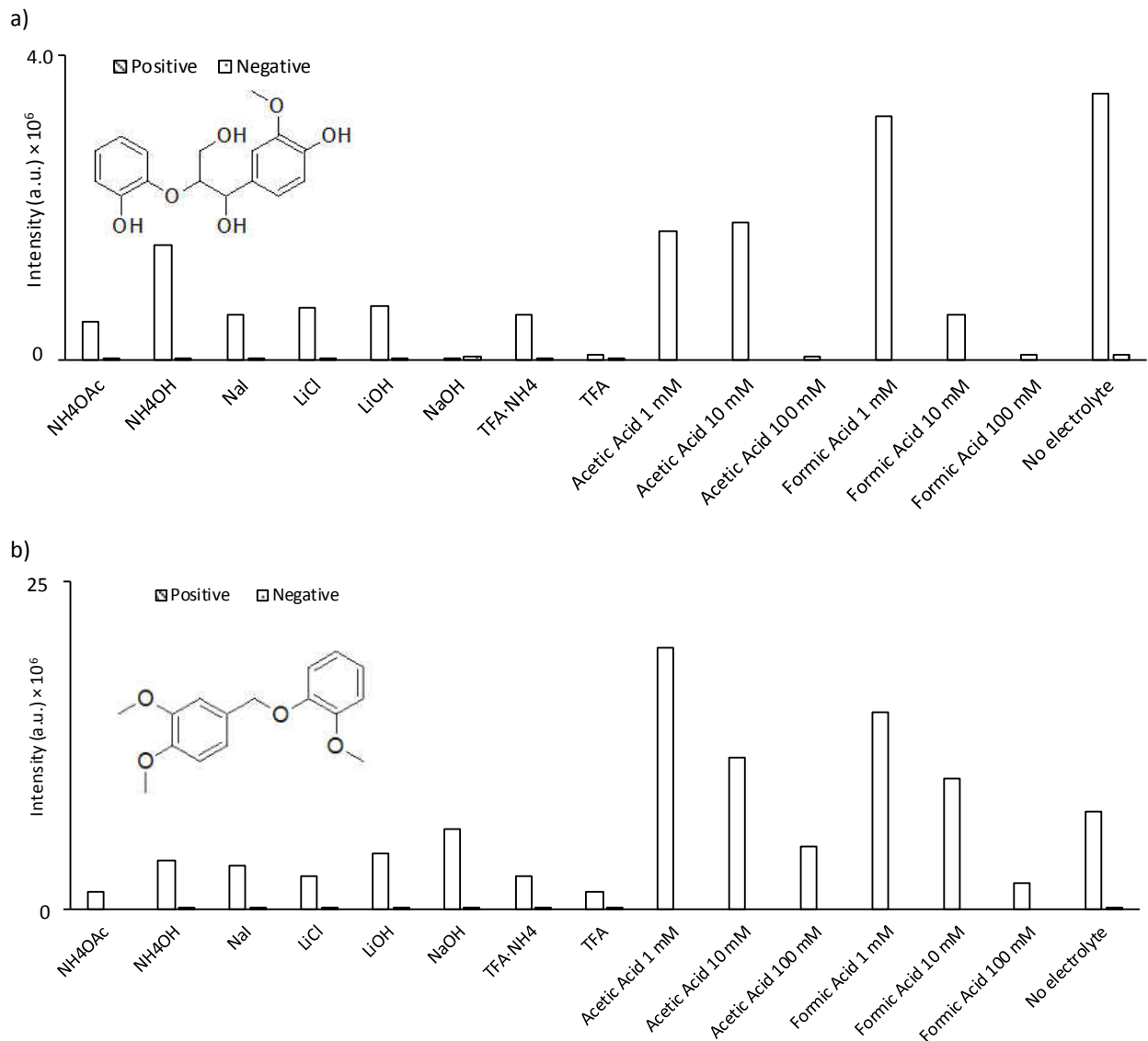


Figure 8. ESI TOF MS response obtained in the presence of different electrolytes via a direct infusion for two representative dimers (a) G-β-2; (b) ET2 in the positive and negative ionization modes. For most of the electrolytes used, the response for $[M+Na]^+$ and deprotonated molecular ions is shown, except for LiCl and LiOH whose application resulted in the formation of $[M+Li]^+$. The electrolyte concentration was $1.0 \text{ mmol} \cdot \text{L}^{-1}$ unless specified otherwise.

Sodium hydroxide, which was previously claimed as an effective ionization agent for lignin model compounds in both positive and negative ESI modes,⁷⁷ did not promote the formation of sodium or protonated adducts for G-β-2 as much as the majority of other evaluated electrolytes (Fig.8a). Moreover, in contrast to the previous work,⁷⁷ excessive fragmentation was observed in

the presence of sodium hydroxide in the positive (Fig. 9c) and negative modes, whereas a “clean” mass spectrum was obtained when either ammonium acetate or acetic acid were used (Fig 9a, b). Perhaps, the reason for a different fragmentation pattern upon ionization of G- β -2 was a varied stability (fragmentation) of ions in different mass analyzers used in previous studies, as Hauptert et al.⁷⁷ utilized a linear quadrupole ion trap MS whereas in our study we used TOF.

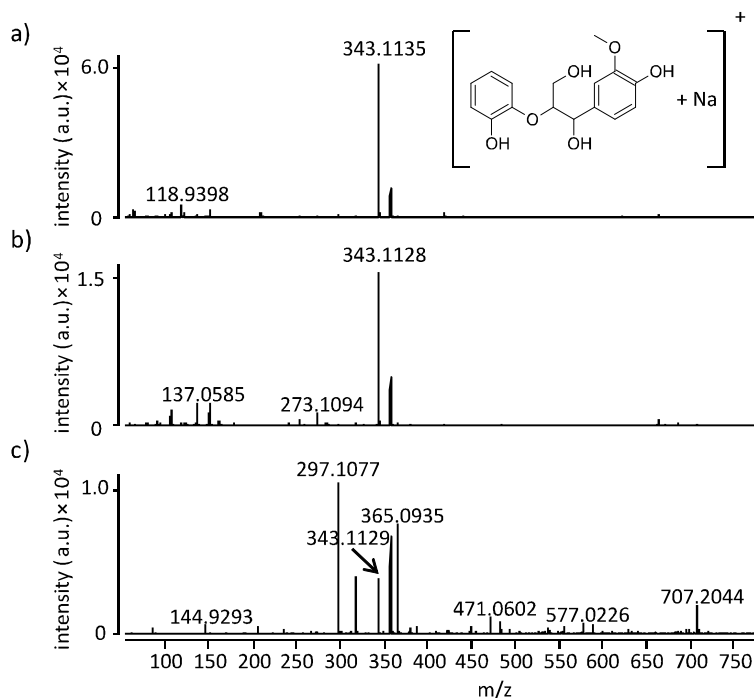


Figure 9. Positive ESI TOF mass spectra of 5 ppm G- β -2 ($[M+Na]^+$ 343.1152 m/z) in the presence of 1.0 $\text{mmol}\cdot\text{L}^{-1}$ of a) ammonium acetate (mass accuracy error 5 ppm); b) acetic acid (mass accuracy error 7 ppm); and c) sodium hydroxide (mass accuracy error 6.7 ppm).

III.2.2. Impact of Oxygenated Functional Groups on ESI Ionization

Based on the screening experiments (*cf.* Fig. 8), formic and acetic acids appeared to be the most efficient electrolytes. Thus, we compared these acids to frequently used ammonium acetate,¹⁴² to evaluate the impact of these electrolytes on the ionization effectiveness of a broader suite of mono-, di- and triarene lignin model compounds featuring different linkages and functional groups (Table 6), and investigated the contribution of various oxygenated functional groups: The results are shown in Table 7. Contrary to the previously preferred negative ionization mode,^{62, 63} we showed ionization of all considered compounds (with hydroxyl, methoxy and carboxyl groups) in the positive ESI mode with both formic/acetic acids and ammonium acetate, although some selectivity toward specific oxygenated functional groups was observed.

The compounds *without* phenolic hydroxyl groups, with multiple *methoxy* groups, or with *aliphatic* hydroxyl groups, were preferentially ionized in the positive mode (the upper portion of Table 7) corroborating the results obtained earlier for non-acidic lignin model compounds.^{77, 143} Thus the positive ESI mode is preferable as similar structural features, i.e., prevailing methoxy over phenolic hydroxyl functional groups, are also characteristic for alkali lignin (4.6 vs. 3.6 moles/1,000 g as claimed by the supplier).

While both electrolyte systems seemed to show satisfactory performance, acids were more effective for the majority of species with no hydroxyl groups and prevailing methoxy groups (Table 7). It is of note that some of the standards showed low response or could not be detected in the negative ESI mode at all, e.g., VER, EST2, ET2, ET3-1, SA, ET3-2, P2, G- β -2). This could perhaps be explained by the absence of hydroxyl groups or their steric hindrance (the structure motifs occurring in these molecules are shown in Table 6). For example, in case of syringaldehyde

(SA) two MeO groups in the *ortho*-position to the hydroxyl moiety made the deprotonation of these compounds difficult.

Highly hydroxylated monomeric phenolic standards with no more than one methoxy group (the bottom portion of Table 7), those containing *carboxyl* groups as well as other compounds of high *acidity* such as VA, V and D2V, showed a higher ionization efficiency in the negative mode, as expected (Table 7). Nevertheless, as mentioned above, such a high ratio of hydroxylation/methoxylation is not characteristic for intact lignin and thus does not seem to be suitable for selection of ionization conditions.

Table 7. ESI TOF MS response with acids (either formic or acetic) and ammonium acetate as ESI electrolytes for representative lignin mono- to trimeric structure model compounds in both positive and negative ionization modes^a

Model Compounds	Numbers of Oxygenated Functional Groups			pK _a	Intensity of the Target Ion Response			
	-OH	-OCH ₃	-COOH		Acid (Formic/Acetic)		Ammonium Acetate	
					Positive	Negative	Positive	Negative
VER	0	2	0	-	++++ ^b	ND ^c	+++	ND
EST2	0	1	0	-	++++	ND	++++	ND
ET2	0	3	0	-	++++	ND	+++	ND
ET3-1	0	5	0	-	++++	ND	+++	ND
ET3-2	1	5	0	-	++++	+	+++	+
P2	2	2	0	9.76	++++	+	+++	+
G-β-2	1 +2 aliphatic	2	0	9.88	++++	+	+++	+
HA	1 +1 aliphatic	1	0	10.19	+++	+	++++	++
ALC2	1 aliphatic	1	0		+++	+	++++	++
S	1	2	0	9.98	++	+++	++++	+
SA	1	2	0	7.8	+++	+	++++	++
VA	1	1	1	4.45	++	+++	+	++++
V	1	1	0	7.38	+	+++	++	++++
D2V	2	2	0	7.04	++	+++	+	++++
G	1	1	0	9.93	++	+++	+	++++
E	1	1	0	10.19	+	++++	+	++++

^a For the majority of analytes, the response was monitored for [M+Na]⁺ and [M-H]⁻ ions in the positive and negative ionization modes, respectively. The electrolyte concentration upon direct infusion was 2.5 mmol·L⁻¹.

^b “++++” indicates the system resulting in the most efficient ionization; “+” indicates the system with the least efficient ionization.

^c “ND” denotes no molecular ions or adducts were detected.

III.2.3. Ionization of Lignin Model Compounds by APCI TOF MS

We also evaluated the applicability of APCI to the analysis of lignin model compounds since this ionization technique was previously reported for the analysis of lignin oligomeric model compounds.^{60, 61, 77} The negative ionization mode in APCI was found to be more efficient than the positive one for the same standards, for which negative ESI was preferable, i.e., D2V, V, VA and G (Fig. 10). Ammonium acetate concentration did not affect the ionization efficiency, which was expected for APCI since ionization primarily occurs in the gas phase. Nevertheless, elevated acid concentrations resulted in the APCI ionization suppression in a similar manner as in ESI.

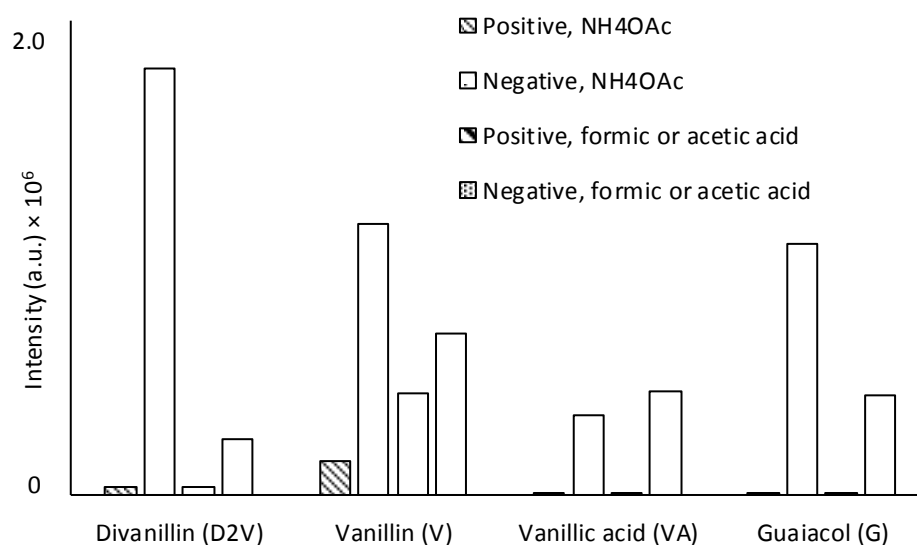
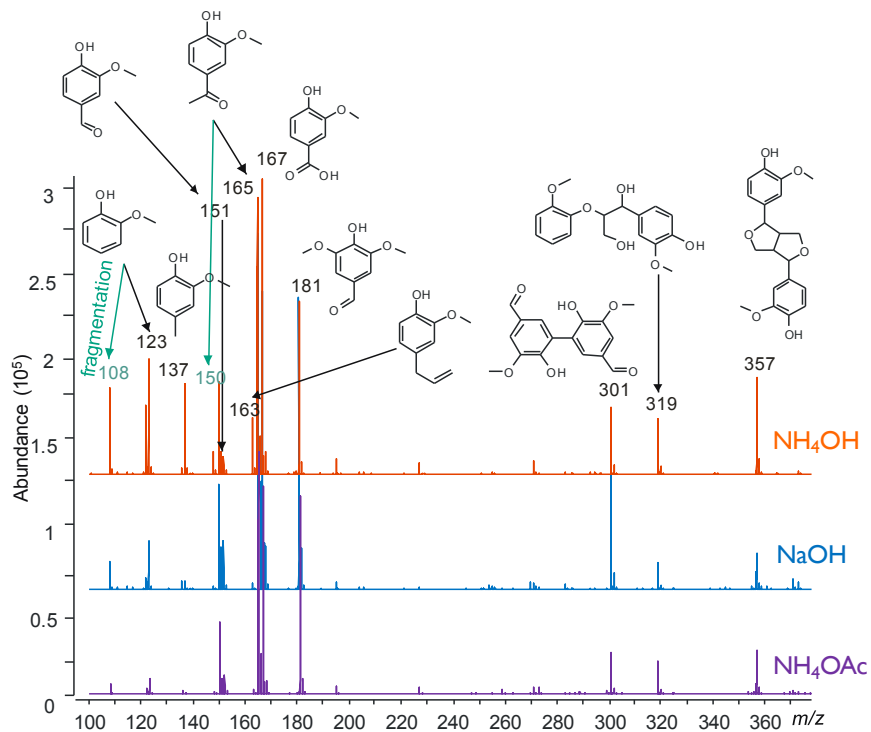


Figure 10. Ionization efficiency of lignin model compounds by APCI TOF MS.

A comparison of the ESI and APCI mass spectra obtained for a mixture of monomeric and dimeric standards upon direct infusion (Fig. 11) showed that in contrast to the reported work⁷⁷ APCI in the negative mode could be potentially applicable for smaller molecule determination, i.e. monomeric species, without an excessive fragmentation and the results were similar to the negative ESI. However, ionization by APCI became hindered for the dimeric species (D2V and G- β -2) (m/z

301 and 319 in Fig. 11). Thus, negative APCI TOF MS could be used for a targeted analysis of monomeric lignin species in mixture, for instance, formed upon degradation and preliminary separated from higher MW degradation products. However, this method is not a method of choice for analysis of mixtures of degradation products or intact lignin itself due to the excessive fragmentation of larger species and a limited by 1,000 m/z range. Therefore, ESI TOF MS rather than APCI TOF MS was considered as a method of choice for analysis of complex mixtures of lignin mono- and oligomeric model compounds and intact lignin.

a)



b)

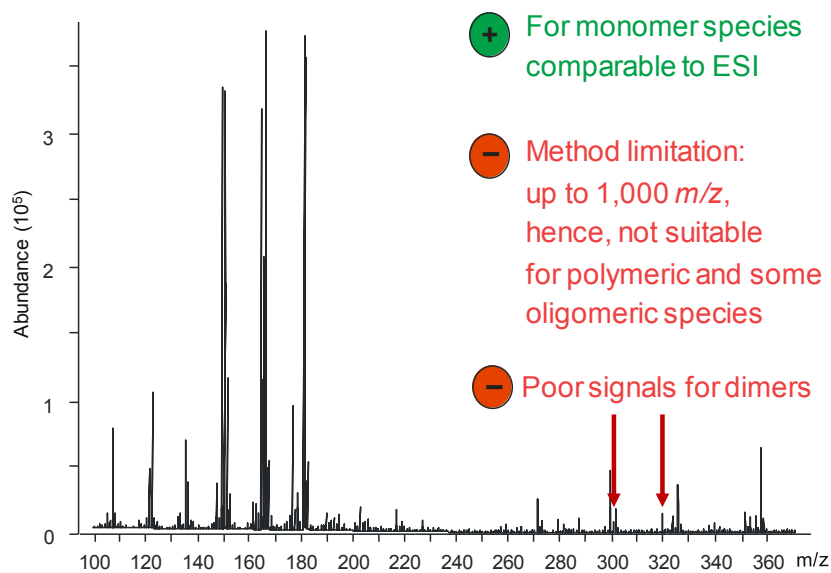


Figure 11. Comparison of mass spectra recorded upon utilizing a) ESI and b) APCI ionization sources in the negative mode.

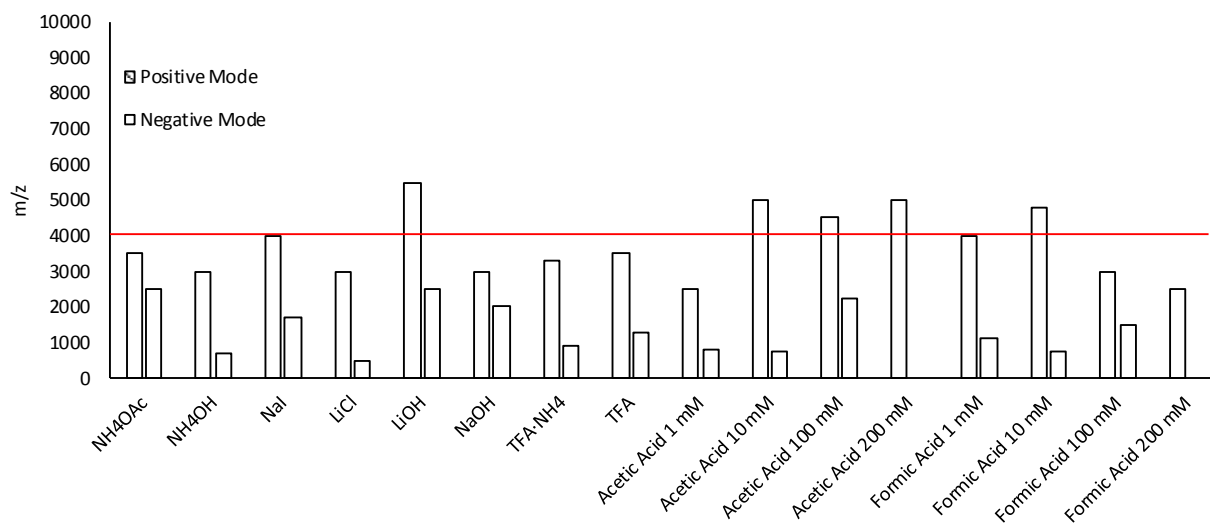
III.2.4. Lignin ESI: Electrolyte Selection

Similarly to lignin model compounds, electrolyte screening was performed for efficient ionization of lignin itself over a broad range of commonly used salts and acids in both the positive and negative modes. The urgent goal was to ensure an effective ionization of higher MW species forming high m/z ions (Fig. 12). Formic acid at its highest concentrations of 100 and 200 mmol·L⁻¹ in the positive ESI mode enhanced the formation of multiply charged species. Following the deconvolution (as explained in the next section), this protocol allowed for detecting the masses of up to 9,000 Da (Fig. 12b).

Under these conditions, the ionization of lower MW lignin model compounds was somewhat suppressed, yet sufficient for their effective detection (*cf.* Fig. 8), thus providing more balanced mass spectra.

Since acetylation is used in a number of studies to enhance lignin's solubility, we investigated its ESI ionization as well. Similar to intact lignin, the positive mode was preferred for derivatized lignin when the hydroxyl groups were substituted with acetyloxy (CH₃COO⁻) groups (Fig 12c). Lignin acetylation prevented a facile deprotonation in the negative mode (Fig. 12c). The acetylated lignin spectrum also featured multiply charged species allowing for subsequent deconvolution (Fig. 12d).

a) Intact alkali lignin. The highest observed m/z prior to deconvolution.



b) Intact alkali lignin. The highest MW (Da) after deconvolution of the mass spectra.

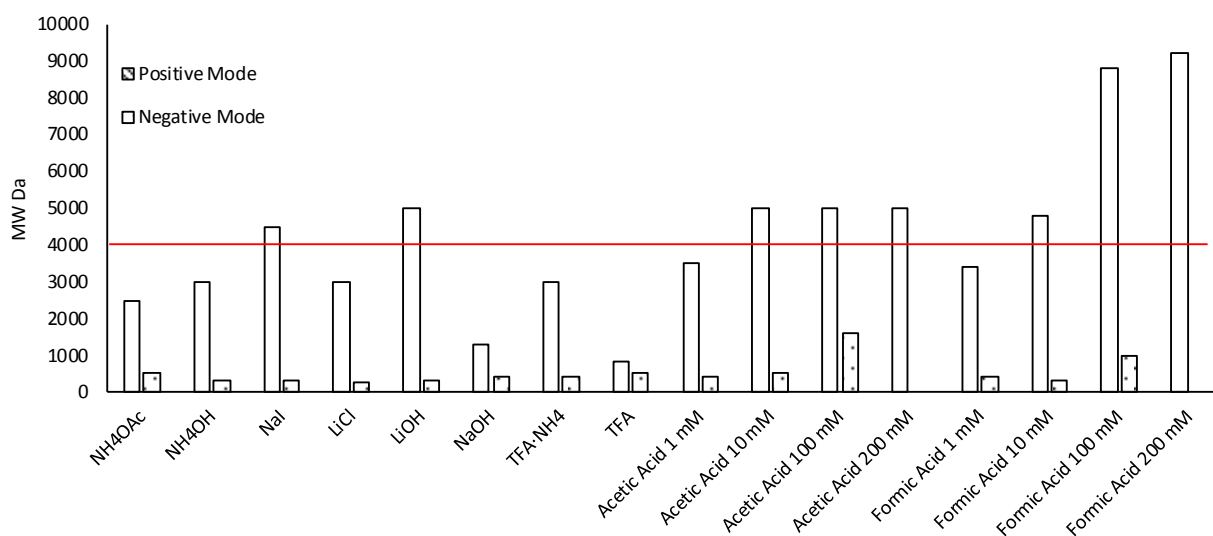
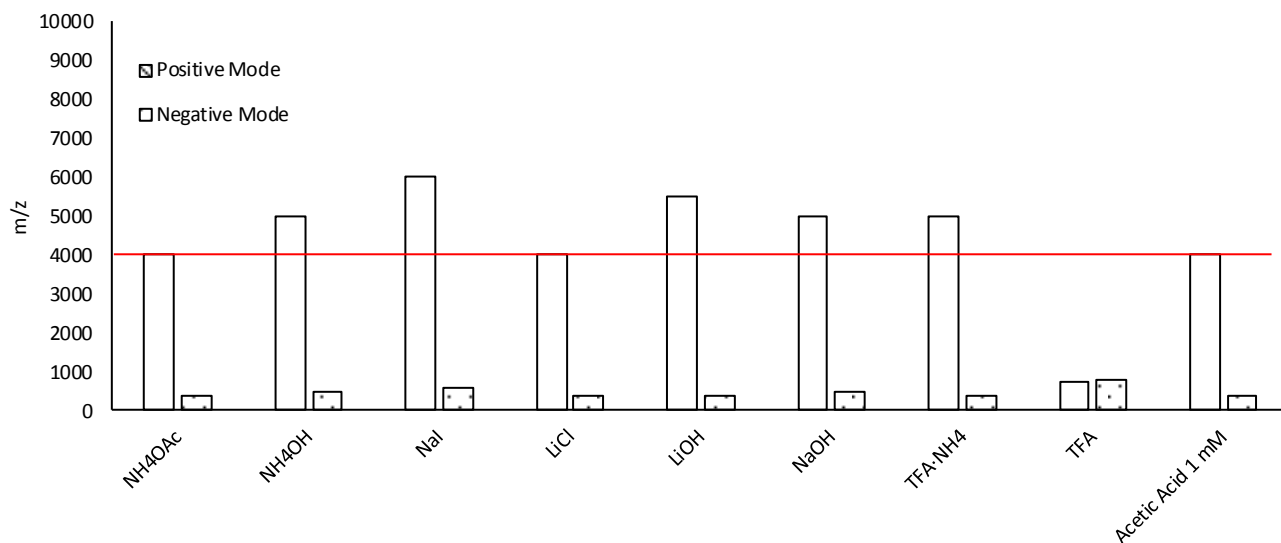


Figure 12. The highest mass-to-charge (m/z) values of the ions detected in the mass spectrum of (a) 15–90 ppm intact alkali lignin and (c) 15 ppm acetylated alkali lignin dissolved in ACN-water 1:1 in the positive and negative ionization modes while using different electrolytes; MW (Da) obtained after spectrum deconvolution of (b) 15–90 ppm intact alkali lignin and (d) 15 ppm acetylated alkali lignin. An electrolyte concentration was $1.0 \text{ mmol} \cdot \text{L}^{-1}$ unless specified otherwise.

Figure 12 cont.

c) Acetylated alkali lignin. The highest m/z prior to deconvolution.



d) Acetylated alkali lignin. The highest MW (Da) after deconvolution of the mass spectra.

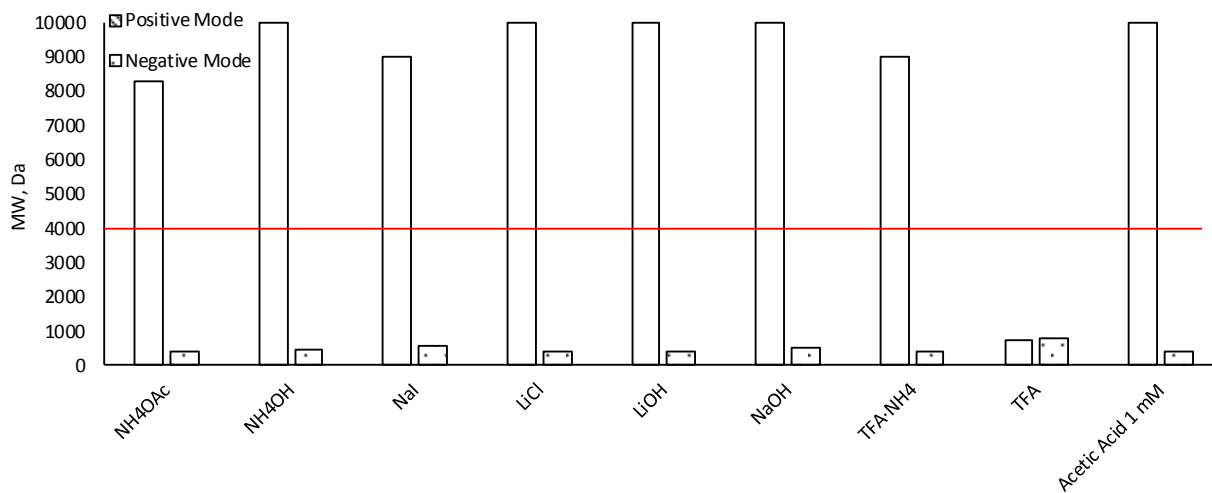


Figure 12. The highest mass-to-charge (m/z) values of the ions detected in the mass spectrum of (a) 15–90 ppm intact alkali lignin and (c) 15 ppm acetylated alkali lignin dissolved in ACN-water 1:1 in the positive and negative ionization modes while using different electrolytes; MW (Da) obtained after spectrum deconvolution of (b) 15–90 ppm intact alkali lignin and (d) 15 ppm acetylated alkali lignin. An electrolyte concentration was $1.0 \text{ mmol} \cdot \text{L}^{-1}$ unless specified otherwise.

III.2.5. Lignin ESI: Mass Spectrum Deconvolution

ESI of lignin in the positive mode in the presence of 100 mmol·L⁻¹ formic acid allowed for minimizing the ionization discrimination. Thus, lower MW species were mainly observed as singly charged ions, whereas high MW lignin constituents carried multiple charges. For example, vanillin was detected as a singly charged ion of 153.0570 *m/z* (protonated adduct [C₈H₈O₃+H]⁺, 16 ppm mass accuracy error) (Fig. 13a). The corresponding deconvoluted species possessed a mass of 152.05 Da (Fig. 13b) calculated based on equations 3 and 7, which was equal to vanillin's MW.

$$153.0570 \cdot 1 - [(1.007825 - 0.000549) \cdot 1] = 152.05 \text{ Da} \quad (7)$$

High MW species were predominantly observed as multiply charged ions, for example the 597.2073 *m/z* ion carried a charge of +7 (the spectrum is shown in Fig. 13c). The mass spectrum deconvolution resulted in a calculated MW of 4173.40 for the corresponding species (equation 8), the spectrum is shown in Fig. 13d.

$$597.2073 \cdot 7 - [(1.007825 - 0.000549) \cdot 7] = 4173.040 \text{ Da} \quad (8)$$

It is of note that the mass spectra prior to and after deconvolution did not depend on the utilized solvent system, thus, the spectra recorded in a THF-water 1:1 (v/v) mixture (Appendix G, Fig. G1) were similar to mass spectra observed in ACN-water (Figs. 13e, f).

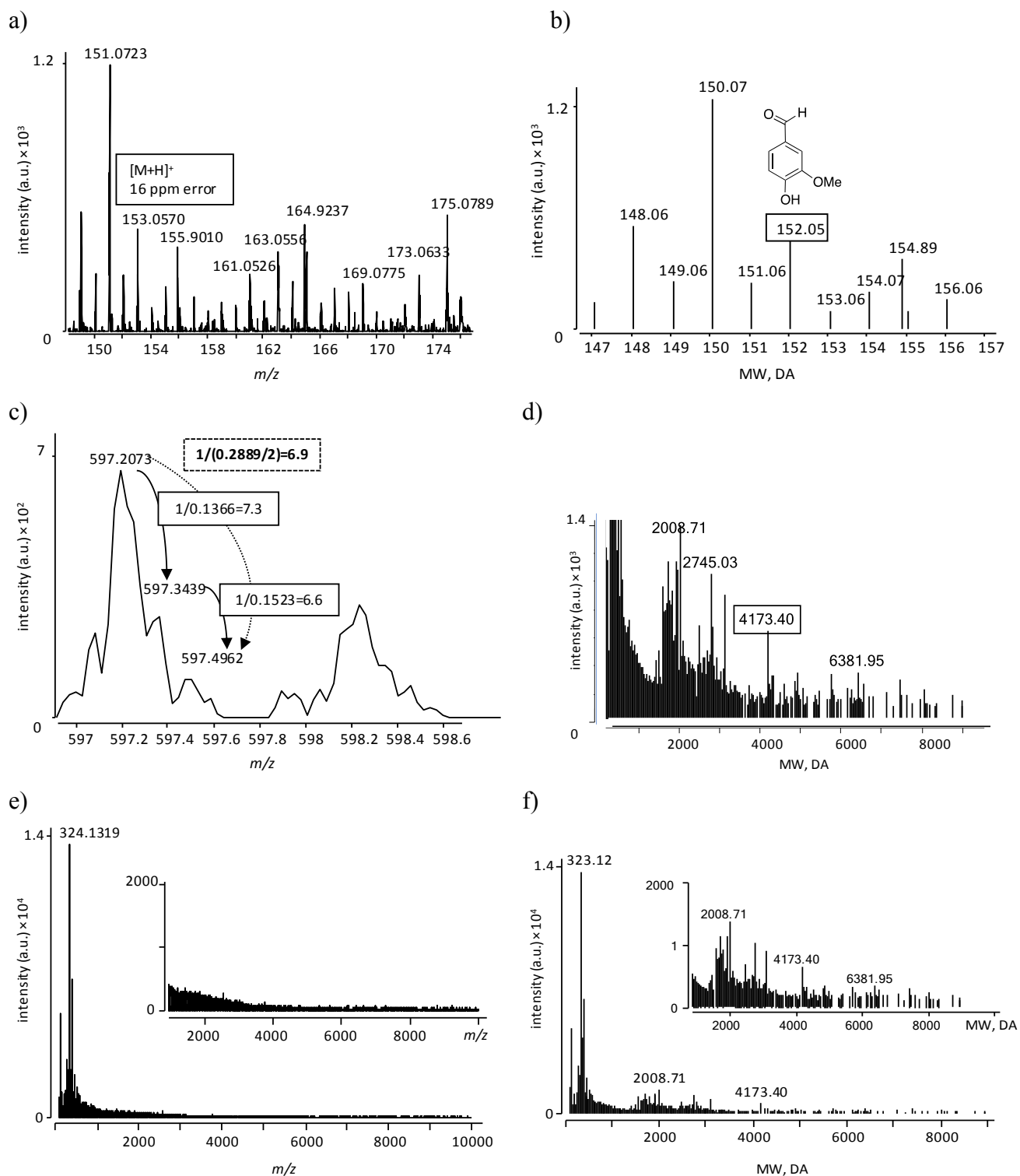


Figure 13. Positive ESI HR TOF mass spectra of an 80 ppm solution of intact lignin in ACN-water (1:1) with 100 mmol·L⁻¹ formic acid: a), c) and e) zoomed and full original mass spectra; b), d) and f) zoomed and full mass spectra after deconvolution.

Thus, analysis of lignin under the suggested ESI conditions allowed for a simultaneous determination of lignin constituents varying in size and structure via direct infusion analysis with minimal sample preparation. An introduced feature of the multiply charged ion formation allowed for an efficient ionization of high MW lignin species, which, to our knowledge, was not previously reported. This approach is an essential contribution to the lignomics toolkit allowing for analysis of higher MW species, as shown in the next section.

III.2.6. Lignin MW Determination by ESI HR TOF MS

To assess lignin MW, we previously adapted an approach from NIST¹³⁶ employing equations 4–6 to the deconvoluted spectral data.¹⁶ This calculation is typically used for evaluating GPC data rather than MS, yet, the obtained values, 1,480 Da, 2,520 Da and 3,790 Da for M_n , M_w and M_z , respectively, were in good agreement with the MW values determined earlier by GPC (Table 8).¹⁶ Interestingly, similar MW values were determined for acetylated lignin, i.e., 1,570 Da, 2,440 Da and 3,530 Da for M_n , M_w and M_z , respectively. This could be explained either by fragmentation with the loss leaving the most abundant molecular ions as ions $[M-CH_3CO^+]$ or incomplete acetylation of lignin due to sterical hindrance, thus still detecting mostly intact lignin. In either case, it appears that the acetylated lignin MS data could also serve for the MW determination of the original, native lignin without a typical mass correction on acetylation.

Table 8. Number-average, weight-average and z-average molecular weight of lignin determined by ESI HR TOF MS, GPC and MALDI HR TOF MS.

	ESI HR TOF MS	GPC ¹⁶	MALDI HR TOF MS
M_n	1,480	1,630	830
M_w	2,520	2,740	1,250
M_z	3,790	3,720	2,230

III.2.7. Ionization: MALDI HR TOF MS vs. ESI HR TOF MS

Similar mass spectra of intact lignin were recorded with MALDI and ESI as ionization sources (compare Fig. 13 to Fig. 6 in section II.2.5). MALDI MS was selected as a reference technique frequently used for polymer MW determination.^{27, 51, 56, 57, 133-135} To achieve the optimal lignin ESI, we evaluated the ionization efficiency with CHCA and HABA matrices and also without a matrix (Appendix B, Fig. B1). The mass spectrum recorded with no matrix was of higher clarity, showing well resolved peaks of higher intensity above 2500 m/z . Apparently, the matrix structurally similar to lignin increased the background and complexity of spectra, perhaps, due to the undesirable association effects occurring during the sample co-crystallization with a matrix.⁵⁵ The recorded LDI mass spectrum (i.e., without a matrix) demonstrated several local maxima at 500, 1000, 2900, 4500 and 6200 m/z (section II.2.5, Fig. 6) with the decreasing signal at m/z values of 7000. The trends in the observed MALDI (LDI) and ESI HR TOF spectra were similar; however, ESI HR TOF MS allowed for obtaining a cleaner deconvoluted spectra for the high MW species.

We evaluated the LDI MS data using the calculations shown in equations 4–6. The determined MW values agreed with the results obtained with GPC and ESI MS (Table 8). The MW elucidated while employing MALDI was shifted toward lower values, perhaps, due to the suppression of high MW species ionization because their detection was limited by the predominant formation of singly charged ions.

III.2.8. Ion Mobility ESI MS: Confirmation of the Multiply Charged Species Formation

To confirm the formation of multiply charged species, intact lignin was analyzed with IM ESI Q-TOF MS (Fig. 14a). Five distinguishable regions observed in the two-dimensional spectrum (drift time (ms) vs. m/z) suggest the occurrence of species carrying either varied charges or

structural conformations (Fig. 14a). The deconvoluted positive IM ESI Q-TOF mass spectrum was similar to that recorded with the TOF MS (Fig. 14b compared to Fig. 13f). Species with a higher MW featured a higher abundance when analyzed by IM MS, as expected due to a better ion focusing typical for this technique. Notably, both deconvoluted spectra featured the same ion species observed after deconvolution.

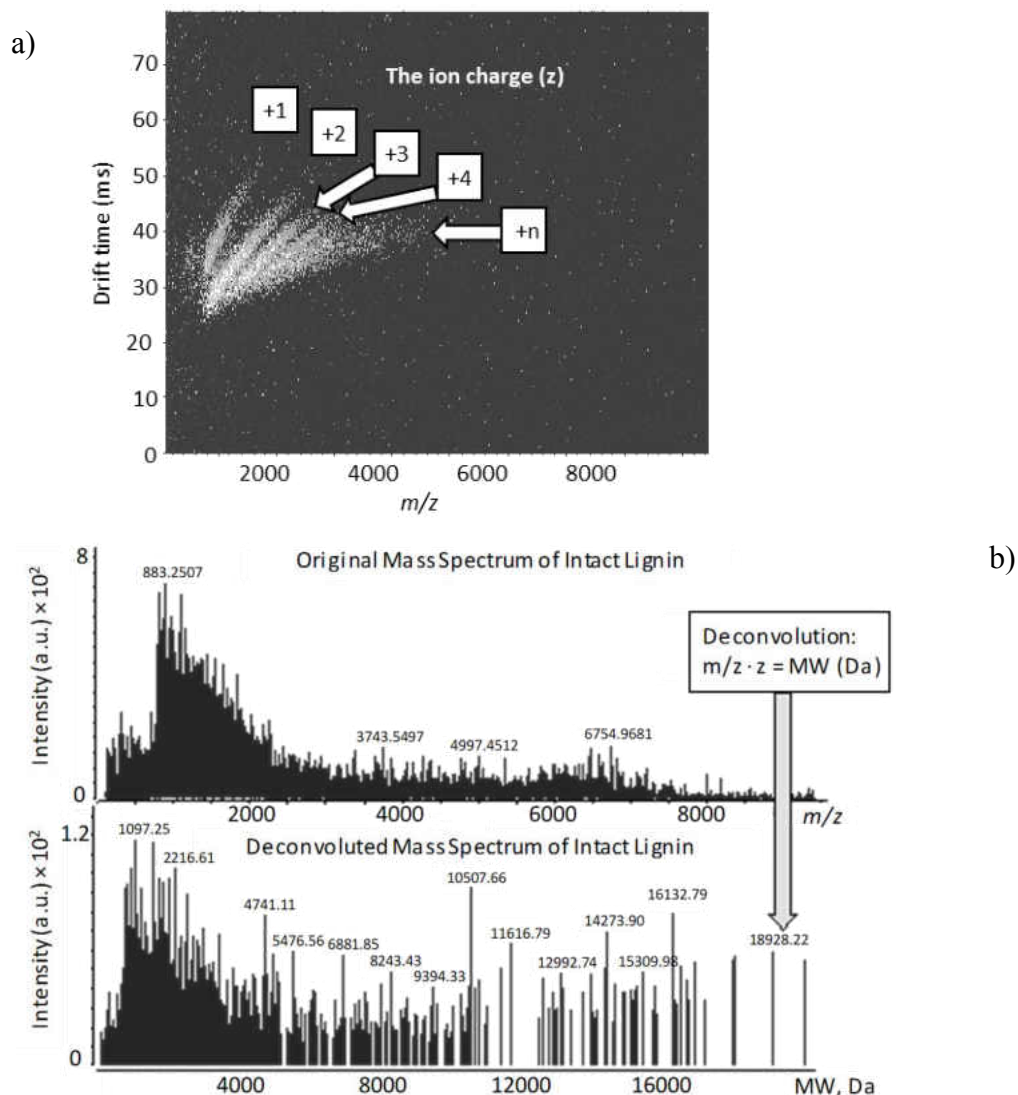


Figure 14. a) Ion mobility image of a 100 ppm solution of intact lignin in ACN-water (1:1) with 100 mmol·L⁻¹ formic acid, recorded in the positive ESI mode. b) Original and deconvoluted mass spectra of a 100 ppm solution of intact lignin in ACN-water (1:1) with 100 mmol·L⁻¹ formic acid recorded in the positive ESI mode. The blank spectrum was subtracted before deconvolution. An accurate deconvolution algorithm is described in equation 3.

With IM ESI HR Q-TOF MS, high MW species with masses up to 20,000 Da were observed, while ESI TOF MS allowed for the detection of species only up to 10,000 Da. This difference (compared to TOF MS) may be due to a higher sensitivity of the newer IM ESI Q-TOF instrument, possibly due to the IM feature allowing for a higher resolution and ion focusing.

CHAPTER IV. LIGNIN FRACTIONATION AND CHARACTERIZATION
BY PREPARATIVE SIZE EXCLUSION CHROMATOGRAPHY

IV.1. Experimental

IV.1.1. Lignin Fractionation via Preparative SEC

Alkali lignin was completely dissolved in a 1:1 (v/v) THF/water mixture at a concentration of 50,000 ppm (w/v) and further diluted with THF to form a lignin solution with a final concentration of 10,000 ppm (w/v) containing 10% of water. No precipitation occurred even when the water content was decreased to 1%.

To perform the SEC column calibration, 200 μ L of a 1% (w/v) standard solutions of PS, PMMA and pinosresinol were injected (Appendix H, Figs. H1 and H2). A linear calibration curve with an R^2 value of 0.9914 was obtained when plotting the retention factors of PS, PMMA standards and pinosresinol vs. logarithm of the standards' MW. The calibration was used to estimate the MW of the collected lignin fractions.

Preparative SEC fractionation was performed on an Agilent 1100 Series HPLC system utilizing a preparative PLgel column (300 \times 25 mm, with 10 μ m particle size and a 1,000 Å pore size). The system was equipped with a diode array detector (DAD). For this work, the analytical flow cell was replaced by a preparative flow cell (Agilent Technologies). Unstabilized THF was used as a mobile phase at a flow rate of 5.0 mL/min. Application of unstabilized THF containing no preservatives was essential to obtain pure lignin fractions without butylated hydroxytoluene or

any other additives used for THF stabilization. An extended loop capillary was installed into the injection loop to perform a 500 μL injection of a 10,000 ppm (w/v) lignin solution.

Several fractionations (with the chromatograms provided in Appendix H, Fig. H3) were performed collecting fractions under similar time windows (allowing to evaluate repeatability) while optimizing the protocol. The final fractionation was conducted in the following elution time windows: 12–14, 14–16, 16–18, 18–20, 20–22, and 22–24 min for the pre-eluate and fractions 0–5, respectively. The fraction collection was performed manually. The procedure was repeated 10 times resulting in a final volume of 100 mL for each of the six collected fractions. Each fraction was dried under a stream of nitrogen to a final volume of 2 mL in order to increase lignin concentration. A 100 mL aliquot of THF was also dried to a final volume of 2 mL representing a blank.

IV.1.2. Analysis of Lignin MW Fractions

IV.1.2.1. HP SEC

The obtained SEC fractions, a blank sample, i.e., concentrated THF, an aliquot of pure THF and an intact lignin solution (50,000 ppm w/v) were analyzed by HP SEC on an Agilent 1100 Series HPLC system equipped with a DAD with an analytical high pressure flow cell, utilizing a PLgel analytical column (300 \times 7.5 mm, with a 5 μm particle and a 1,000 Å pore sizes, 500–60,000 Da separation range) equipped with a PLgel guard column (50 \times 7.5 mm). The SEC column was calibrated with PS standards (Appendix I, Fig. I1). Unstabilized THF was used as a mobile phase at a flow rate of 1.0 mL/min. The injection volume for all samples was set to 20 μL .

IV.1.2.2. TCA

A thermal optical analyzer from Sunset Laboratory Inc. (Portland, OR, USA) was employed to obtain quantitative thermal carbon evolution profiles enabling a comprehensive carbon fractionation and characterization.^{144, 145} For TCA analysis, a 20 μ L aliquot of sample was spiked on a Pall Flex 2500QAT-UP tissue quartz filter (Pall Corp, East Hills, NY, USA), dried on a hot plate at 40 °C for 4 min and placed into the oven. The sample was desorbed and pyrolyzed at desired temperature steps for specific times. A detailed description of the applied TCA protocol can be found elsewhere.^{144, 145} Briefly, the temperatures 30, 200 and 300 °C were employed for thermal desorption and 400, 500 and 890 °C for pyrolysis in helium atmosphere, followed by oven cooling to 550 °C, introduction of an oxidizing carrier gas mixture of He with 10% of O₂ and heating to 890 °C, to evolve the coked carbon fraction. All the evolved species were converted to CO₂ and then to methane, thus allowing for quantification with a flame ionization detection. The TCA instrument was calibrated with sucrose, the consistency of calibration was ensured by a daily introduction of one standard.

IV.1.2.3. STEM, DLS Analysis and Zeta Potential Measurements

A Hitachi SU8010 scanning electron microscope equipped with a transmission electron detector (Hitachi High-Technologies Corp., Japan) operated at 30 kV was used to obtain the STEM images of lignin nanoparticles (NPs) and their aggregates. Lignin fraction solutions obtained upon fractionation and the subsequent evaporation as well as a 10,000 ppm (w/v) intact lignin solution were diluted 1,000 times with water, deposited on a carbon film 200 mesh copper grid (Electron Microscopy Sciences, Hatfield, PA, USA) and dried at 40 °C overnight.

A Zetasizer particle analyzer, model Nano-ZS (Malvern Instruments, UK) was used to measure hydrodynamic diameters and surface charges of lignin particles utilizing a disposable

folded capillary cell. The pre-eluate solution was diluted 50 times with water, whereas fractions 1 and 5, and fractions 2–4 were diluted 200 and 40 times, respectively, to maintain an equal concentration of lignin products.

IV.2. Results and Discussion

To provide insight into the molecular structure of the lignin reducing complexity of sample, we fractionated lignin using preparative SEC to obtain presumably more homogenous samples featuring a narrower molecular size distribution. As demonstrated in Chapter II, the application of a highly cross-linked porous polystyrene/divinylbenzene matrix-based (PSDVB) stationary phase allowed for lignin separation based solely on its MW.¹⁶ The suggested SEC analysis conditions¹⁶ were deemed and subsequently shown to be suitable for lignin size- and MW-based separation and fractionation.

We performed characterization of the fractions utilizing a suite of methods while using traditional chemistry approaches as well as nanoparticle characterization.

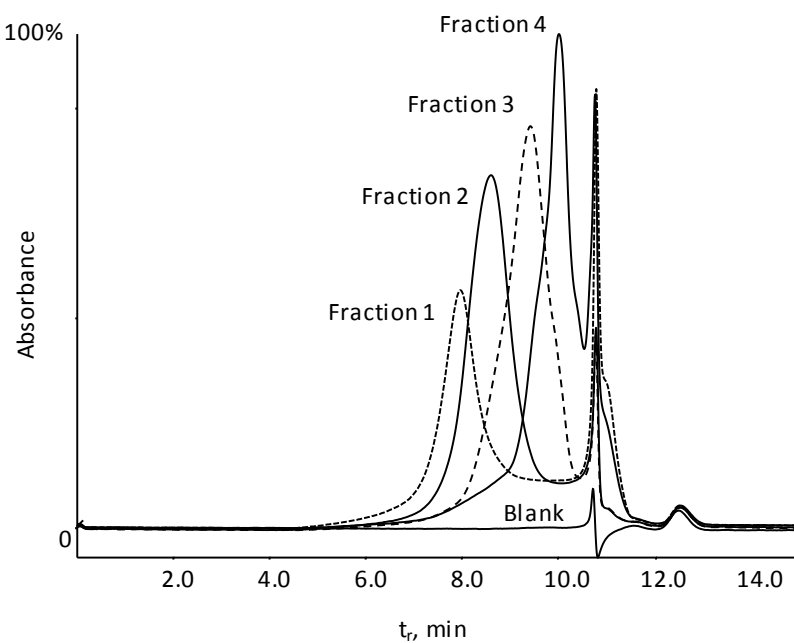
IV.2.1. Lignin Fractionation on Analytical SEC

First, the fractionation conditions were validated on an analytical SEC column (Appendix H, Fig. H3a) and the obtained fractions were re-analyzed on the same column (Fig. 15a). The fractions eluted in the expected order corresponding to the retention time windows, in which they were collected. Each of the fractions featured a narrower molecular size distribution than the original lignin (Fig. 15a). The calculated M_n values for fractions 1–4 were 9,980 Da, 3,150 Da, 1,330 Da, and 1,210 Da, respectively, while intact lignin had an M_n of 1,500 Da.

The TCA results confirmed the effective fractionation by a proportional increase and decrease of the carbon content in the corresponding fractions, i.e., fraction 4 featured large amounts

of volatile species compared to the other fractions. At the same time, fraction 4 showed the lowest quantity of carbon evolving at 870 °C and then in the presence of oxygen (Fig. 15b). By contrast, fraction 1, which was presumably composed of mainly high-MW species, had the lowest amount of volatile species, while over 60% of carbon in this fraction evolved at the highest temperature, e.g., 870 °C both without and then in the presence of oxygen (Fig. 15b).

a)



b)

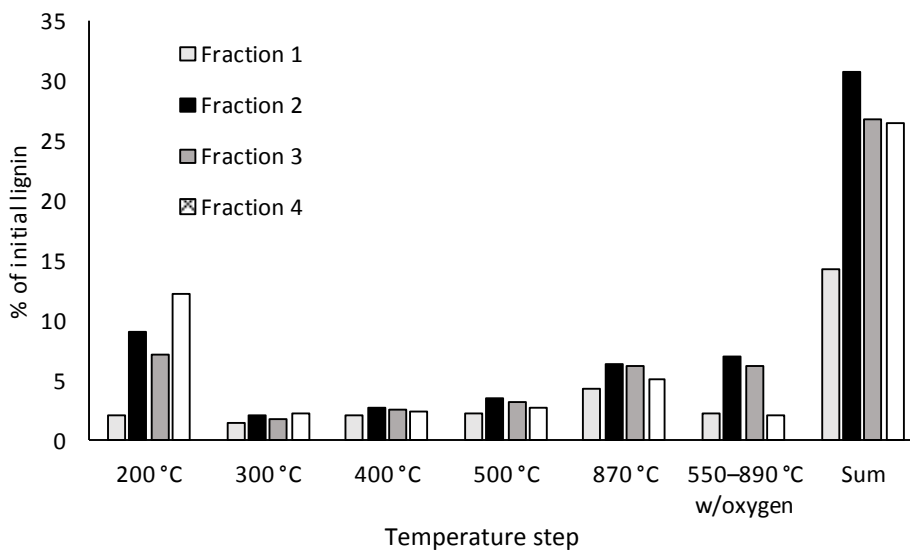


Figure 15. The validation of lignin fractionation conditions employing analytical SEC column: a) HP SEC elution profiles of the fractions; b) TCA profiles of lignin fractions.

IV.2.2. Lignin Fractionation on Preparative SEC

The use of preparative-scale SEC column allowed us to increase lignin loadings, and thus collect the fractions with a higher lignin concentration by performing fewer injections. As a result, a narrower MW distribution of species within the fractions was achieved. For a better understanding of lignin properties, we performed four fractionation replicates with the modified retention time windows allowing for a simultaneous optimization of the fractionation procedure.

In two initial fractionation experiment replicates, the first fraction (fraction 1) was collected within the first two minutes from the start of the lignin elution peak on the SEC-DAD (212-750 nm) chromatogram as shown in Appendix H, Figs. H3b, c. In these cases when the fractions were re-analyzed by HP SEC, fraction 1, which was expected to consist of species with the highest MW, featured two maxima on the SEC chromatogram highlighted with the arrows (Fig. 16a). One of the maxima corresponded to high MW species as expected, whereas the other maximum corresponded to the species of the smallest molecular size (Fig. 16a). Furthermore, the TCA profiles of fraction 1 demonstrated a surprisingly high amount of volatile species evolving at 200 °C (Fig. 16b) while none was expected.

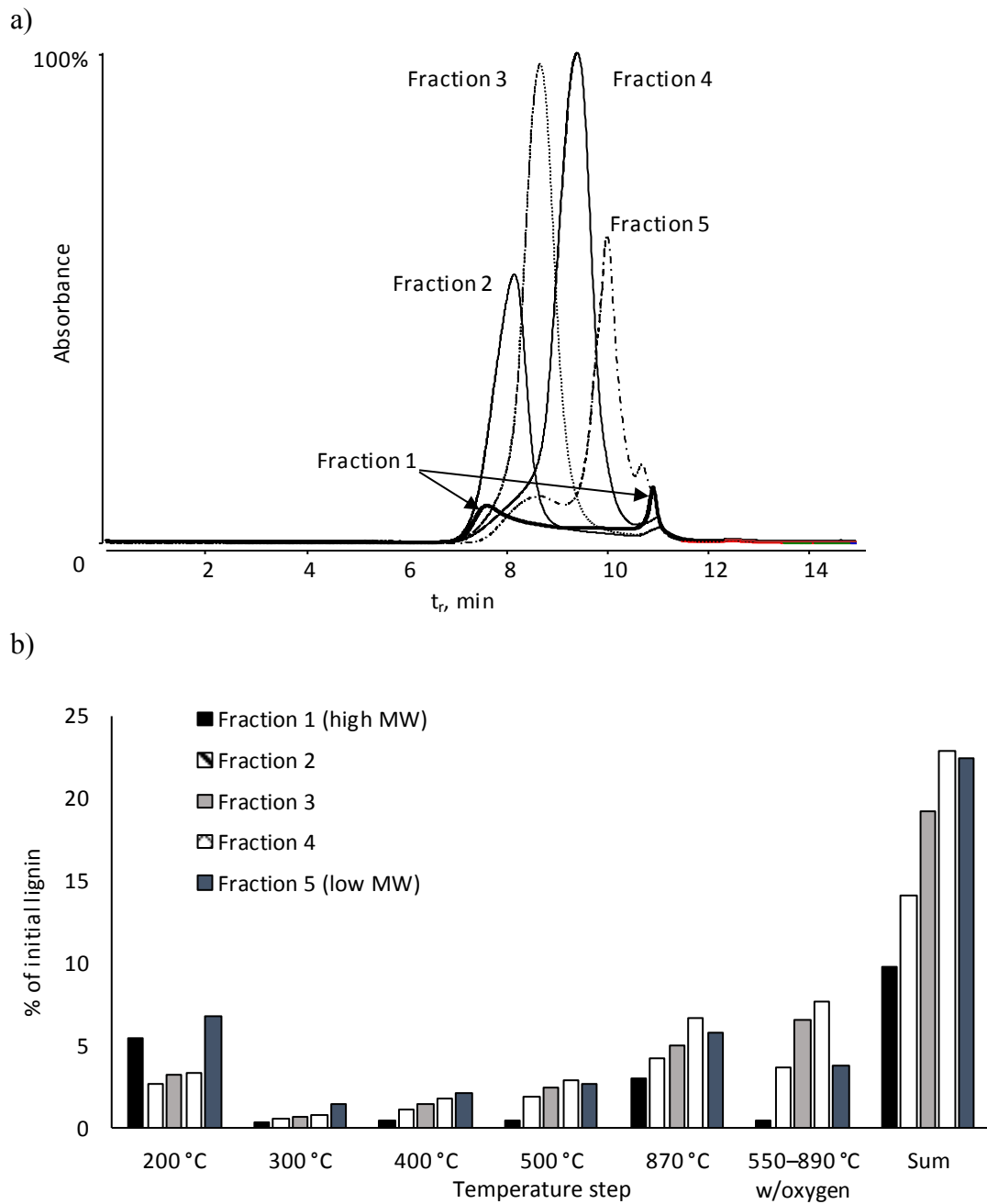
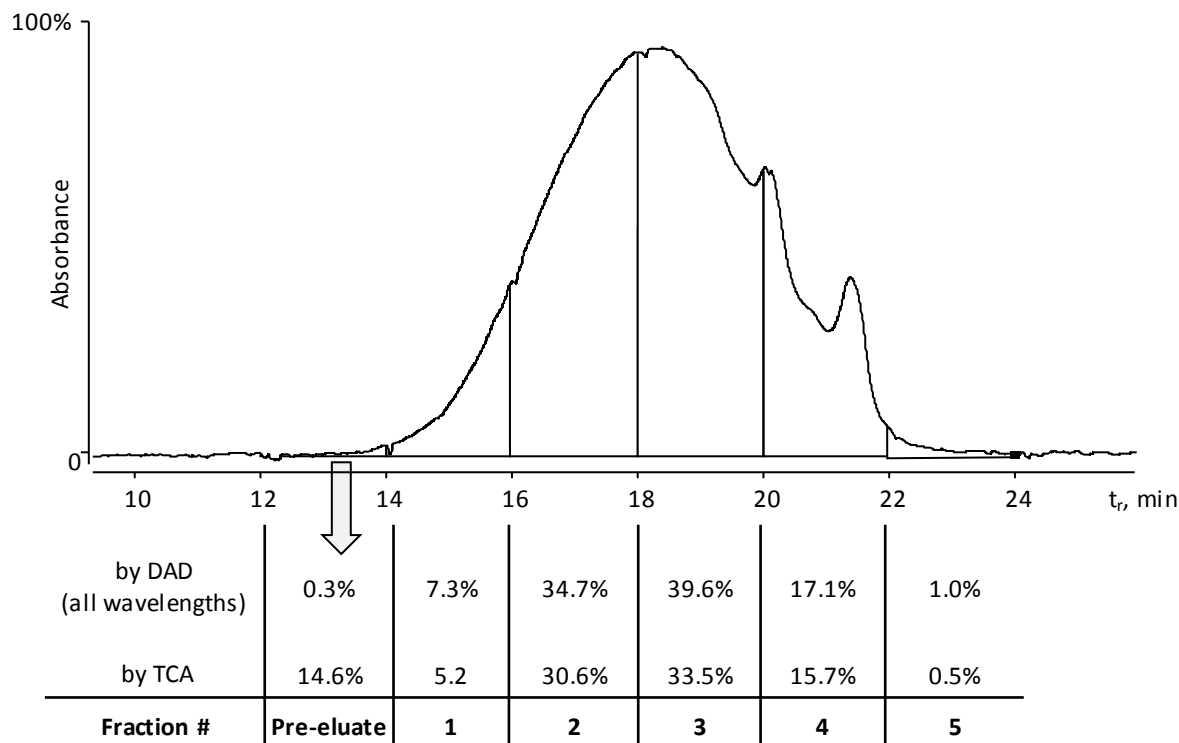


Figure 16. a) HP SEC and b) TCA profiles of lignin fractions (initial SEC fractionation) when the pre-eluate and fraction 1 were collected jointly.

To investigate the origin of the species supposedly co-eluting with high MW lignin constituents in fraction 1, we collected the pre-eluate of fraction 1 separately (Fig. 17a, Appendix H, Figs. H3d, e). The pre-eluate was not expected to have a high concentration of any

lignin-constituting chemicals because of a low DAD signal intensity at retention times when the pre-eluate was collected (the chromatogram and the corresponding area under the peak are shown in Fig. 17a). However, the TCA results showed that the pre-eluate contributed to ca. 10-15% of all lignin products separated by the preparative SEC (Fig. 17a). Thus, the pre-eluate contained such a portion of intact lignin, which did not absorb light in the UV-Vis spectral region restricted by THF cut-off (220–750 nm) and eluting earlier than a high MW UV-absorbing lignin fraction in the preparative SEC. These features suggest its non-phenolic origin.

a) Preparative SEC elution profile of lignin with the corresponding fraction areas and their relative carbon content determined by TCA.



b) HP SEC elution profiles of lignin MW fractions.

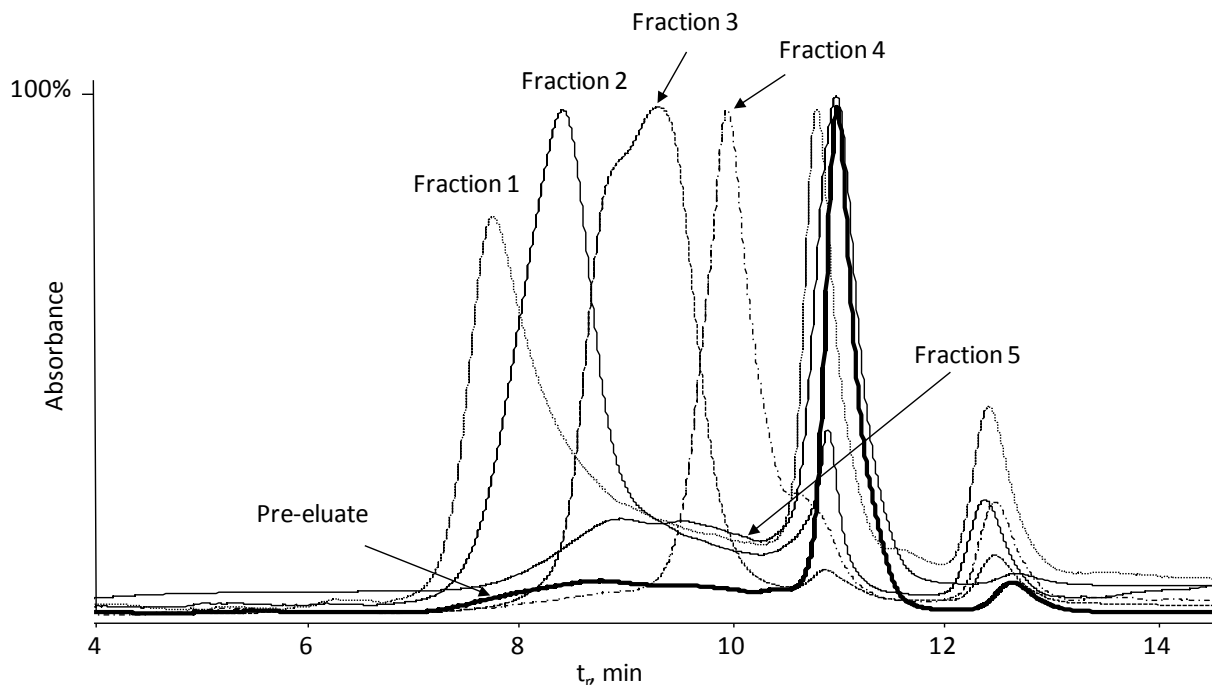


Figure 17. a) Lignin elution profile in the preparative SEC with the corresponding fraction areas and their relative carbon content determined by TCA; b) HP SEC and b) TCA profiles of lignin fractions when fraction 1 and the pre-eluate were collected separately.

Figure 17 cont.

c) TCA profiles of lignin MW fractions

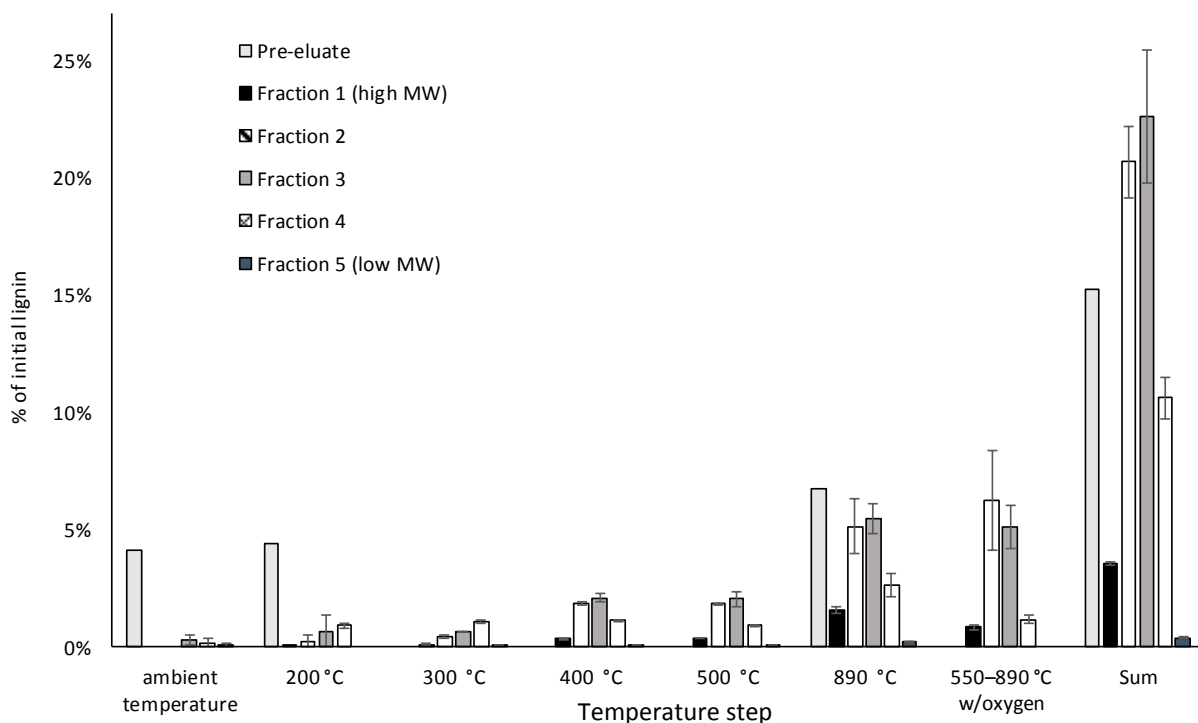


Figure 17. a) Lignin elution profile in the preparative SEC with the corresponding fraction areas and their relative carbon content determined by TCA; b) HP SEC and b) TCA profiles of lignin fractions when fraction 1 and the pre-eluate were collected separately.

IV.2.2.1. HP SEC and TCA of the Pre-Eluate

When analyzed by HP SEC-DAD, the pre-eluate was shown to be predominantly composed of small molecular size species eluting later in the analysis (Fig. 17b) with the retention time similar to that of low-MW species. This observation suggested the presence of low-MW species in the pre-eluate of lignin in the preparative SEC, which eluted without being retained in the SEC stationary phase pores when injected on the preparative column in a mixture with lignin. These species tended to behave like the true low-MW size species when they were isolated and re-analyzed separately from lignin (*cf.* Fig. 17b). High volatility of a significant portion (65% of carbon in this fraction, Appendix H, Fig. H4) of the pre-eluate species is shown by TCA evolving

already at low temperatures (the ambient temperature and 200 °C steps) thus supporting this suggestion (Fig. 17c). Also, the TCA analysis of the pre-eluate did not show any species evolving at the coked fraction when oxygen was introduced into the system, thus supporting the less cross-linked (presumably, non-lignin like) structure of the species in the pre-eluate.

Perhaps, carbohydrates may be the impurities in lignin appearing in the pre-eluate. In trees, lignin is known to interact with polysaccharides, particularly hemicellulose, leading to the formation of other chemical species, glycoconjugates, known as lignin-carbohydrate complex.¹⁴⁶ The difficulty in separating lignin from carbohydrates in wood was first described in 1866¹⁴⁷ and remains relevant until now.¹⁴⁶ Furthermore, Tunc et al.¹⁴⁸ showed that lignin-carbohydrate complexes eluted at lower retention volumes (times) when analyzing original ball-milled wood on a PLgel column, whereas the enzyme treatment led to a shift of the SEC elution profile towards longer retention times suggesting the solubilization of lignin-carbohydrate complexes.¹⁴⁸ Furthermore, the TCA profile of levoglucosan (Appendix H, Fig. H5) demonstrated a similar to the pre-eluate carbon distribution across the temperature step with a high amount of carbon evolving at low temperature steps and minimal amount of carbon evolving in the presence of oxygen.

IV.2.2.2. HP SEC and TCA of Lignin Fractions

Fraction 1 elution after the pre-eluate (black bars in Fig. 17b and Appendix H, Fig. H4) demonstrated a typical for TCA profile high-MW species with ca. 62 % of carbon in this fraction evolving at 890 °C without and then in the presence of oxygen. This fraction also featured low amounts of carbon evolving at the ambient temperature and at 200 °C, e.g., 13% (relative) for a fresh sample. An aged sample did not feature any carbon evolved at these temperature steps suggesting a re-polymerization of low MW species.

Both fractions 2 and 3 had 28% and 24% (relative) of coked carbon, respectively, which evidenced the presence of some higher MW species in both of these fractions with their higher content in fraction 2. Less than 13% (relative) of carbon evolved during the first two temperature steps in these fractions suggesting a low content of volatile low-MW species in fractions 2 and 3. Moreover, these values decreased to 1% and 4% (relative) for fractions 2 and 3, respectively, as a result of sample aging for 3 months evidencing the occurrence of re-polymerization.

In contrast, fraction 4 featured an opposite trend to fractions 1–3 in carbon distribution across the temperature steps, with 34% (relative) of carbon evolving at an ambient temperature and 200 °C for the fresh sample and 9% (relative) for the aged sample. Additionally, 20% (relative) of carbon evolved at 300 and 400 °C steps for both the fresh and aged samples. A higher relative amount of carbon evolving at 300 and 400 °C compared to fractions 1–3 suggested fraction 4 to contain oligomeric species. Also, this fraction demonstrated a lower amount of coked carbon and thus less of high MW species compared to fractions 1–3. Such a composition of fraction 4 was expected considering the later elution time of this fraction (20–22 min).

Finally, fraction 5 had 43% (relative) of carbon evolving at the low temperature steps (the ambient temperature and 200 °C) for the fresh sample and 16% (relative) for the aged sample. The loss of volatile species and/or re-polymerization may explain the decrease of carbon desorbing at low temperatures. Increase in the relative amount of carbon evolving at 890 °C without oxygen from 11% to 53% (relative) supported the occurrence of re-polymerization. Finally, fraction 5 did not feature any coked carbon for both the fresh and aged samples as expected for a low MW fraction abundant with monomeric phenol derivatives.

To summarize, TCA results supported the non-lignin nature of the pre-eluate fraction featuring high amounts of volatile species and no coked carbon. Fraction 1 demonstrated a TCA

profile typical for high-MW species with most of the carbon evolving at the highest temperatures and getting coked. By contrast, a low MW fraction 5 had the highest amount of volatile species and none of coked carbon. Oligomeric species were observed in the highest amounts in fractions 2–4.

Furthermore, the decreasing amount of volatile species with a concomitant increase in the 890 °C portion suggested the occurrence of re-polymerization as a result of sample storage at 4 °C.

IV.2.2.3. Molecular Weight and Molecular Size of Lignin Fractions and the Pre-Eluate

The M_n and M_w values determined for the lignin fractions and intact lignin by HP SEC are shown in Table 9. These numbers were in good agreement with the expected MW values being consistent with the elution order of the fractions.

Table 9. MW, average hydrodynamic diameter and zeta-potential of the particles in lignin fractions and the pre-eluate determined by SEC and DLS.

	Pre-eluate	Fraction 1	Fraction 2	Fraction 3	Fraction 4	Fraction 5	Original Lignin
M_n, Da (SEC)	ND	4,790	2,820	1,340	790	250	1,600
M_w, Da (SEC)	ND	5,970	3,820	2,630	2,600	310	2,700
Average hydrodynamic diameter, nm (DLS)	407 ± 63	384 ± 23	140 ± 4	150 ± 19	ND	ND	97 ± 3
Zeta-potential, mV (DLS)	-48.6	-47.4	-51.1	-42.6	-36.5	-28.7	-40.7

Based on the preliminary data obtained with DLS, intact lignin featured a surprisingly narrow distribution of the hydrodynamic size in the aqueous solution, 97 ± 3 nm (Table 9). Moreover, the particles of a larger size were observed in the higher MW fractions with a size of 140–150 nm for oligomeric lignin fractions 2 and 3 and 384 ± 23 nm for high MW fraction 1. Perhaps, larger molecules, which predominantly occur in the higher MW fractions, are more prone to nanoparticle formation when they are isolated from the low MW portion of lignin and other impurities, i.e., carbohydrates. Such aggregates of a larger size were observed in STEM images of fraction 1 (Appendix H, Fig H6a). The amorphous nature of carbohydrates, e.g., hemicellulose, may have resulted in the formation of larger size aggregates, over 400 nm, detected by DLS, with unclear contours as shown in STEM images (Appendix H, Fig H7a). No distinguishable particles were detected by DLS when analyzing lower MW fractions of lignin. The STEM images supported these results because no nanoparticles were observed in the sample of fraction 5 (Appendix H, Figs. H6e, H7f).

A correlation between the hydrodynamic diameter of the particles and the M_n values determined by SEC suggested that larger particles or aggregates were formed in the solution of higher MW lignin species (Fig. 18a). Furthermore, the lower MW fractions 4 and 5 demonstrated a lower absolute zeta-potential values (Fig. 18b), and thus a lower stability in the solution (i.e., a tendency to aggregate) expected for low MW lignin constituents featuring.

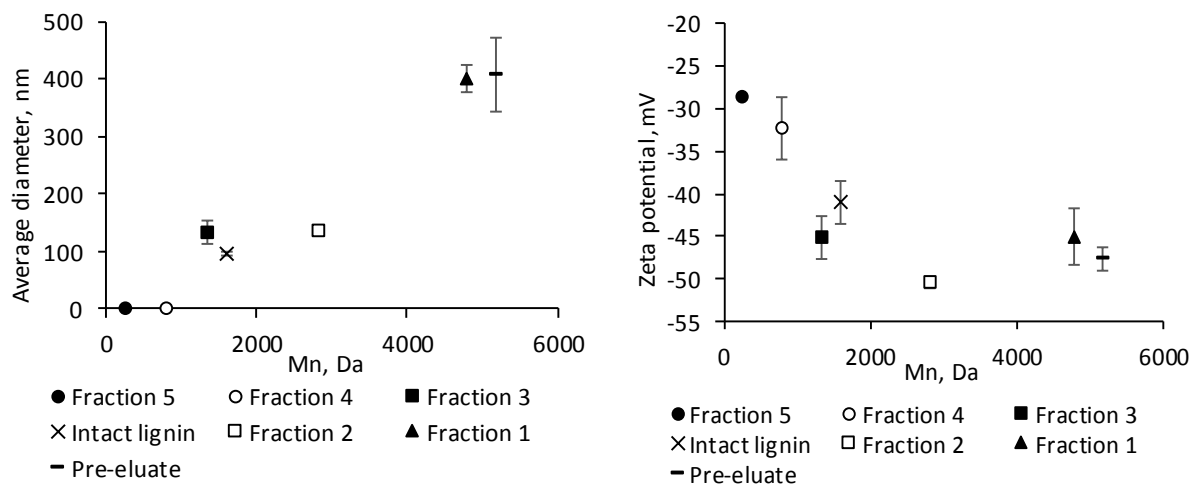


Figure 18. a) Average hydrodynamic diameter and b) zeta-potential of the particles in the solution of lignin MW fractions and the pre-eluate determined by DLS.

CHAPTER V. APPLICATION OF THE DEVELOPED METHODS TO SYNTHETIC POLYMERS AND DEGRADED LIGNIN

V.1. Characterization of Biomodified Lignin Using Liquid Chromatography

V.1.1. Experimental

The SEC method for accurate MW determination of lignin, which was shown to be unaffected by secondary non-SEC interactions, and the RP HPLC method for the assessment of lignin structural changes described in II.2.6 were applied to lignin samples subjected to biomodification with fungus *Coriolus versicolor* (*C. versicolor*). A detailed description of the performed biotreatment can be found elsewhere.¹⁴⁹⁻¹⁵¹ The biotreatment was performed without and then in the presence of 2% dimethyl sulfoxide (DMSO).

For SEC, the samples were diluted with a 1:1 (v/v) THF-water mixture prior to the analysis. A control sample consisting of THF, water and DMSO 49, 49 and 2% (v/v), respectively, was analyzed to account for the solvent background. Its chromatogram was subtracted from samples' chromatograms prior to MW calculation. The M_n and M_w values were calculated as described in section II.1.4 using formulas 1–2.

For RP HPLC, an HPLC Zorbax Eclipse Plus C18 column (pore size 95 Å), 3.5 μm particle size, 2.1 \times 150 mm with a guard column, 2.1 \times 12.5 mm, was utilized. The RP HPLC method is described in section II.1. Briefly, the mobile phase consisted of 0.5 $\text{mmol}\cdot\text{L}^{-1}$ NH_4OAc in water (solvent A), and 0.5 $\text{mmol}\cdot\text{L}^{-1}$ NH_4OAc in ACN (solvent B). A gradient elution program was used for the analysis starting with an isocratic elution at 10% of solvent B for 5 min, and then followed

by a linear gradient to 95% B from 5 to 50 min. The flow rate was $0.3 \text{ mL}\cdot\text{min}^{-1}$. The DAD detection was performed in a range of 190 to 700 nm with a step of 2 nm. The samples were analyzed prior to the biotreatment, then after 1, 3 and 6 days of the treatment.

V.1.2. Results and Discussion

V.1.2.1. Lignin MW Increase upon Biomodification by SEC

The developed SEC method showed different elution profiles for untreated lignin and that treated with white rot fungi *C. versicolor*, with the latter eluting earlier (Fig. 19).^{149, 150} The earlier SEC elution suggested that the biotreatment resulted in an increase in lignin MW. The calculated M_n and M_w values corroborated this observation showing an increase from 1,750 Da to 4,780 Da and from 4,690 Da to 28,760 Da, respectively. The observed MW increase indicated intermolecular cross-linking being the major reaction path in lignin biomodification.

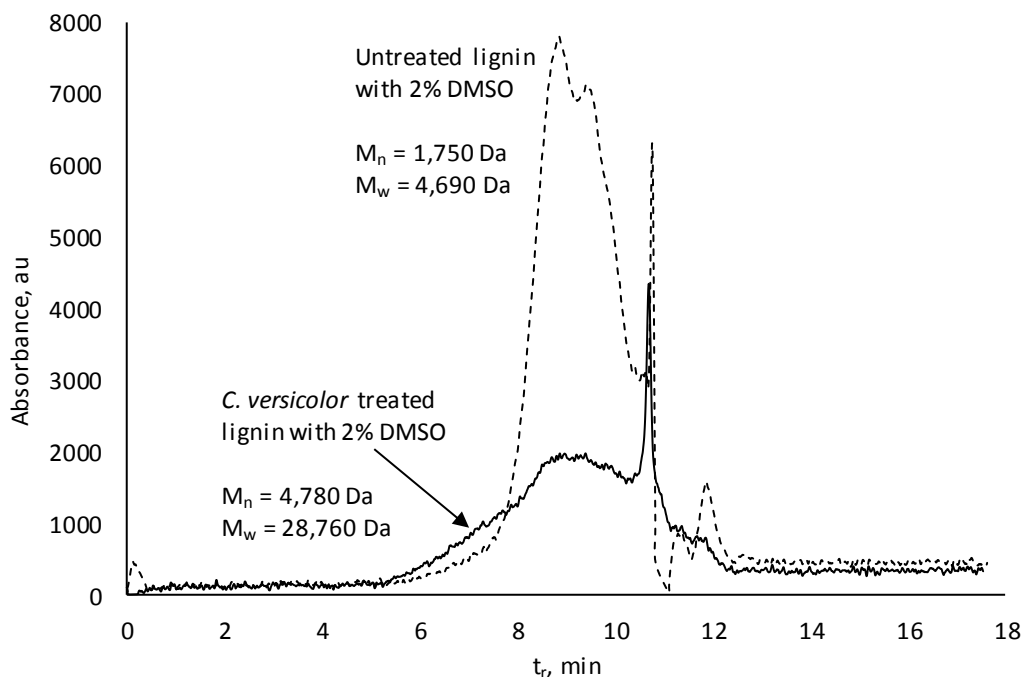


Figure 19. SEC elution profiles of the intact untreated and *C. versicolor*-treated lignin after subtracting the chromatogram of the control sample.

V.1.2.2. HPLC for Lignin Structural Changes Elucidation upon Biomodification

The analysis of the biomodified lignin with RP HPLC showed that lignin structure was changed as a result of the biotreatment (Fig. 20). Additional peaks developed at earlier elution times in the fungal-treated lignin samples with and without DMSO.

Addition of 2% DMSO to the samples resulted in complete lignin dissolution in contrast to the samples without DMSO. An incomplete dissolution of lignin without DMSO resulted in a low DAD signal intensity throughout the chromatographic analysis of the water-soluble lignin portion. Nevertheless, the sample fungal treatment resulted in the formation of the water-soluble species, which eluted between 17 and 20 min and were detected by the DAD (Fig. 20a). Also, we confirmed that the DMSO addition to the samples did not result in the RP HPLC method artifacts, so the retention time of the internal standard (IS) was consistent in the chromatograms of the samples with and without DMSO (Fig. 20).

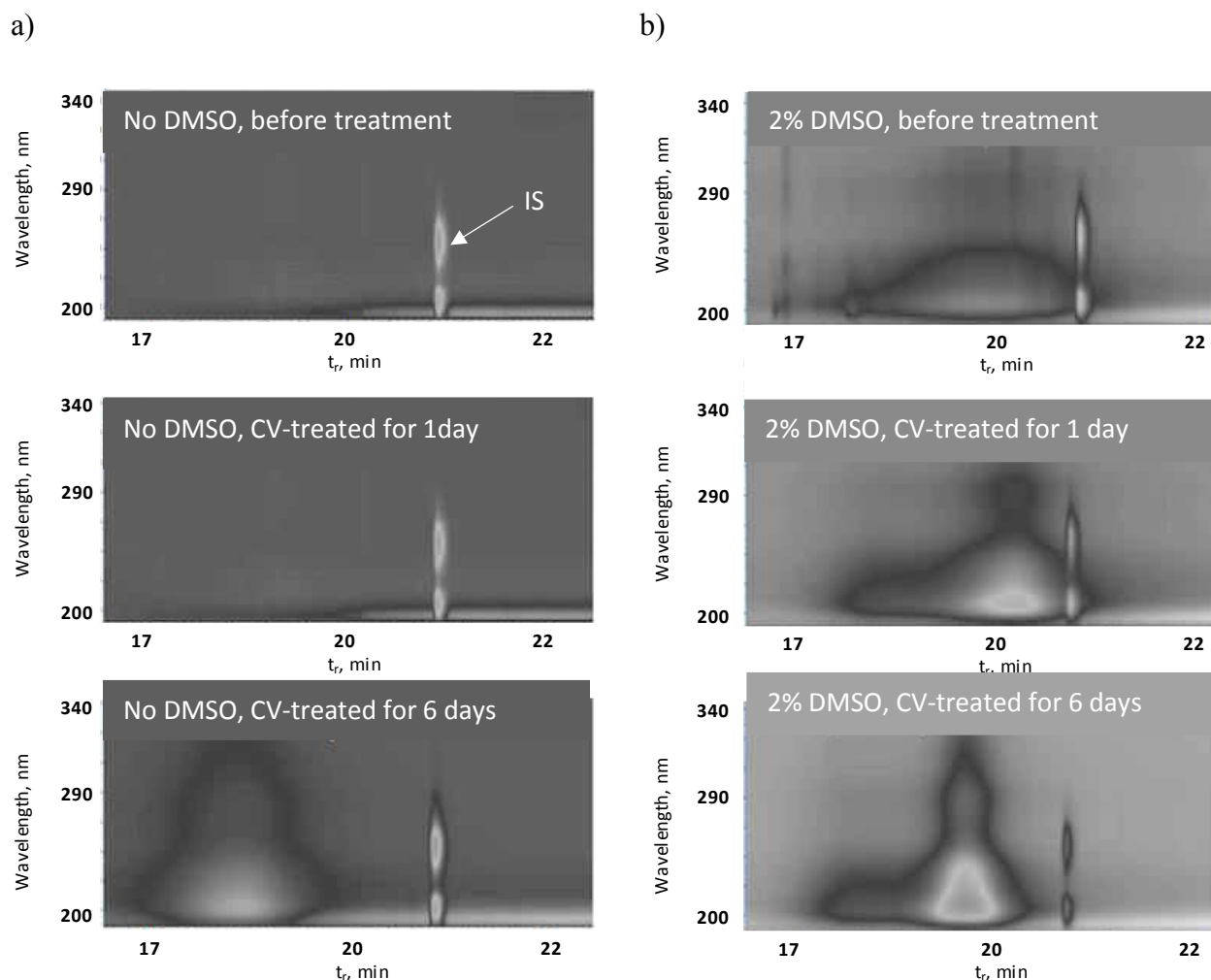
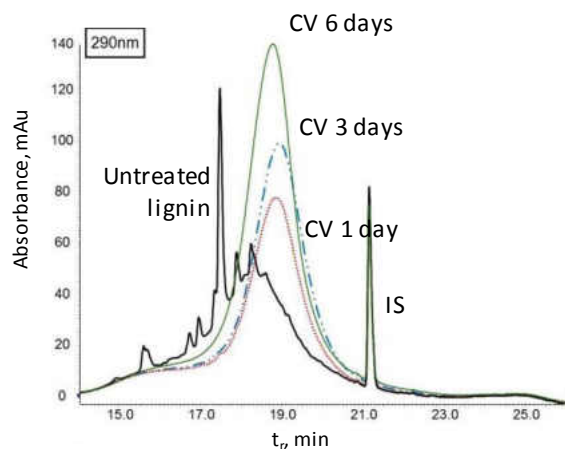


Figure 20. The RP HPLC-DAD contour plots of the original lignin and its fungal biotransformation product a) without and b) in the presence of DMSO.

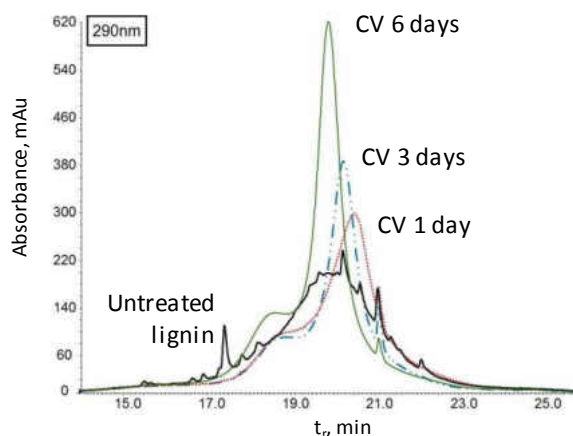
The major changes in the RP HPLC-DAD elution profiles were observed at 205, 290 and 540 nm, thus these wavelengths were chosen for monitoring the sample modification. For the samples treated in the presence of DMSO, the chromatographic peaks recorded at 290 and 540 nm shifted toward shorter retention times as a result of the fungal treatment (Fig. 21). This effect was more pronounced for the increased treatment times. As the analysis was performed on the reversed-phase column, the earlier elution suggested an increase of the product polarity, i.e., the extent of the biomodified sample oxygenation, compared to the untreated lignin (Fig. 21). This observation

also corroborated the increase in lignin solubility in water observed after the fungal treatment without and then in the presence of DMSO.

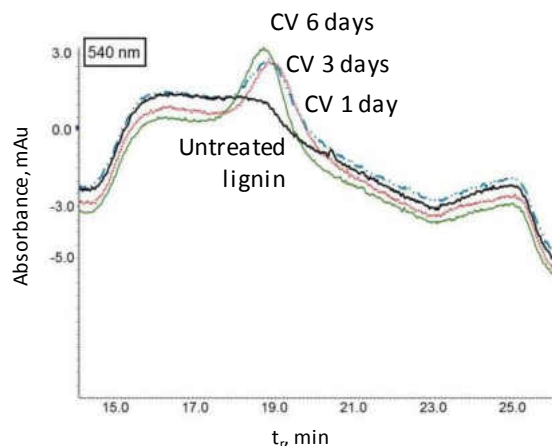
a) No DMSO



b) 2% DMSO



c)



d)

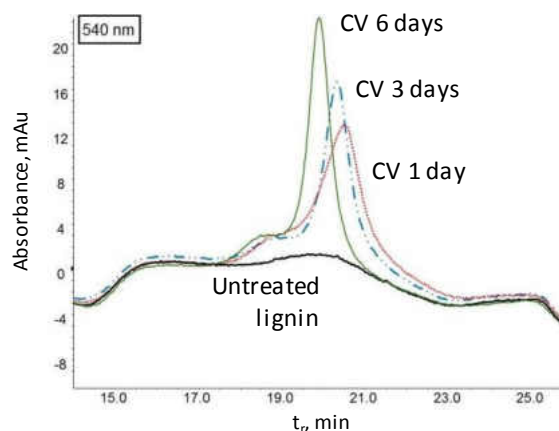


Figure 21. The extracted wavelength RP HPLC-DAD chromatograms (15–25 min) at 290 nm and 540 nm of the original lignin and its fungal biotransformation product a, c) without and b,d) in the presence of DMSO

The narrowing of the product's peak observed both with and without DMSO may indicate a decrease of the sample polydispersity (Fig. 21). The changes observed by RP HPLC were consistent with the proposed^{150, 151} intramolecular cross-linking of lignin oligomers, which would increase the sample uniformity (i.e., decrease polydispersity).

V.2. Lignin MW Decrease upon Thermal Treatment with Hydrogen Peroxide

V.2.1. Experimental

The developed SEC method for determining MW of lignin, which was shown to be unaffected by secondary non-SEC interactions, was also employed for characterization hydrotreated lignin samples. Thermal hydrotreatment of alkali lignin (1.0 g) was performed in an autoclave for 30 min at 120 °C under 17 psi in the pressure rated glass tubes (50 mL). The treatments in an aqueous system (100 % water) and an aqueous system with methanol 25% (v/v) with addition of hydrogen peroxide at the concentrations 0%, 5% and 10% (v/v) (total volume 25 mL). Prior to the analysis the hydrotreated samples were diluted with THF prior to the SEC analysis to decrease the water content to 5%. The M_n and M_w values were calculated as described in section II.1.4 using formulas 1–2.

V.2.2. Results and Discussion

The SEC elution profiles of the water-soluble fractions of lignin after its autoclaving in the presence of hydrogen peroxide shifted towards longer retention times compared to the sample without hydrogen peroxide in both 100% aqueous and methanol-containing systems (Fig. 22). Furthermore, the highest concentrations of hydrogen peroxide (10% in 100% aqueous media) resulted in a later elution of lignin compared to the sample treated with 5% of hydrogen peroxide (Fig. 22a). This effect was not observed in the methanol-water system (Fig. 22b). Perhaps, methanol increases lignin solubilization and leads to a greater sample dissolution, thus minimizing the solubilizing effect of hydrogen peroxide observed at its lower concentrations (5%) in water.

This trend suggested that the presence of hydrogen peroxide promoted the degradation of the water-soluble lignin portion. The calculated MW values supported this observation, as M_n of the autoclaved lignin in the presence of hydrogen peroxide decreased to 770 and 470 Da for 5%

H₂O₂ and 10% H₂O₂, respectively, compared to 1,300 Da determined for the sample autoclaved in 100% water without H₂O₂ (Table 10). The same trend was observed in the methanol-water system with the M_n value decreasing from 1,310 Da to 580 Da without hydrogen peroxide and then in the presence of 10% H₂O₂, respectively (Table 10).

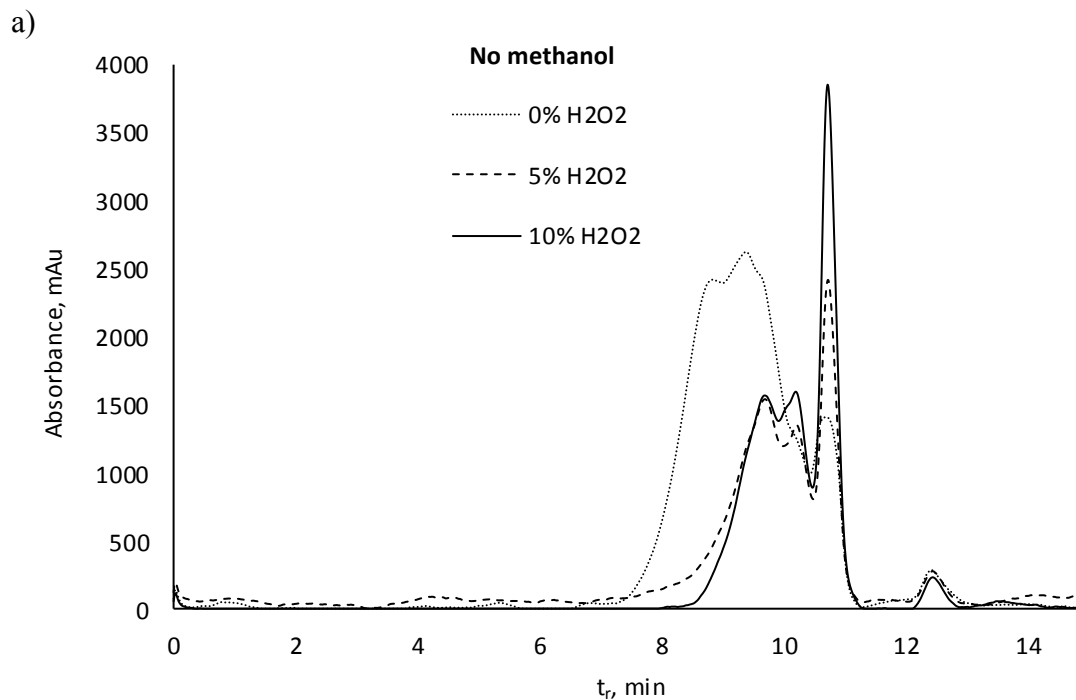


Figure 22. SEC elution profiles of the water-soluble portion of lignin autoclaved in the presence of 0%, 5% and 10% of H₂O₂ (v/v) a) in a 100% aqueous system; b) in an aqueous system containing 25% of methanol.

Figure 22 cont.

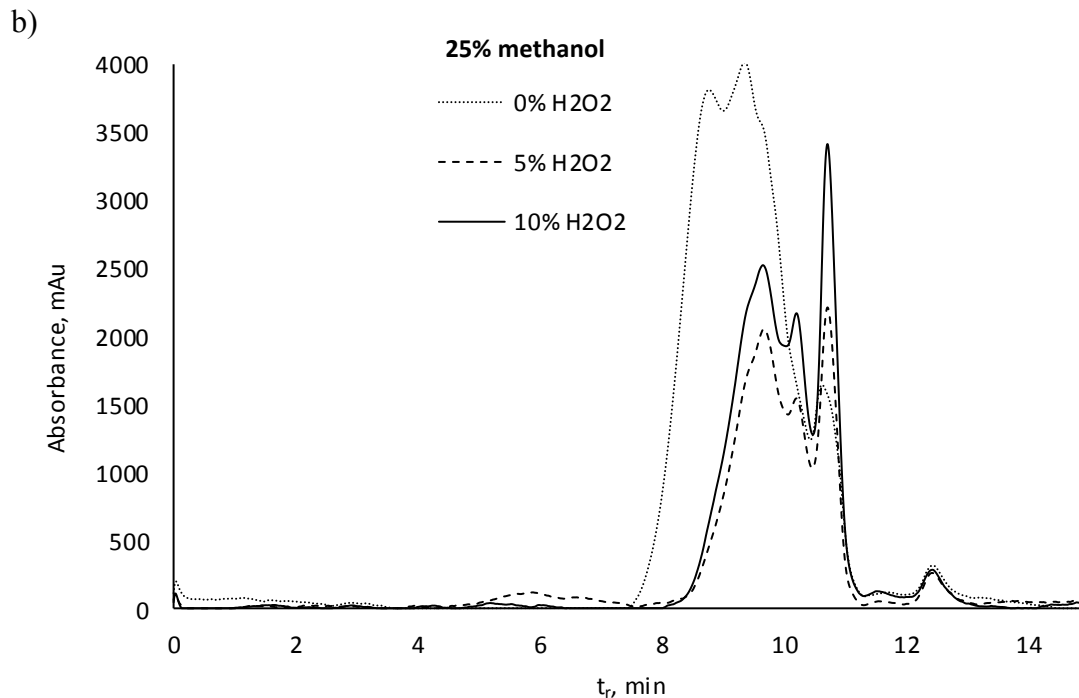


Figure 22. SEC elution profiles of the water-soluble portion of lignin autoclaved in the presence of 0%, 5% and 10% of H₂O₂ (v/v) a) in a 100% aqueous system; b) in an aqueous system containing 25% of methanol.

Table 10. Molecular weight of the water-soluble portion of lignin autoclaved in the presence of 0%, 5% and 10% of H₂O₂ (v/v) in 100% water and in the aqueous system containing 25% of methanol.

	Without methanol	25% methanol
0% H₂O₂	M _n = 1,300 Da M _w = 2,430 Da	M _n = 1,310 Da M _w = 2,360 Da
5% H₂O₂	M _n = 770 Da M _w = 2,140 Da	M _n = 600 Da M _w = 930 Da
10% H₂O₂	M _n = 470 Da M _w = 780 Da	M _n = 580 Da M _w = 920 Da

Notably, the elucidated MW of water-soluble autoclaved lignin without H₂O₂ in water and the water-methanol system were lower than the values determined for the intact lignin sample fully

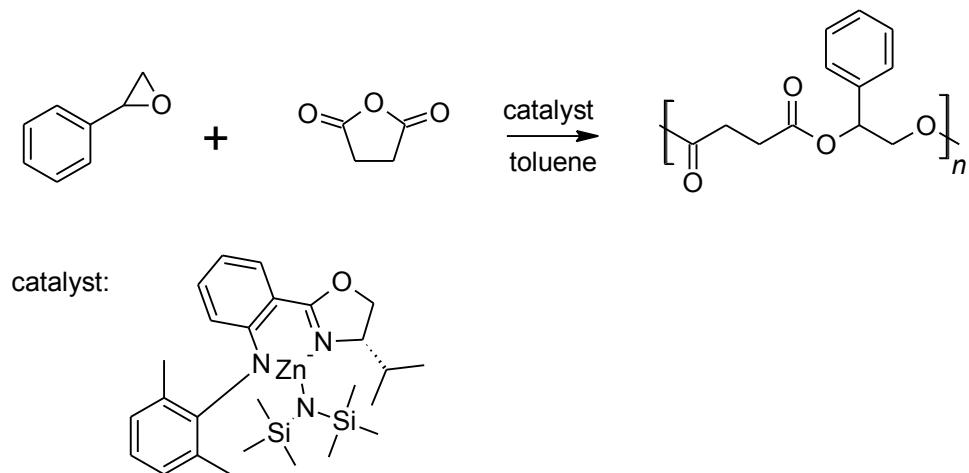
dissolved in the THF-water system reported in section II.2.4 (1,630 and 2,740 Da for M_n and M_w , respectively). This may be a result of a selective solubilization of a low-MW portion of lignin in a water-methanol system during autoclaving.

V.3. ESI HR TOF MS for the MW Determination of Synthetic Polymers

V.3.1. Experimental

The developed ESI HR TOF-MS method described in Chapter III was employed for an assessment of MW distribution of a group of synthetic polymers using the feature of multiply charged ion formation. Molecular weights of 1) narrow MW distribution polypropylene glycol (PPG) standards; 2) a copolymer of styrene oxide and maleic anhydride; and 3) narrow MW distribution polyethylene glycol (PEG) standards in a mixture were determined using direct infusion (DI) MS analysis. Also, RP HPLC-MS was applied for separation and MW elucidation to a mixture of narrow MW distribution PEG standards. Analysis details are provided in Table 11.

Narrow MW distribution PPG standards with the M_n values of 1,130 Da, 1880 Da, 2,780 Da and 3,100 Da were purchased from Sigma Aldrich. Three mixtures of narrow MW distribution PEG standards with the M_n values of 1) 232 Da, 879 Da, 3,850 Da, 14,900 Da (PEG mixture 1); 2) 547 Da, 2,980 Da, 10,600 Da, 34,000 Da (PEG mixture 2) and 3) 269 Da, 1,380 Da, 5,610 Da, 22,100 Da (PEG mixture 3) were obtained from Fluka. The copolymer of styrene oxide and maleic anhydride was synthesized using zinc amido-oxazolate catalyst/styrene oxide/maleic anhydride (ratio 1:200:200) in toluene at 100 °C, for 0.33 hour (Scheme 1). The details of this synthesis are provided elsewhere.¹⁵²



Scheme 1. The ring-opening copolymerization of styrene oxide with maleic anhydride using zinc complex.

Table 11. Optimized conditions for DI-MS and HPLC-MS analysis of the selected synthetic polymers.

Analyte	Conc.	DI or HPLC	Solvent	Electrolyte	Flow rate, $\mu\text{L}/\text{min}$	Electrospray potential, V	Fragmentor potential, V	Nebulization T, $^{\circ}\text{C}$	Nebulization p, psi	Drying gas flow rate, L/min
PPG	100 ppm	DI	ACN-water 1:1 (v/v)	NH_4OAc , $10 \text{ mmol}\cdot\text{L}^{-1}$	5	4750	350	350	20	4
PEG	100 ppm	DI	ACN-water 1:1 (v/v)	NH_4OAc , $0.5 \text{ mmol}\cdot\text{L}^{-1}$	5	5500	150	300	20	4
The copolymer of styrene oxide and maleic anhydride	5 ppm	DI	ACN-water 1:1 (v/v)	NH_4OAc , $2.5 \text{ mmol}\cdot\text{L}^{-1}$	5	4500	200	300	25	4
PEG	1000 ppm	RP HPLC Zorbax Eclipse Plus C18 column	A: water w/10 $\text{mmol}\cdot\text{L}^{-1}$ NH_4OAc ; B: ACN w/10 $\text{mmol}\cdot\text{L}^{-1}$ NH_4OAc ^a	NH_4OAc , $10 \text{ mmol}\cdot\text{L}^{-1}$	300	4500	150	350	25	12

^a The RP HPLC gradient elution method is described in section II.1.

V.3.2. Results and Discussion

The developed ESI HR TOF MS method (section III.2.2.3) was shown to be an effective tool in lignomics. In this project, the method potential for elucidating polymer MW was assessed through its application to a suite of representative polymers including PPG, PEG and a copolymer of styrene oxide and maleic anhydride.

V.3.2.1. PPG MW Determination via Direct Infusion

The MW values for four PPG standards were determined via DI ESI HR TOF MS. The results were in good agreement with the M_n values provided by the supplier (Table 12).

Table 12. Number-average molecular weight for PPG standards determined by ESI HR TOF MS and claimed by the supplier.

Standard	M_n determined by ESI HR TOF MS	M_n provided by the supplier
PPG-1000	1,130	1,000
PPG-2000	1,880	2,000
PPG-2700	2,780	2,700
PPG-3500	3,100	3,500

The mass spectra of the PPG standards before and after deconvolution are provided in Appendix J (Fig. J1). The spectrum of the PPG standard featuring lower MW, i.e., $M_n = 1,000$ Da did not undergo changes upon the deconvolution since the ions were exclusively single charged. By contrast, the PPG standard with the expected M_n of 2,000 Da featured the double charged species in its mass spectrum. The ions with the charge of up to +4 were detected in the mass spectra of higher MW PPG-2000 and PPG-3500. This is demonstrated in a mass spectrum of a PPG ion

carrying a charge of +4 is shown in Appendix J (Fig. J2) along with the calculation for its native MW elucidation.

V.3.2.2. Determination of the MW of a Copolymer via Direct Infusion

The MW of a copolymer of styrene oxide and maleic anhydride was determined via DI ESI HR TOF MS (Fig. 23). The results were in good agreement with the M_n , M_w and M_z values determined by GPC analysis on a PLgel Mixed-D column calibrated with PS standards, utilizing a refractive index detector (Table 13). Furthermore, the M_p (molar mass at the peak maximum) value determined by GPC was 2,990 Da. The mass distribution observed in the mass spectrum after deconvolution (Fig. 23) featured the species with a mass of 2,910.96 Da as the most abundant one. This result closely matched the M_p value determined by GPC.

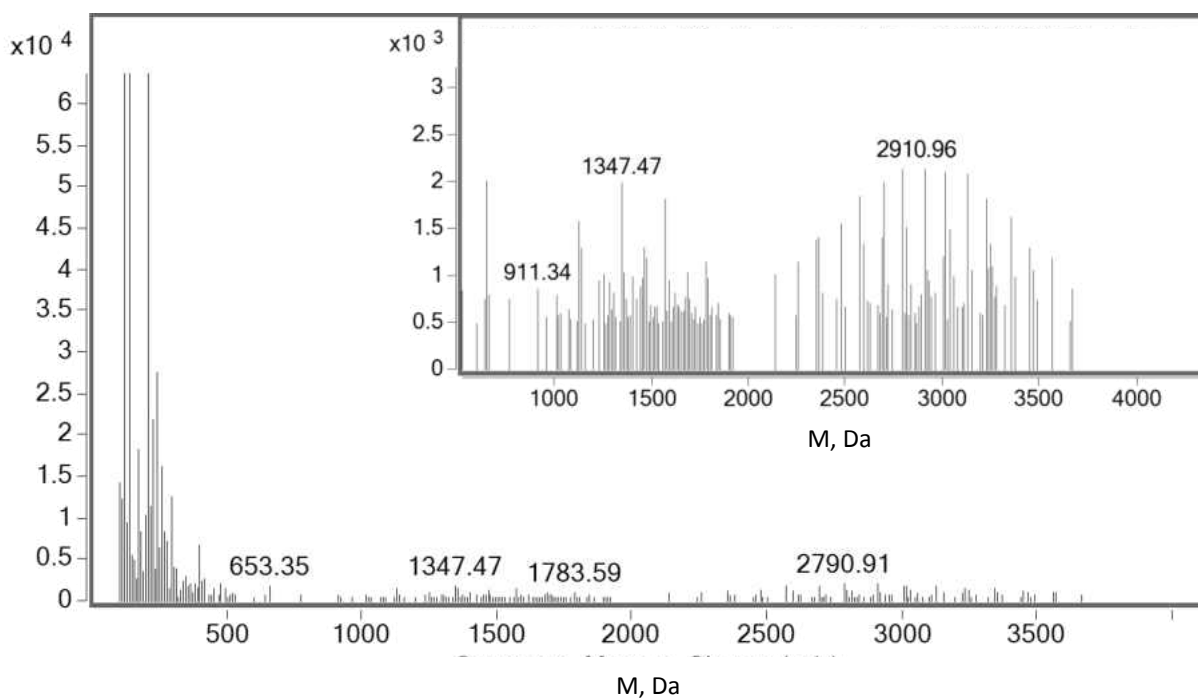


Figure 23. Deconvoluted ESI mass spectrum of a copolymer of styrene oxide and maleic anhydride analyzed by DI ESI HR TOF MS.

Table 13. Molecular weight (Da) of copolymer of styrene oxide and maleic anhydride determined by GPC and ESI HR TOF MS.

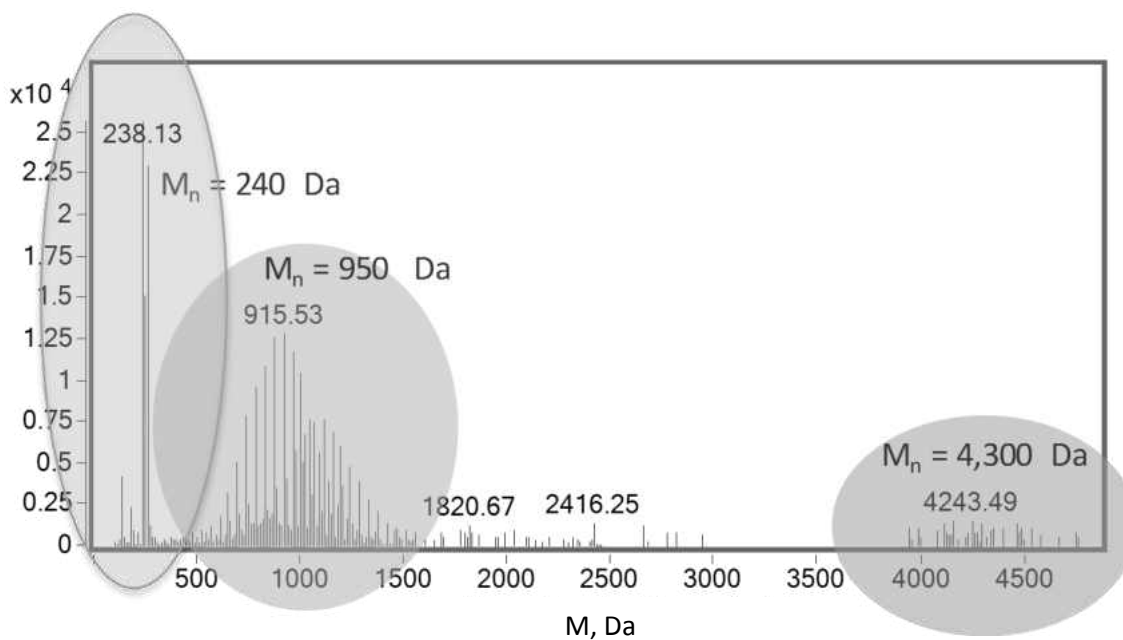
	GPC	ESI HR TOF MS
M_n	2,640	2,340
M_w	3,000	2,600
M_z	3,380	2,790

Thus, the method allowed for a rapid DI analysis with a minimal sample preparation providing an accurate MW distribution. Also, unlike SEC, the MS method is reference-free, thus it does not require a calibration with structurally similar standards.

V.3.2.3. PEG MW Determination via Direct Infusion of a Polymer Mixture

The MW values of PEG standards were determined via DI of a mixture of four standards. Three and two out of four PEG standards were detected by ESI HR TOF MS in mixtures 1 and 2 showing three and two distributions in the deconvoluted mass spectra, respectively (Fig. 24).

a)



b)

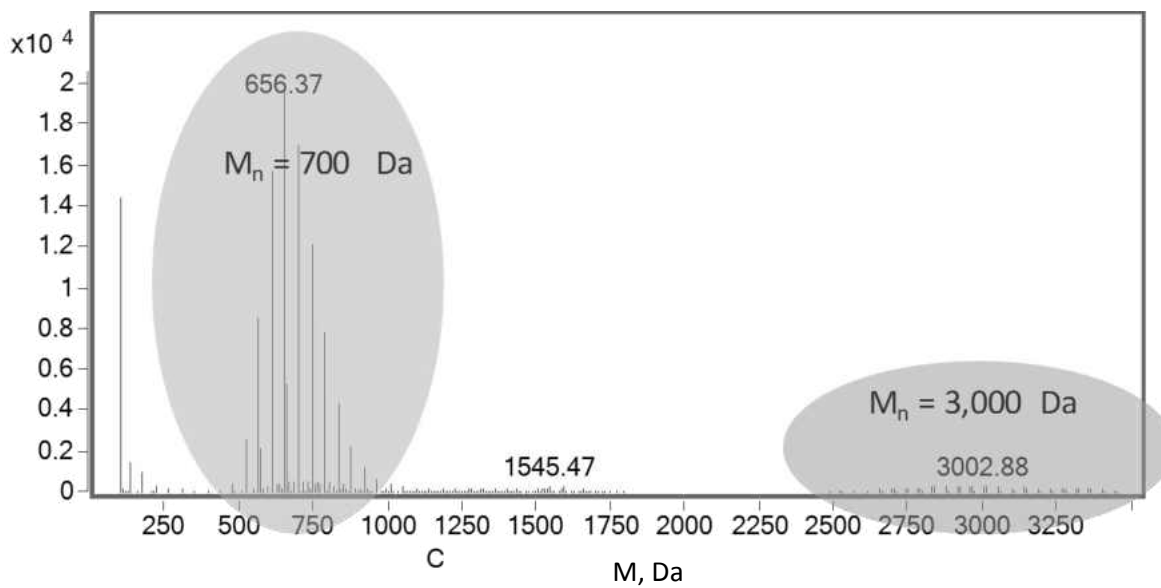


Figure 24. Deconvoluted ESI mass spectrum of PEG standard mixtures a) 1 and b) 2 analyzed by DI ESI HR TOF MS.

The determined M_n and M_w values for the detected standards were in good agreement with those provided by the supplier (Table 14).

Table 14. Molecular weight (M_n / M_w , Da) of PEG narrow MW distribution standards analyzed in a mixture by ESI HR TOF MS and claimed by the supplier.

Determined by ESI HR TOF MS	Provided by the supplier
Mixture 1	
240 / 250	232 / 232
950 / 990	879 / 985
4,300 / 4,310	3,850 / 4,270
Mixture 2	
700 / 710	547 / 636
3,000 / 3,020	2,980 / 3,060

V.3.2.4. PEG MW Determination via RP HPLC of a Polymer Mixture

The MW values of three PEG standards in mixture 3 were determined via RP HPLC with ESI HR TOF MS detection. Three out of four PEG standards were detected in the chromatogram and their MW values were accurately determined upon the corresponding mass spectrum deconvolution. The RP HPLC chromatogram is shown in Appendix J, Fig. J3. Mass spectra prior to and after deconvolution at the retention times of 16.3, 18.1 and 18.8 min corresponding to the PEG standards with the M_n values of 269, 1,380 and 5,610 Da, respectively, claimed by the supplier are shown in Appendix J, Fig. J4. The determined M_n and M_w values were in good agreement with those provided by the supplier (Table 15).

Table 15. Molecular weight (M_n / M_w , Da) of PEG narrow MW distribution standards (mixture 3) analyzed in a mixture by ESI HR TOF MS and claimed by the supplier.

Determined by ESI HR TOF MS	Provided by the supplier
330 / 340	269 / 330
1,470 / 1,500	1,380 / 1,490
6,000 / 6,040	5,610 / 6,510

It is of note that we included only the species of the distribution around 6,000 Da in the deconvoluted mass spectrum for calculating the MW values for the most retained PEG standard with the M_n of 5,610 Da claimed by the supplier. Including the other species that did not belong to the distribution would result in the underestimation of the polymer MW. Those species may be a result of the polymer fragmentation in the source or a partial carryover of the lower MW PEG species.

Thus, the developed ESI HR TOF MS method was successfully applied to characterizing MW of synthetic polymers including PEG, PPG and the synthesized copolymer of styrene oxide and maleic anhydride. The method was applied as a stand-alone MS analysis via direct infusion or in combination with RP HPLC.

CONCLUSIONS

In this dissertation, I have shown the complexity of analyzing lignin and the challenges of its accurate characterization. The ultimate goal of the work was development of methods contributing to lignomics. This was carried out through investigation of separation mechanisms in liquid chromatography, and optimization of conditions for SEC as well as ESI HR-MS. Further investigation of lignin structure was enabled by preparative fractionation of lignin. Finally, we have successfully employed the developed methods in a vast array of areas, demonstrating their applicability.

Liquid Chromatography of Lignin

The detrimental effect of unwanted interactions encountered in SEC of lignin was demonstrated and their sources were identified. Then, an approach to evaluate the applicability of a size exclusion chromatographic system to lignin MW determination was developed through evaluation of the column performance in separation of a suite of mono- to polymeric model compounds. We evaluated several SEC columns with three different stationary phases and showed that the aqueous-based GFC with an HPMA stationary phase (Waters Ultrahydrogel column) was strongly affected by both the polymeric standard nature and model compound functionalities: The separation of the latter occurred based on their pK_a values instead of the MW. The organic solvent-based GPC with THF as a mobile phase was also affected by the chemical nature of polymeric

standards if a column with the GDVB stationary phase (Jordi Gel GBR column) was utilized, however the effect was less pronounced than in GFC. This GPC column did not allow for the size-based separation of the functionality-rich analytes, e.g., lignin structure model compounds. The separation was strongly affected by non-SEC interactions; perhaps, hydrogen bonding occurring when either hydroxylated HPMA or glucose-rich GDVB were used as stationary phases. Thus, the preference in lignin analysis should be given to nonpolar stationary phase materials, which are not prone to hydrogen bonding.

The PSDVB stationary phase (Agilent PLgel 500 Å and 1000 Å columns) showed a correct MW-based separation of various polymeric standards regardless of their nature, as well as of low-MW lignin structure model compounds providing a size-based separation from 150 to 26,000 Da. We proved that PS and PMMA standards could be reliably used for the SEC column calibration if an appropriate stationary phase was utilized. The 5 μm , 1000 Å GPC column provided a better separation of the polymeric standards compared to a 10 μm , 500 Å column showing a prevailing effect of the particle size on the resolution compared to pore size.

The lignin MW was determined utilizing the PLgel 1000 Å column, which was calibrated with both PS and PMMA standards, and the obtained MW values corroborated the MALDI (LDI) results. The obtained M_n value of 1,900 Da was similar to those reported in literature whereas the determined M_w of 3,060 Da was lower than the values reported earlier. These results suggest that lignin is not as highly polymerized as was assumed earlier.

To compare the SEC data with those of MS used as a reference method, we implemented a modified NIST approach¹³⁶ for calculating mean MW values based on MS data. To the best of our knowledge, this method of MW elucidation has not been applied to lignin in the previous studies. The determined number-average MW corroborated the SEC results. We demonstrated an

increase in lignin PDI and MW to unrealistic values as a result of acetylation procedure and proposed an alternate approach to eliminate the acetylation step without sacrificing the lignin solubility in THF-water.

HR MS as a Tool for Lignomics

An ESI TOF MS method for intact lignin analysis was developed allowing for a simultaneous detection of both low and high MW species via direct infusion with minimal sample preparation. The most efficient ionization conditions were achieved in the positive ESI mode with 100 mmol·L⁻¹ formic acid as an electrolyte. For the first time, the formation of multiply charged ions promoting the ionization of high MW lignin species was shown. Determination of multiply charged ions was possible due to an inherently high resolving power of an applied HR TOF mass analyzer. To elucidate MW, the mass spectrum was deconvoluted. The obtained M_n , M_w , and M_z values of 1,480 Da, 2,520 Da and 3,790 Da, respectively, were in good agreement with those determined previously for similar samples by gel permeation chromatography. The presence of multiply charged lignin ions was confirmed by IM MS using ESI IM HR Q-TOF MS. The developed method may extend the lignomics toolkit while targeting higher-MW species.

Lignin Fractionation and Characterization by Preparative SEC

It was shown that intact alkali lignin had impurities of a lower MW, which may have a carbohydrate nature. These impurities unexpectedly elute prior to high MW lignin species in SEC and may skew the determined MW values if the detector rather than DAD is used as a detector. The fractionated lignin features narrower MW distributions with the high MW species occurring

in the first eluted fractions and volatile, low-MW species recovered in the latest SEC fractions. We performed the preliminary evaluation of the particle size distribution in the solution as well as in the dried samples and showed that the separate fractions tend to form nanoparticles of a larger size than intact lignin. Lower MW fractions did not form nanoparticles in the solution and possessed the lowest stability assessed based on the zeta-potential values.

To further understand the chemical composition of each fraction and the pre-eluate, particularly, to confirm the carbohydrate nature of the chemicals occurring in fraction 1, pyr-GC-MS, FTIR, ^1H NMR as well as ^{31}P NMR analyses will be performed in the future work.

Applications of the Developed Methods

The HPLC applicability for polymer analysis as a complement to SEC allowing one to obtain additional information on sample's polarity for a more comprehensive characterization was demonstrated. Useful information on sample polarity of biomodified lignin was collected via RP HPLC. The developed SEC method was applied to the lignin hydrotreated samples and the MW decrease upon thermal treatment with hydrogen peroxide was shown.

The developed ESI HR TOF MS method was successfully applied to characterizing MW of synthetic polymers including PEG, PPG and synthesized copolymer of styrene oxide and maleic anhydride. It allowed for a rapid direct infusion analysis of polymers for MW elucidation with a minimal sample preparation. The method provided an accurate MW distribution, which was confirmed by SEC.

APPENDICES

Appendix A

Low MW species representing lignin used for SEC performance evaluation. Chromatograms of polymeric, low MW lignin model compounds and intact lignin on various SEC columns

Table A1. Low MW species representing lignin with their structures used for the evaluation of the column separation performance.

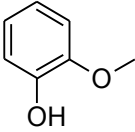
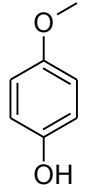
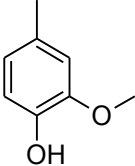
	Compounds	Class of methoxy-phenols (extra functional groups)	Molecular Formula	Chemical Structure	MW (g·mol ⁻¹)	pK _a	Supplier/ Synthesized	Purity
1	Guaiacol	G	C ₇ H ₈ O ₂		124.24	9.93	Acros Organics ^a	≥99%
2	<i>p</i> -Guaiacol	G	C ₇ H ₈ O ₂		124.24	9.90	Pfaltz and Bauer ^b	99%
3	Creosol	alkyl-G	C ₈ H ₁₀ O ₂		138.16	10.34	Sigma-Aldrich ^c	≥98%

Table A1. cont.

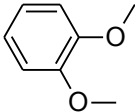
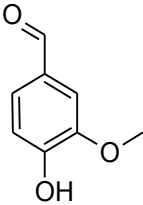
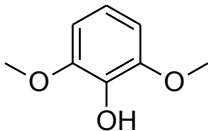
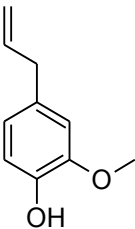
	Compounds	Class of methoxy-phenols (extra functional groups)	Molecular Formula	Chemical Structure	MW (g·mol⁻¹)	pK_a	Supplier/ Synthesized	Purity
4	Veratrole	–	C ₈ H ₁₀ O ₂		138.16	~40	Sigma-Aldrich	99%
5	Vanillin	carbonyl-G	C ₈ H ₈ O ₃		152.15	7.38	Sigma-Aldrich	99%
6	Syringol	methoxy-G	C ₈ H ₁₀ O ₃		154.16	9.98	Acros Organics	99%
7	Eugenol	alkenyl-G	C ₁₀ H ₁₂ O ₂		164.20	10.19	Acros Organics	99%

Table A1. cont.

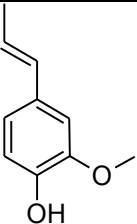
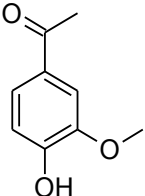
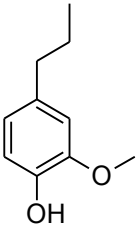
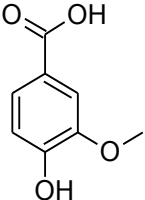
Compounds	Class of methoxy-phenols (extra functional groups)	Molecular Formula	Chemical Structure	MW (g·mol ⁻¹)	pK _a	Supplier/ Synthesized	Purity	
8	Isoeugenol	alkenyl-G	C ₁₀ H ₁₂ O ₂		164.20	9.89	Sigma-Aldrich	98.8%
9	4'-Hydroxy-3'-methoxyacetophenone	carbonyl-G	C ₉ H ₁₀ O ₃		166.17	7.81	Sigma-Aldrich	98%
10	4-Propylguaiacol	alkyl-G	C ₁₀ H ₁₄ O ₂		166.22	10.29	Sigma-Aldrich	≥99%
11	Vanillic acid	carboxyl-G	C ₈ H ₈ O ₄		168.15	4.45	Fluka ^d	97%

Table A1. cont.

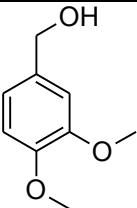
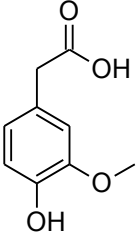
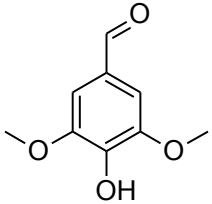
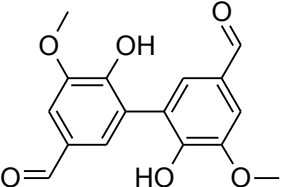
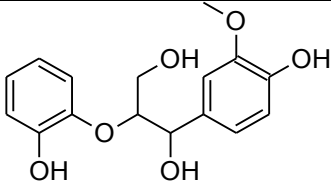
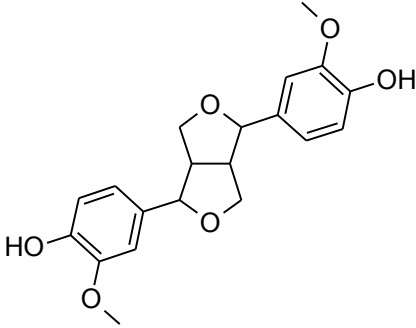
Compounds	Class of methoxy-phenols (extra functional groups)	Molecular Formula	Chemical Structure	MW (g·mol ⁻¹)	pK _a	Supplier/ Synthesized	Purity	
12	Veratrole alcohol	–	C ₉ H ₁₂ O ₃		168.19	>16	Sigma-Aldrich	96%
13	Homovanillic acid	carboxyl-G	C ₉ H ₁₀ O ₄		182.15	4.41	Acros Organics	98%
14	Syringaldehyde	carbonyl-G	C ₉ H ₁₀ O ₄		182.17	7.8	Sigma-Aldrich	98%
15	Dehydrodivanillin	carbonyl-G	C ₁₆ H ₁₄ O ₆		302.07	7.04	In-house synthesis based on ^{124, 128} .	≥95%

Table A1. cont.

Compounds	Class of methoxy-phenols (extra functional groups)	Molecular Formula	Chemical Structure	MW (g·mol ⁻¹)	pK _a	Supplier/ Synthesized	Purity	
16	Guaiacylglycerol- β -guaiacyl ether	≥ 2 hydroxy-G	C ₁₇ H ₂₀ O ₆		320.34	9.88	In-house synthesis based on ¹²⁶ .	$\geq 95\%$
17	Pinoresinol	≥ 2 hydroxy-G	C ₂₀ H ₂₂ O ₆		358.38	9.76	Sigma-Aldrich ^c	$\geq 95\%$

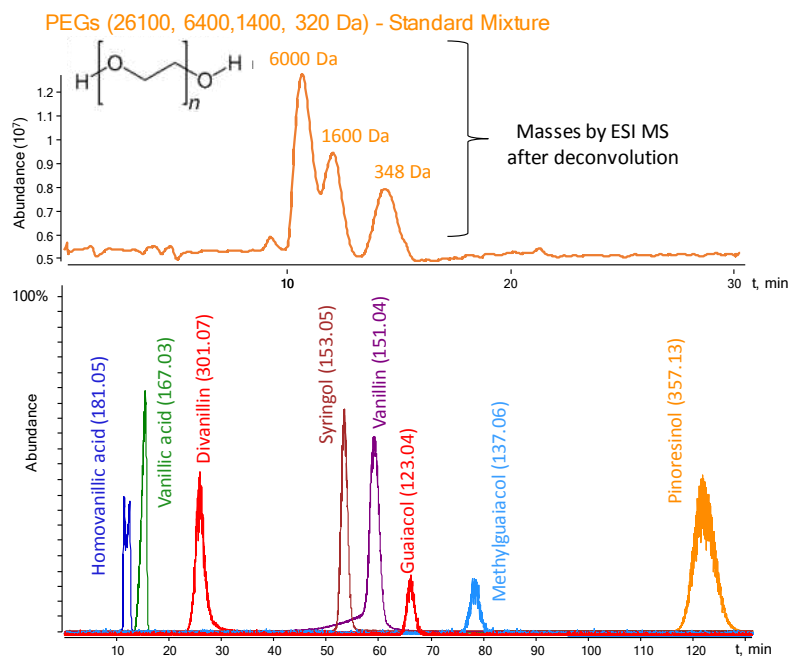
^a Acros Organics (Morris Plains, NJ, USA)

^b Pfaltz and Bauer (Waterbury, CT, USA)

^c Sigma-Aldrich (St. Louis, MO, USA)

^d Fluka (Steinheim, Germany)

a) HPMA



b) GDVB

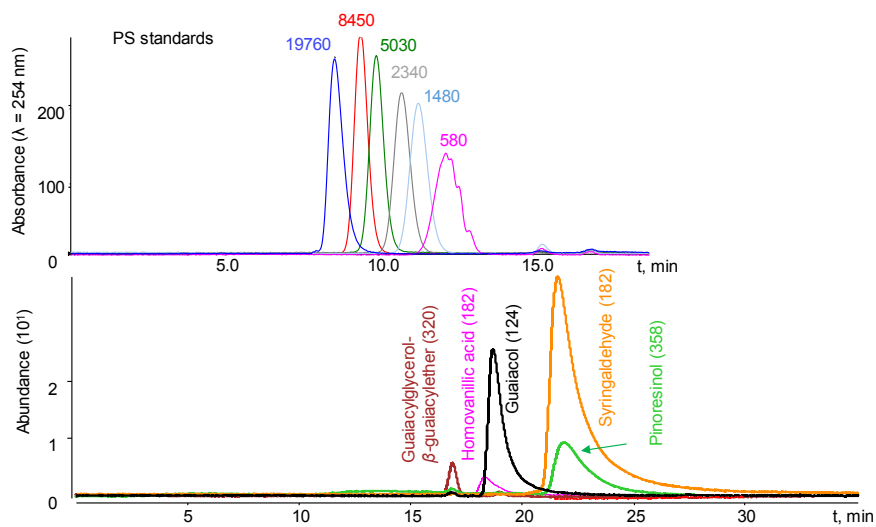


Figure A1. Overlaid DAD chromatograms of lignin structure model compounds and polymeric standards on various stationary phases: a) HPMA; b) GDVB; c) PSDVB.

Figure A1 cont.

c) PSDVB

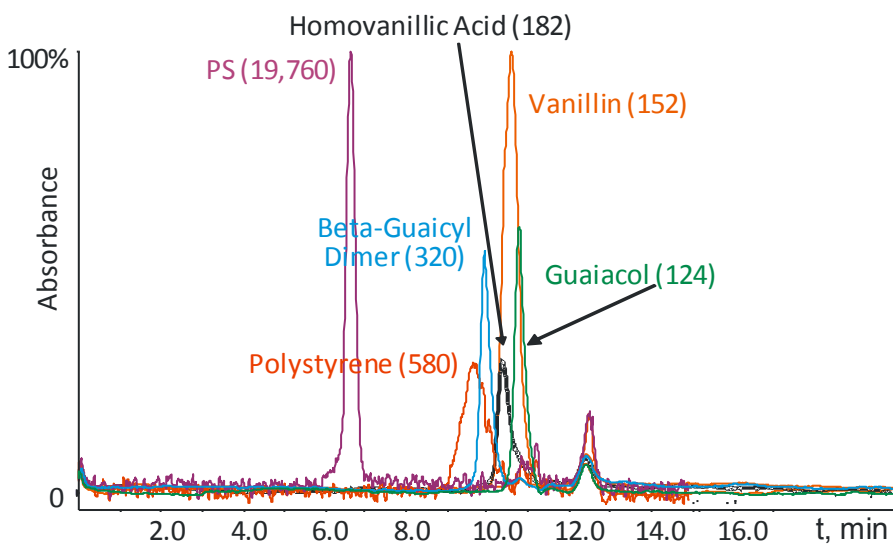
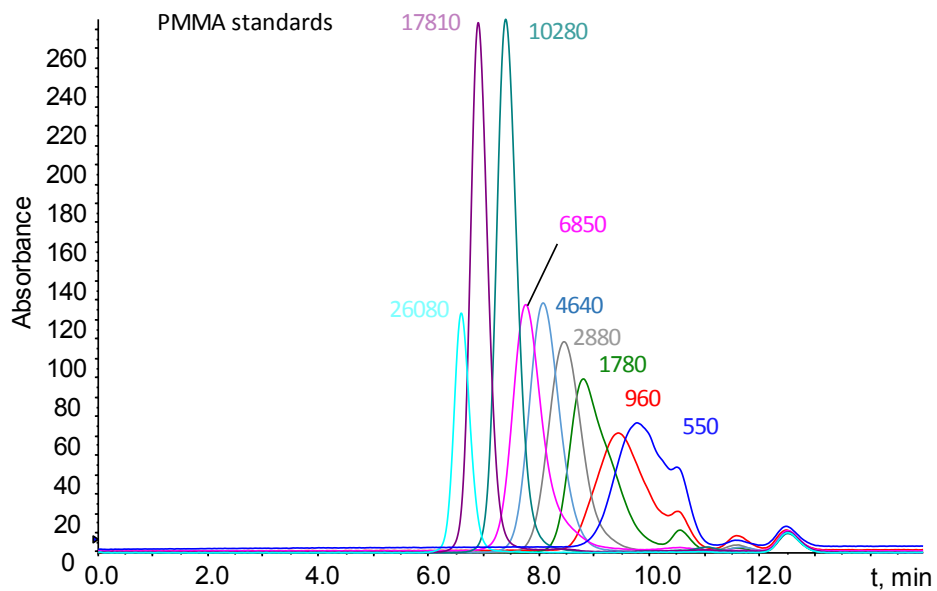
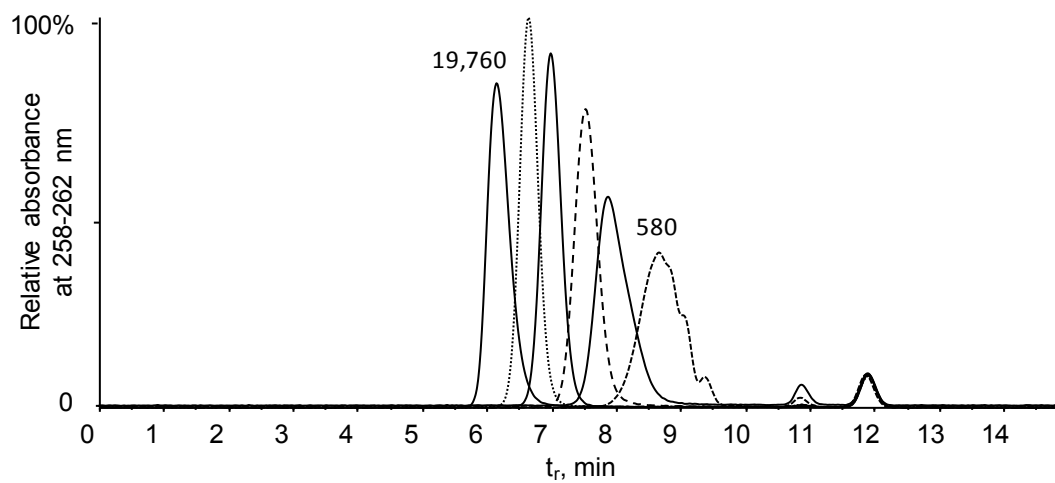


Figure A1. Overlaid DAD chromatograms of lignin structure model compounds and polymeric standards on various stationary phases: a) HPMA; b) GDVB; c) PSDVB.

a)



b)

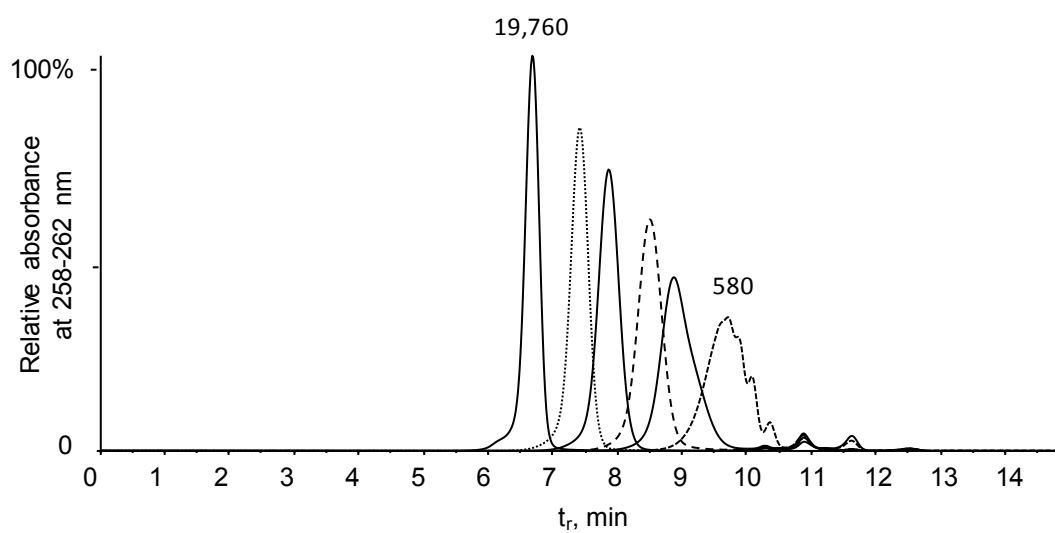


Figure A2. Overlaid DAD chromatograms of PS standards (580–19760 Da) analyzed on (a) the PLgel 500 Å and (b) the PLgel 1000 Å columns.

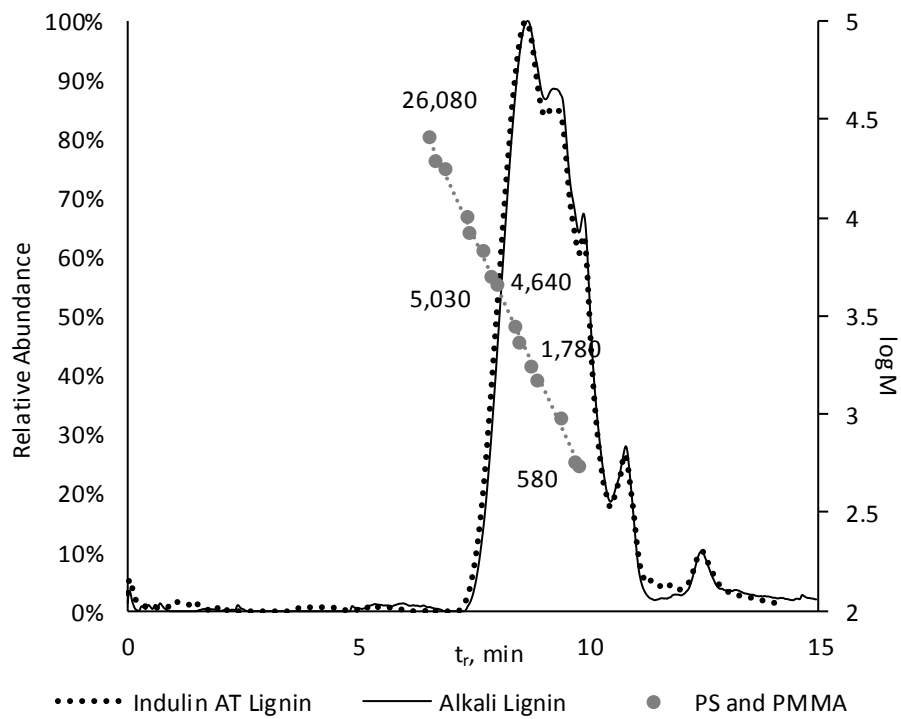


Figure A3. Alkali and Indulin AT lignin elution profiles on the PSDVB stationary phase (the PLgel 1000 Å column).

Appendix B

MALDI mass spectra of alkali lignin recorded in the presence of various matrices

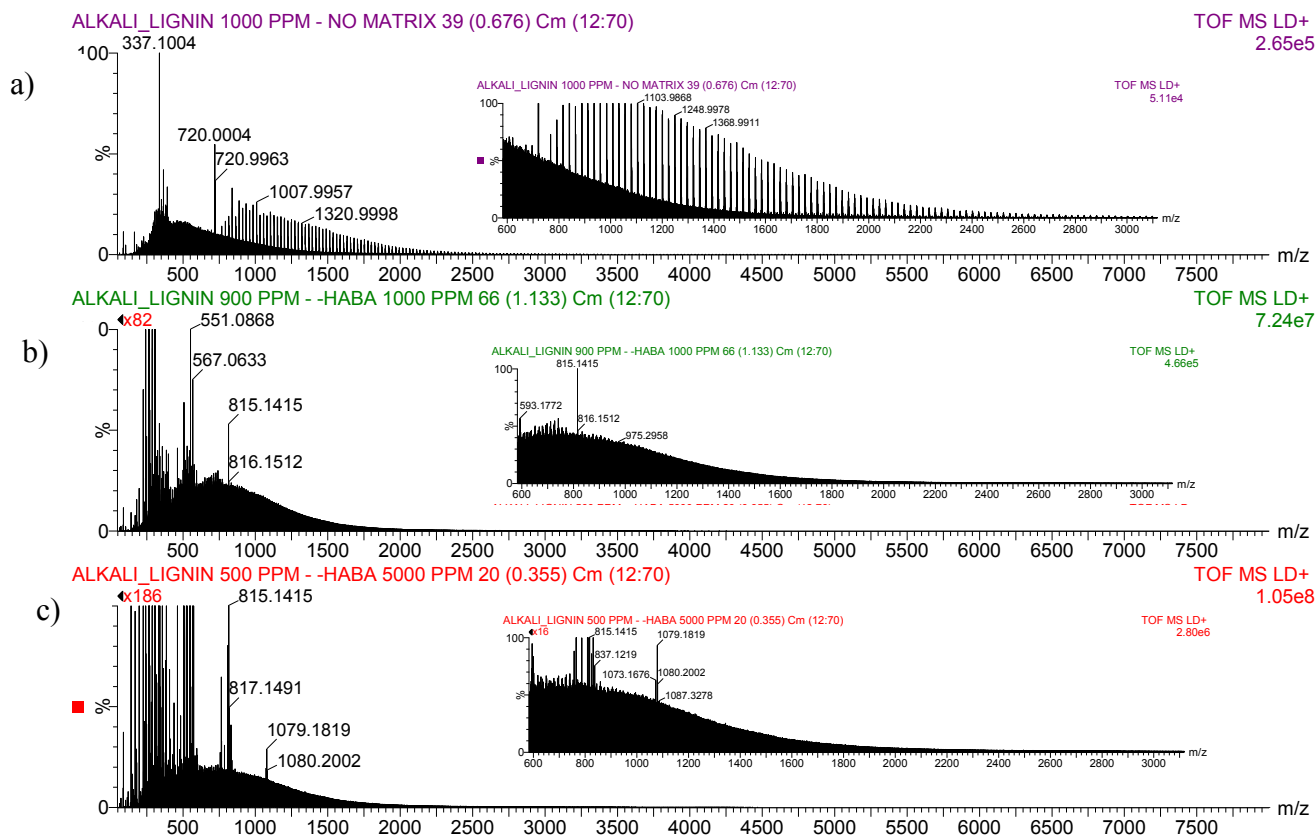


Figure B1. MALDI mass spectrum of alkali lignin with various matrices: a) without a matrix; b) 2-(4-hydroxyphenylazo)benzoic acid (ration with lignin 1:1); c) 2-(4-hydroxyphenylazo)benzoic acid (10-times excess compared to lignin); d) 2-(4-hydroxyphenylazo)benzoic acid (5-times excess compared to lignin); e) α -cyano-4-hydroxycinnamic acid (5-times excess compared to lignin).

Figure B1 cont.

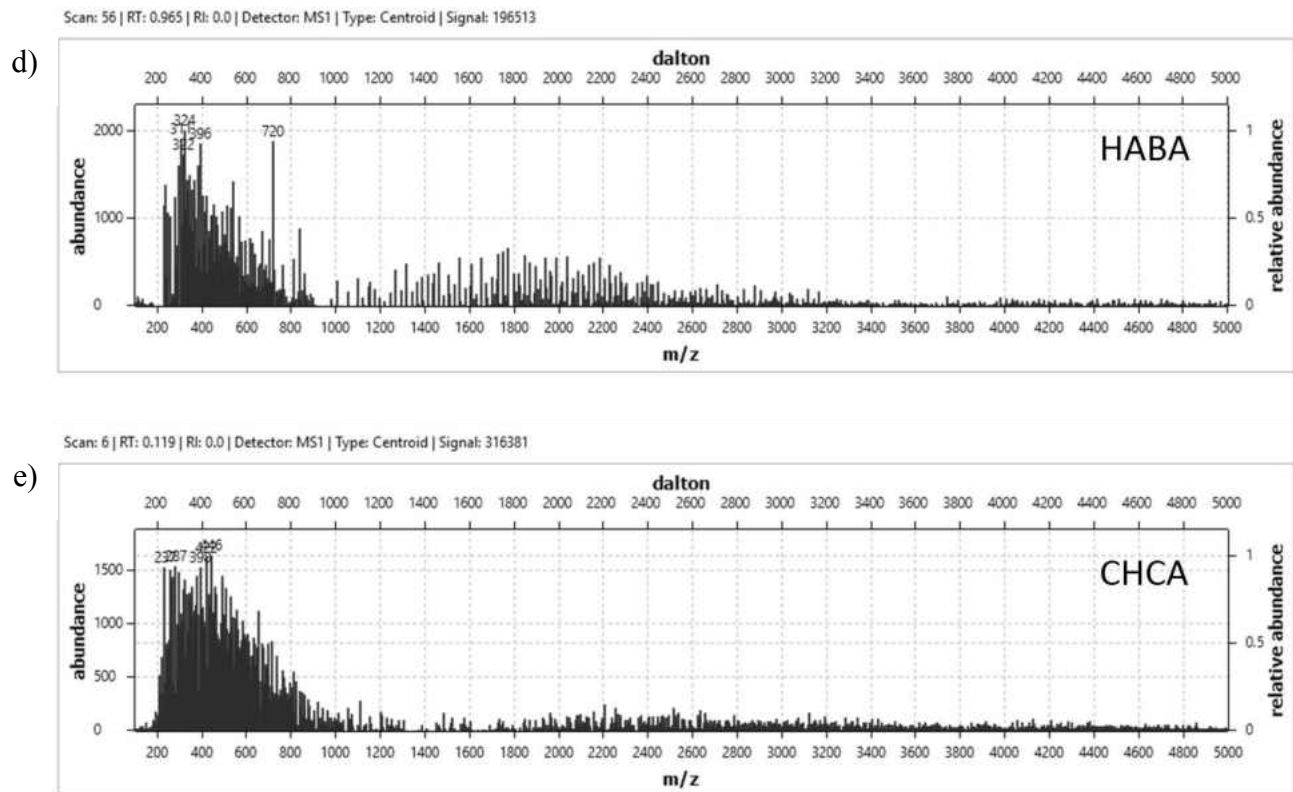
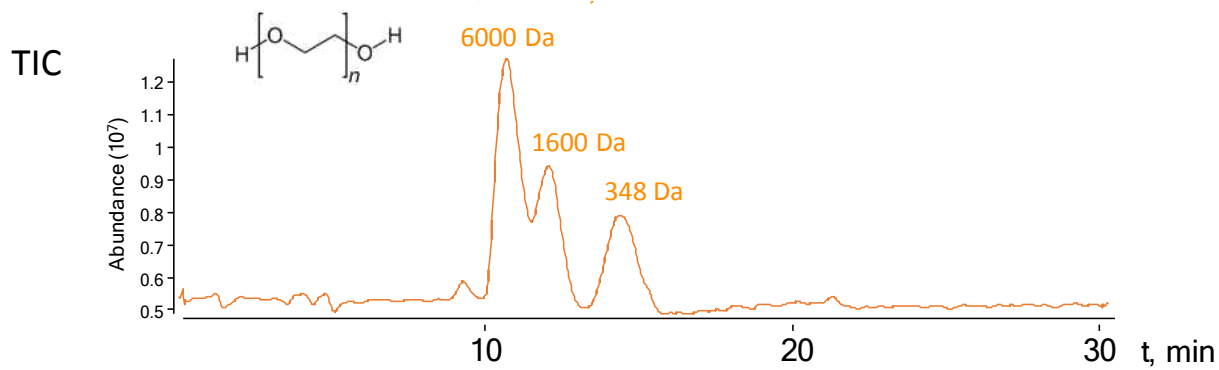


Figure B1. MALDI mass spectrum of alkali lignin with various matrices: a) without a matrix; b) 2-(4-hydroxyphenylazo)benzoic acid (ration with lignin 1:1); c) 2-(4-hydroxyphenylazo)benzoic acid (10-times excess compared to lignin); d) 2-(4-hydroxyphenylazo)benzoic acid (5-times excess compared to lignin); e) α -cyano-4-hydroxycinnamic acid (5-times excess compared to lignin).

Appendix C

Chromatograms of polymeric and low-MW model compounds

a)



b)

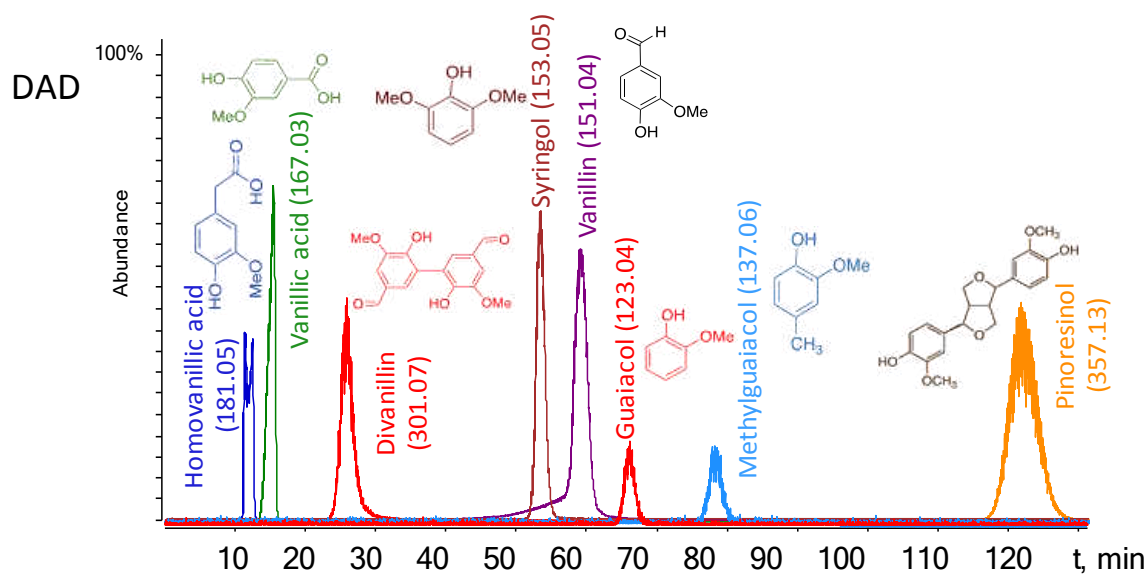
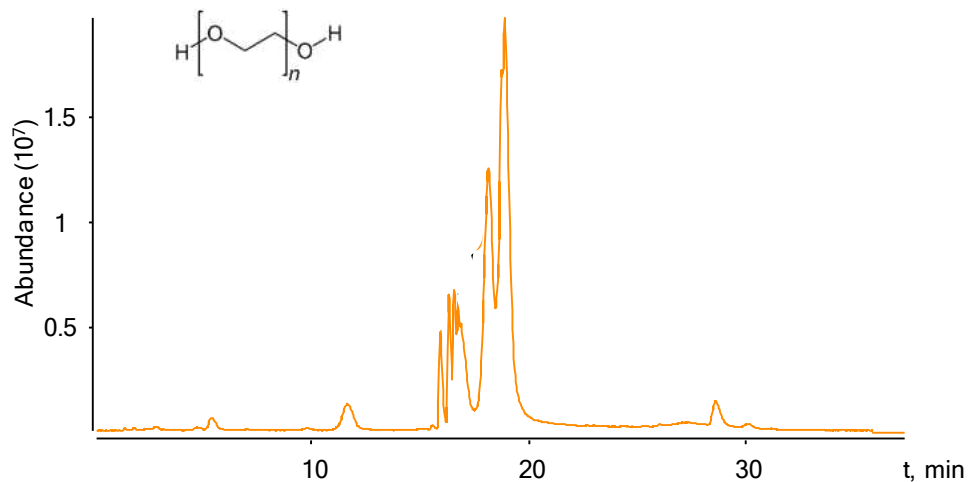


Figure C1. a) TIC chromatogram of PEG standards (26100, 6400, 1400 and 320 Da) and b) overlaid DAD chromatograms of low MW lignin model compounds analyzed on GFC Ultrahydrogel 120 Å column.

a)



b)

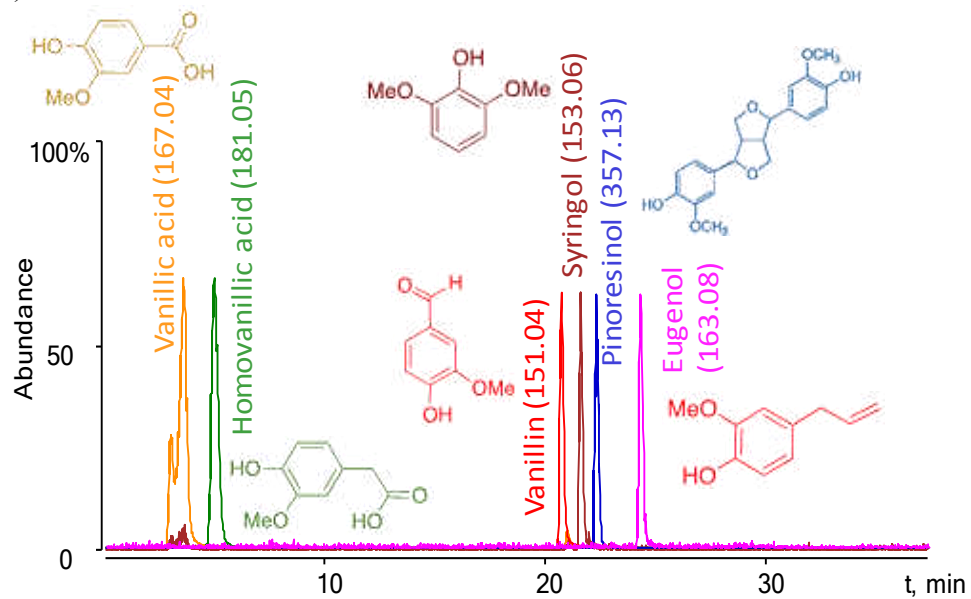


Figure C2. a) TIC chromatogram of PEG standards (26100, 6400, 1400 and 320 Da) and b) overlaid DAD chromatograms of low MW lignin model compounds analyzed on Zorbax Eclipse Plus C18 column with pore size 95 Å.

Appendix D

Table D1. Lignin model compounds and their structures employed in ESI HR MS optimization.

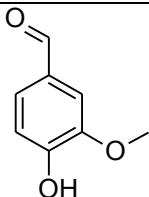
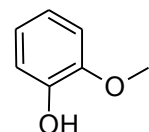
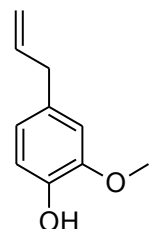
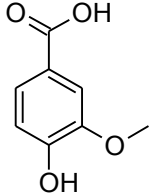
Compounds	Acronym	Chemical Structure	MW (g·mol ⁻¹)	Supplier/Synthesized	Purity
Vanillin	V		152.15	Sigma-Aldrich ^a	99%
Guaiacol	G		124.24	Sigma-Aldrich	98%
Eugenol	E		164.20	Acros Organics ^b	99%
Vanillic acid	VA		168.15	Fluka ^c	97%

Table D1. cont.

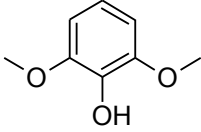
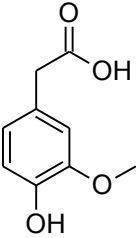
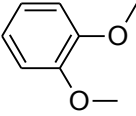
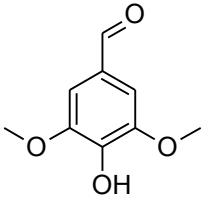
Compounds	Acronym	Chemical Structure	MW (g·mol ⁻¹)	Supplier/Synthesized	Purity
Syringol	S		154.16	Acros Organics	99%
Homovanillyl alcohol	HA		168.19	Sigma-Aldrich	99%
Veratrole	VER		138.16	Sigma-Aldrich	99%
Syringaldehyde	SA		182.17	Sigma-Aldrich	98%

Table D1. cont.

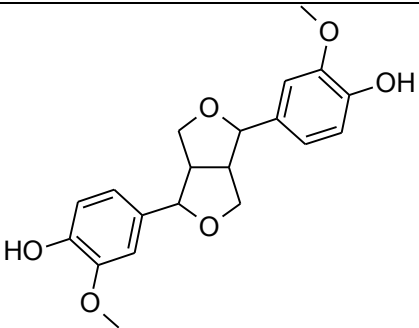
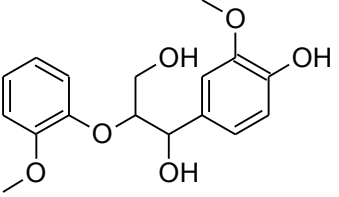
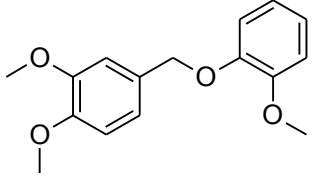
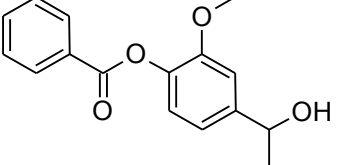
Compounds	Acronym	Chemical Structure	MW (g·mol ⁻¹)	Supplier/Synthesized	Purity
Pinoresinol	P2		358.38	Sigma-Aldrich	≥95%
Guaiacylglycerol-β-guaiacyl ether	G-β-2		320.34	In-house synthesis based on ¹²⁶ .	≥95%
1,2-Dimethoxy-4-[(2-methoxyphenoxy)methyl]benzene (henceforth called the ether dimer)	ET2		274.12	In-house synthesis based on ¹³⁷ .	≥95%
4-(1-Hydroxyethyl)-2-methoxyphenyl benzoate (henceforth called the alcohol dimer)	ALC2		272.10	In-house synthesis based on ¹³⁷ .	≥95%

Table D1. cont.

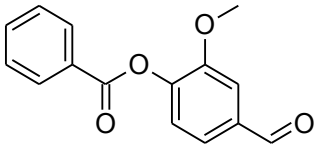
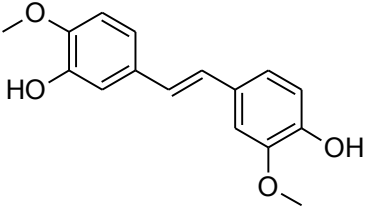
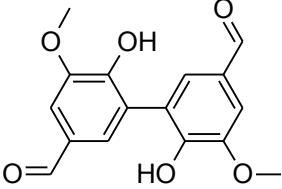
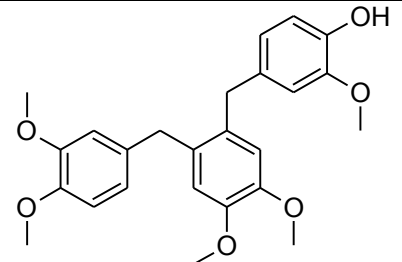
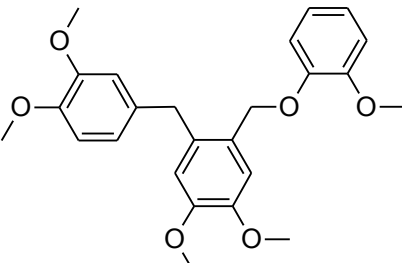
Compounds	Acronym	Chemical Structure	MW (g·mol ⁻¹)	Supplier/Synthesized	Purity
4-Formyl-2-methoxyphenyl benzoate (henceforth called the ester dimer)	EST2		256.07	In-house synthesis based on ¹³⁷ .	≥95%
(<i>E</i>)-4,4'-(Ethene-1,2-diyl)bis(2-methoxyphenol) (henceforth called the alkene dimer)	ALK2		272.10	In-house synthesis based on ¹³⁷ .	≥95%
Dehydrodivanillin	D2V		302.07	In-house synthesis based on ^{124, 128} .	≥95%

Table D1. cont.

Compounds	Acronym	Chemical Structure	MW (g·mol ⁻¹)	Supplier/Synthesized	Purity
4-[2-(3,4-Dimethoxybenzyl)-4,5-dimethoxybenzyl]-2-methoxyphenol and 1-(3,4-dimethoxybenzyl)-4,5-dimethoxy-2-[(2-methoxyphenoxy)methyl]benzene (henceforth called the ether trimers)	ET3-1		424.19	In-house synthesis based on ¹³⁷ .	≥95%
	ET3-2				

^a Sigma-Aldrich (St. Louis, MO, USA)

^b Acros Organics (Morris Plains, NJ, USA)

^c Fluka (Steinheim, Germany)

Appendix E

Table E1. The response (peak area) for target ion $[M+H]^+$ ($155.070 \pm 0.030 m/z$) via FIA of 5 ppm syringol in MeOH/Water (1:1) analyzed in the positive ionization mode.

Ionization source	Electrolyte, concentration in sample/mobile phase, mmol·L ⁻¹	Flow rate, mL·min ⁻¹	Responses	
			Sample contains electrolyte	Mobile phase contains electrolyte
ESI	ammonium acetate, 12.5/2.5	0.2	$12.5 \cdot 10^6$	$13.6 \cdot 10^6$
ESI	ammonium acetate, 15 /2.5	0.3	$7.8 \cdot 10^6$	$7.9 \cdot 10^6$
APCI	formic acid 25/5	0.2	$7.8 \cdot 10^6$	$7.9 \cdot 10^6$

Appendix F

Calibration of ESI TOF MS with cesium iodide to minimize mass error at the extended m/z range

n	M (CsI)n	(CsI)nCs+	n	M (CsI)n	(CsI)nCs+
1	259.8099	392.7148	16	4156.959	4289.864
2	519.6199	652.5248	17	4416.769	4549.674
3	779.4298	912.3347	18	4676.579	4809.484
4	1039.24	1172.145	19	4936.389	5069.293
5	1299.05	1431.955	20	5196.199	5329.103
6	1558.86	1691.764	21	5456.008	5588.913
7	1818.669	1951.574	22	5715.818	5848.723
8	2078.479	2211.384	23	5975.628	6108.533
9	2338.289	2471.194	24	6235.438	6368.343
10	2598.099	2731.004	25	6495.248	6628.153
11	2857.909	2990.814	26	6755.058	6887.963
12	3117.719	3250.624	27	7014.868	7147.773
13	3377.529	3510.434	28	7274.678	7407.583
14	3637.339	3770.244	29	7534.488	7667.393
15	3897.149	4030.054	30	7794.298	7927.203
16	4156.959	4289.864	31	8054.108	8187.013
17	4416.769	4549.674	32	8313.918	8446.823

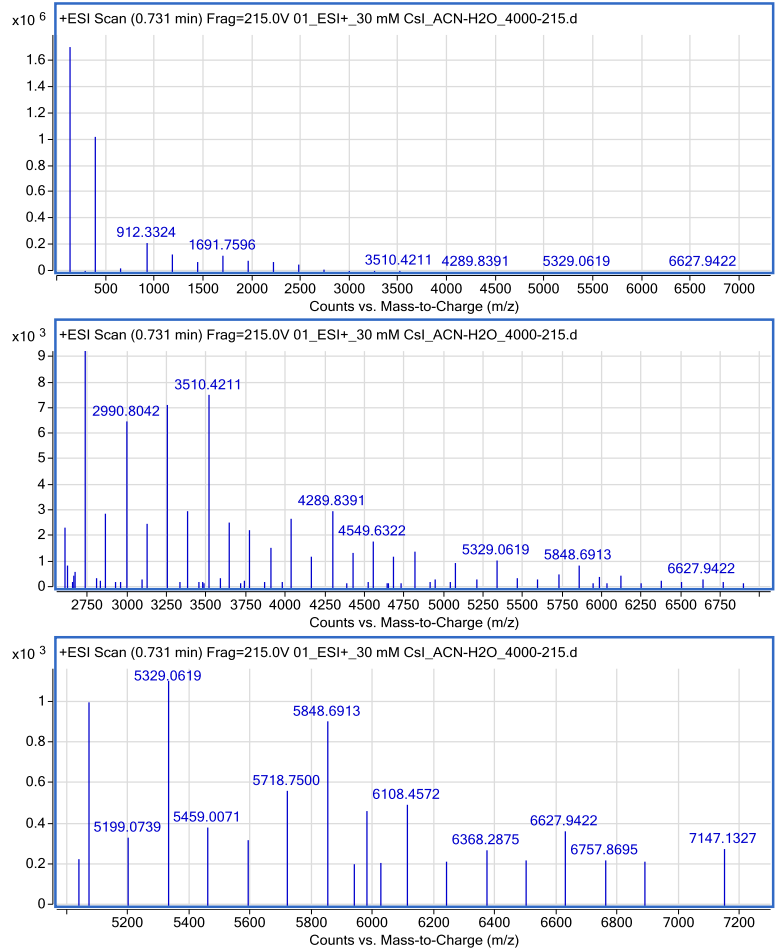


Figure F1. Molecular weight of $(CsI)_n$ clusters and calculated masses of the corresponding $[(CsI)_n + Cs]^+$ ion clusters and their ESI positive mass spectra: Full scale (50–7,500 m/z); zoomed in (2,500–7,000 m/z) and 5,000–7,200 m/z .

Appendix G

ESI mass spectra of lignin in a THF-water solvent system

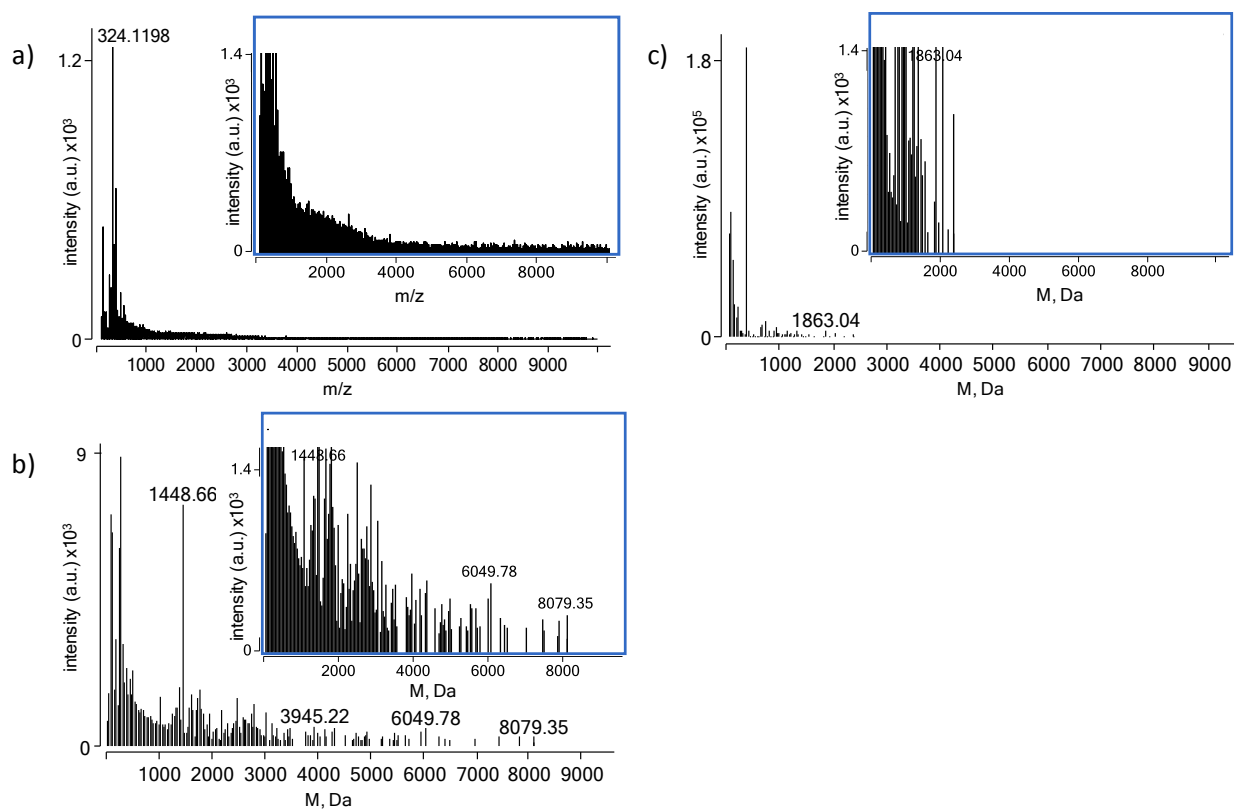


Figure G1. Positive ESI mass spectra of (a, b) a 90 ppm solution of intact lignin in THF-water (1:1) with $100 \text{ mmol}\cdot\text{L}^{-1}$ formic acid and (c) the same solution without lignin, i.e., blank. a) Raw alkali lignin spectrum after blank subtraction; b) deconvoluted lignin spectrum after blank subtraction; and c) deconvoluted spectrum of the blank.

Appendix H

Preparative SEC: SEC system calibration, lignin fractionation and analysis of the fractions

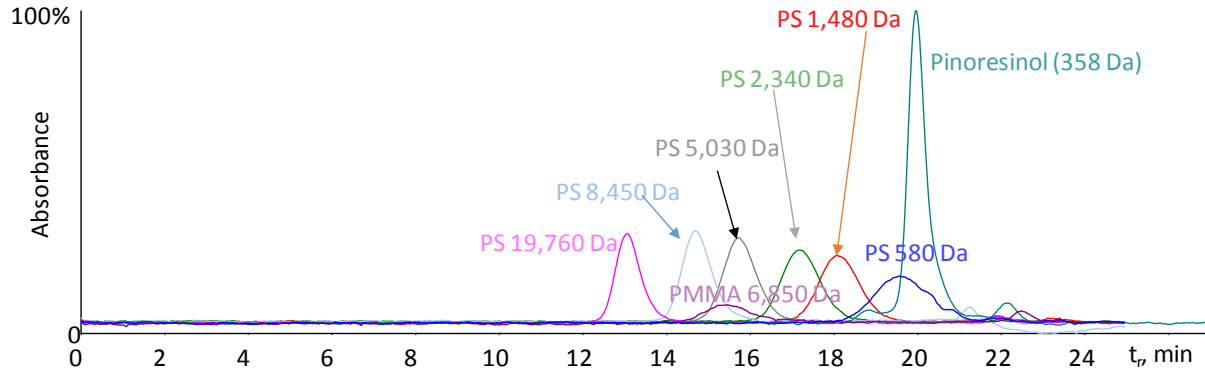
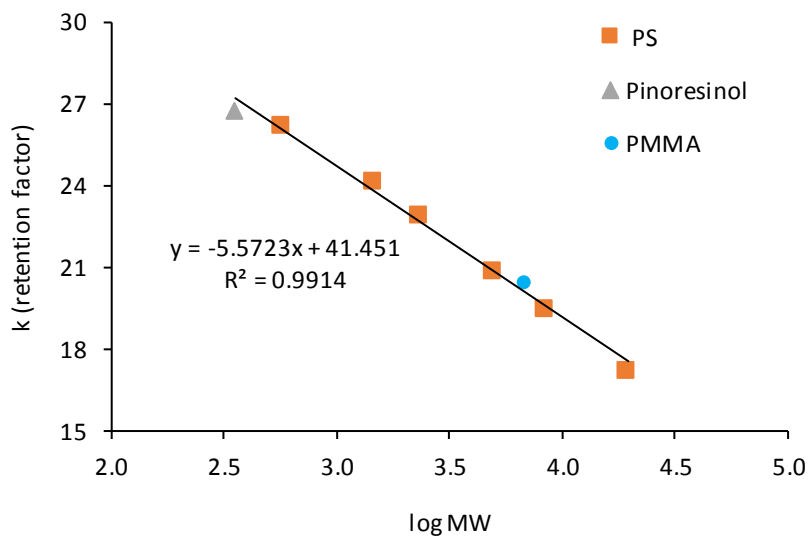


Figure H1. Overlaid DAD chromatograms of PS standards (580–19,760 Da) and pinoresinol analyzed on the preparative PLgel 1000 Å SEC column.

a)



b)

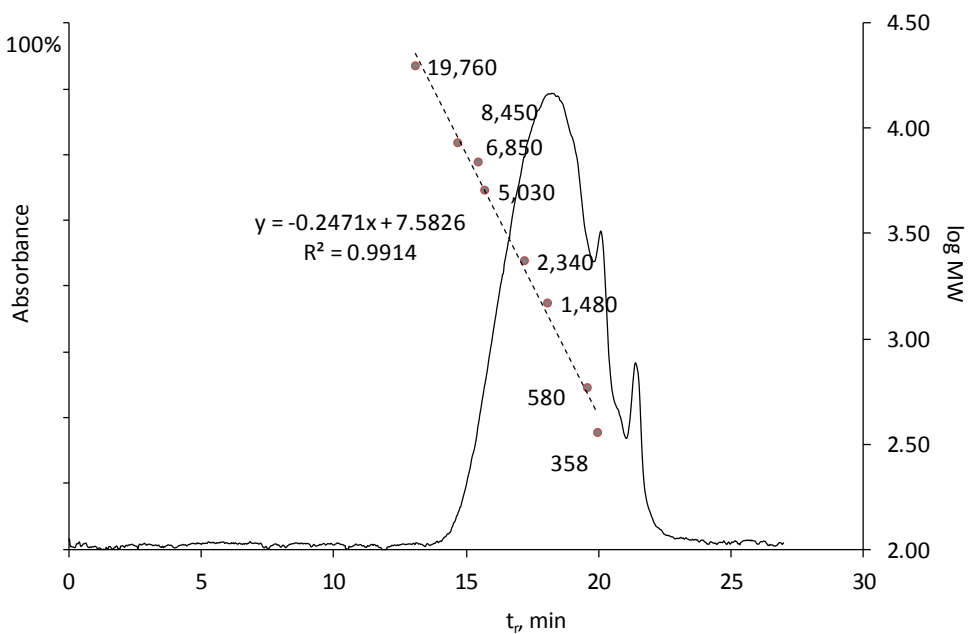


Figure H2. a) Retention factor (k) of PS, PMMA and pinoresinol vs. log MW in preparative SEC; b) log MW vs. retention time of PS, PMMA and pinoresinol

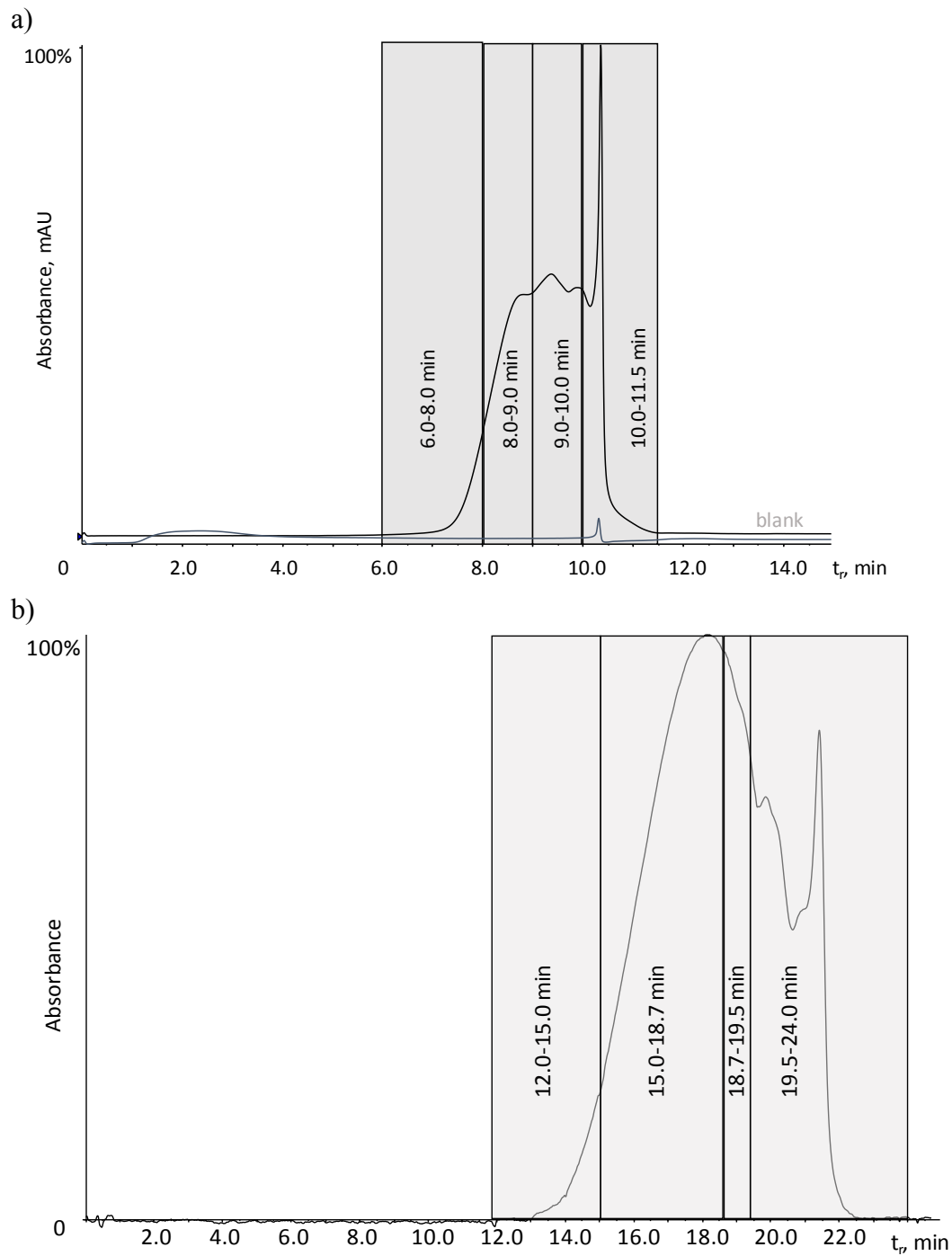


Figure H3. Fractionation experiments performed utilizing a) an analytical SEC 1000 Å PLgel column and b-e) preparative PLgel 1000 Å SEC column with fraction collected in the various retention time windows.

Figure H3 cont.

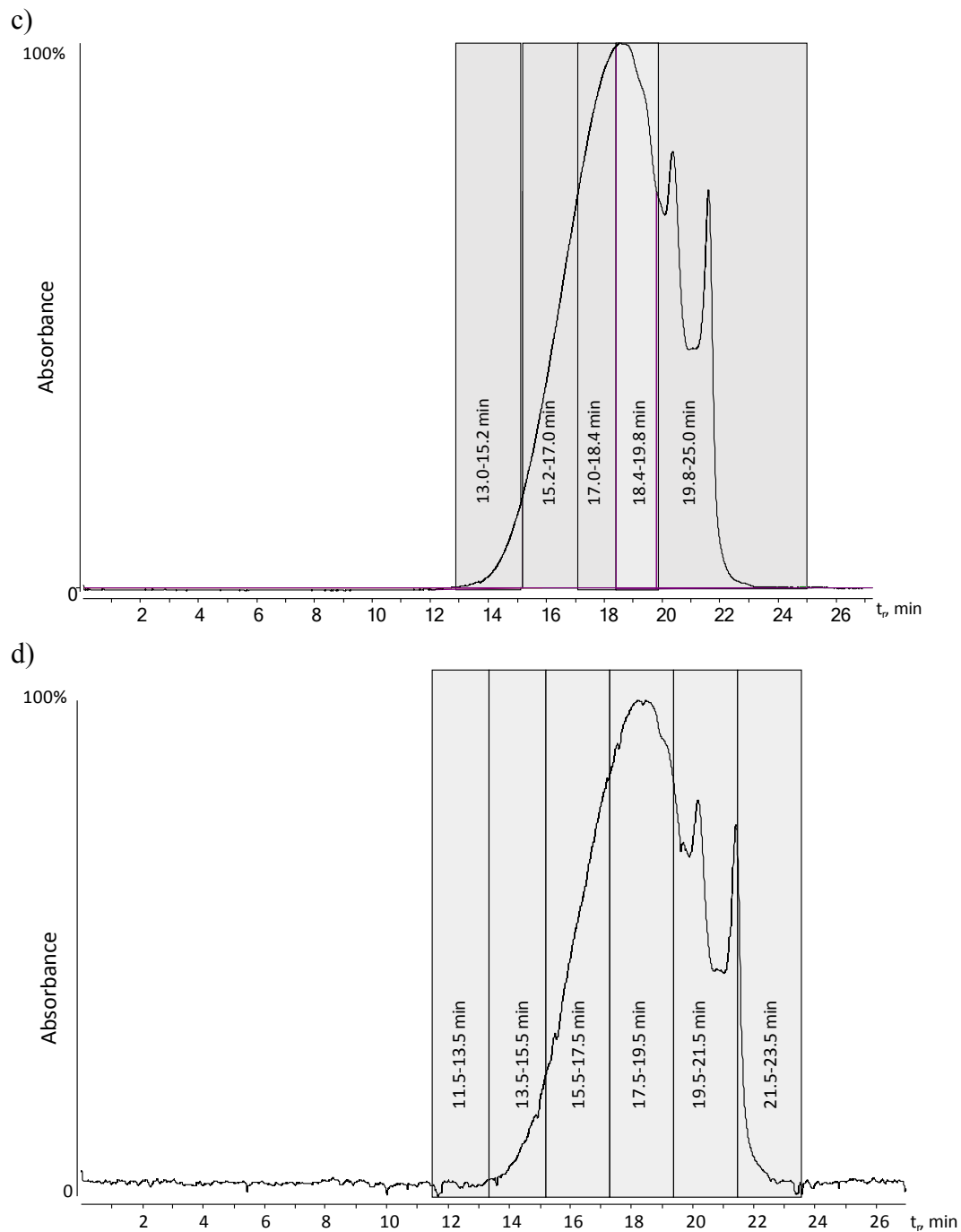


Figure H3. Fractionation experiments performed utilizing a) an analytical SEC 1000 Å PLgel column and b-e) preparative PLgel 1000 Å SEC column with fraction collected in the various retention time windows.

Figure H3 cont.

e)

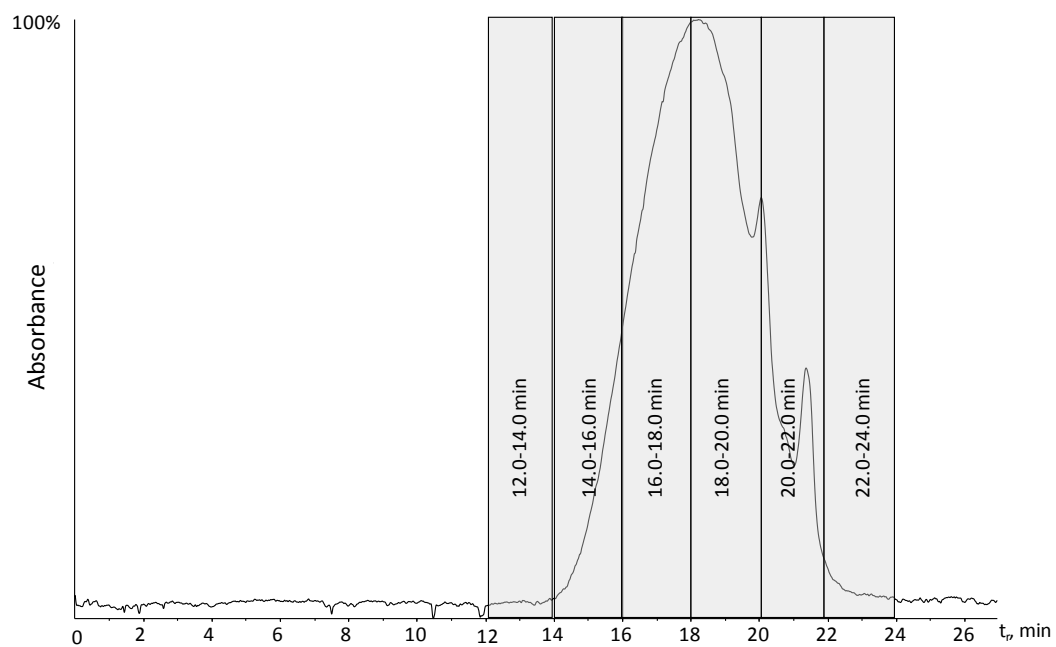


Figure H3. Fractionation experiments performed utilizing a) an analytical SEC 1000 Å PLgel column and b-e) preparative PLgel 1000 Å SEC column with fraction collected in the various retention time windows.

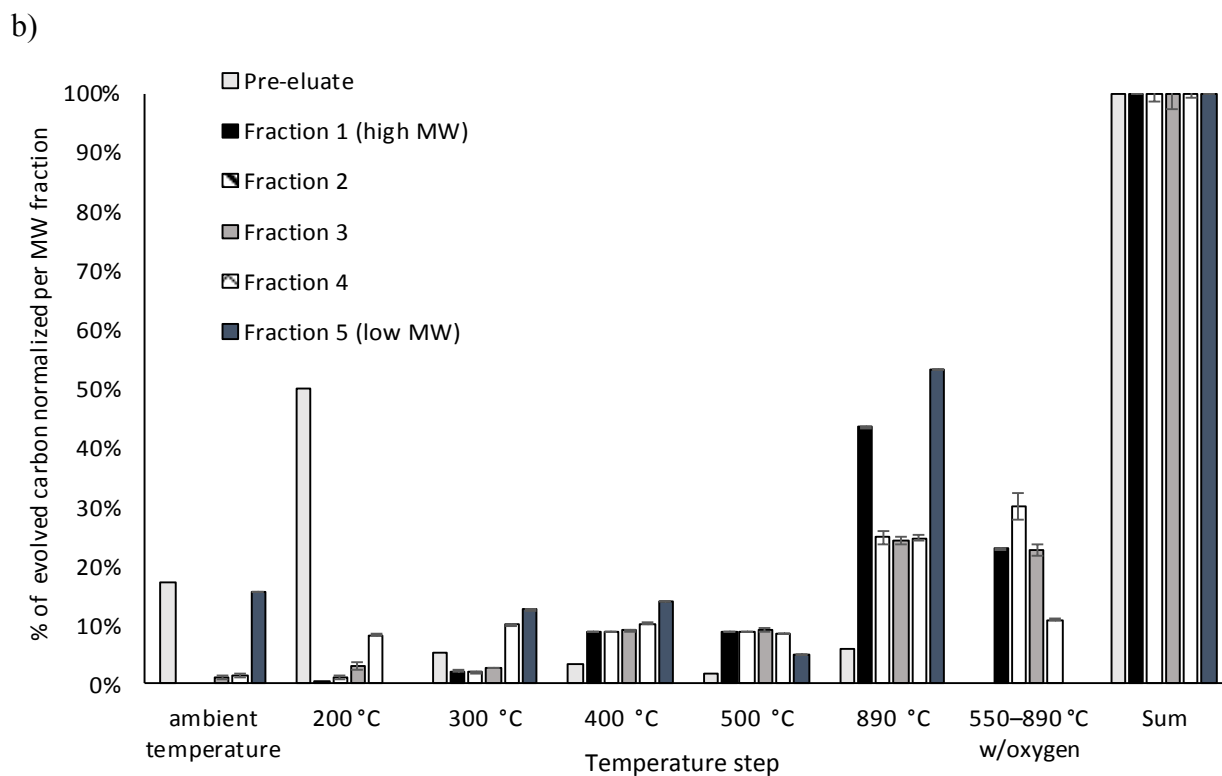
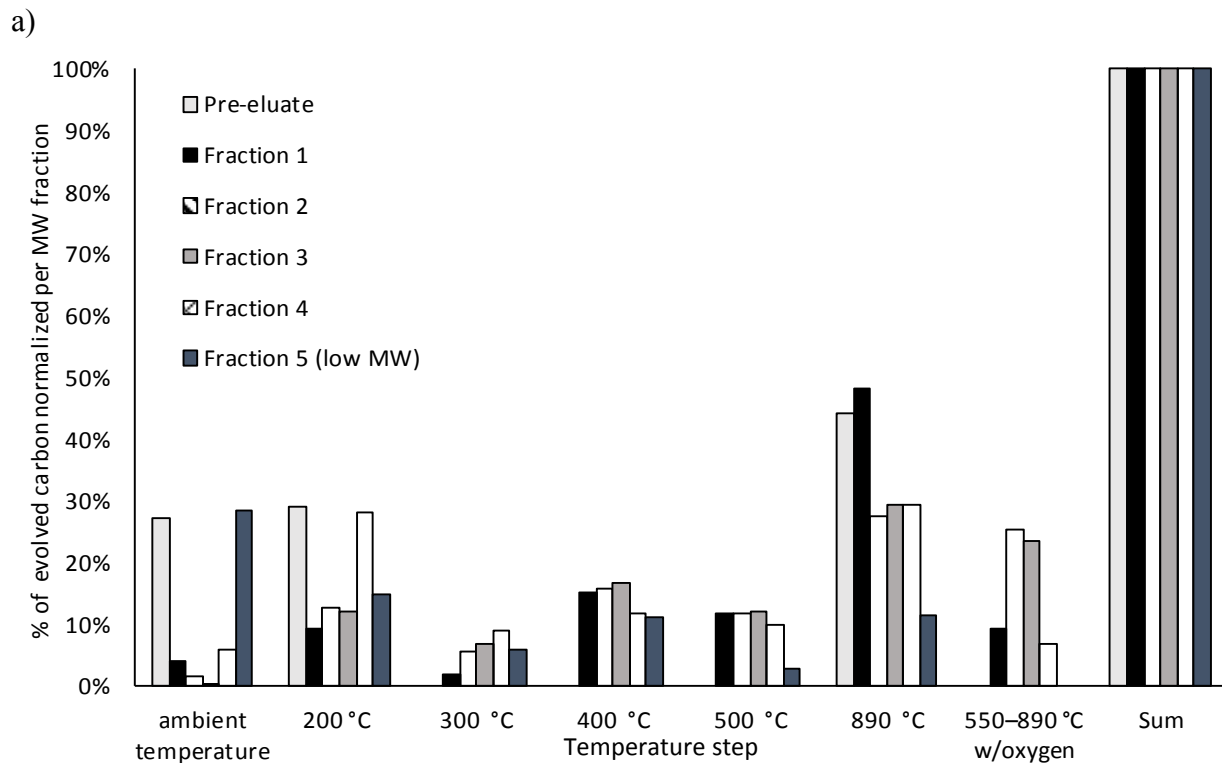


Figure H4. TCA profiles normalized per each lignin MW fraction obtained by fractionation employing the preparative SEC for a) fresh sample; b) aged over 3 month sample.

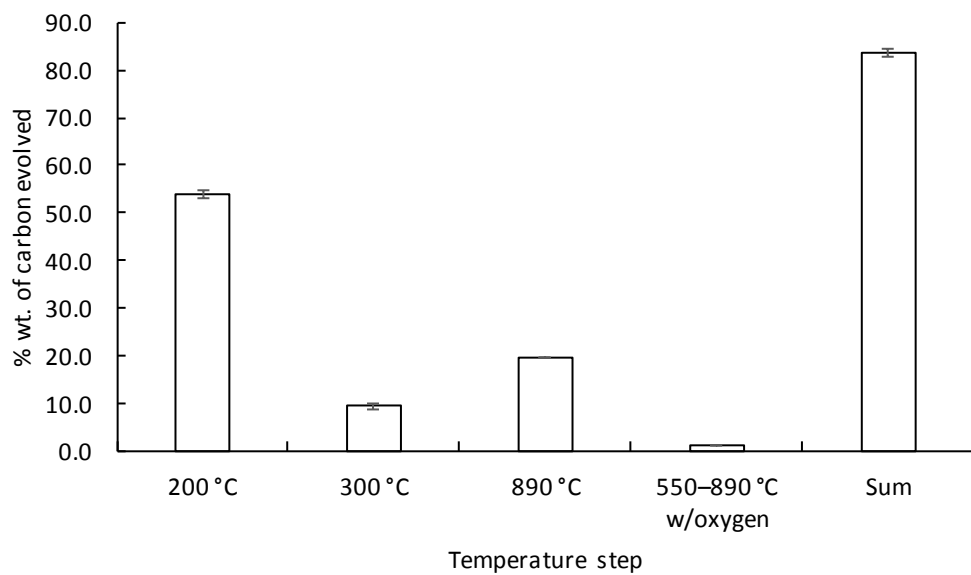


Figure H5. TGA profile of levoglucosan.

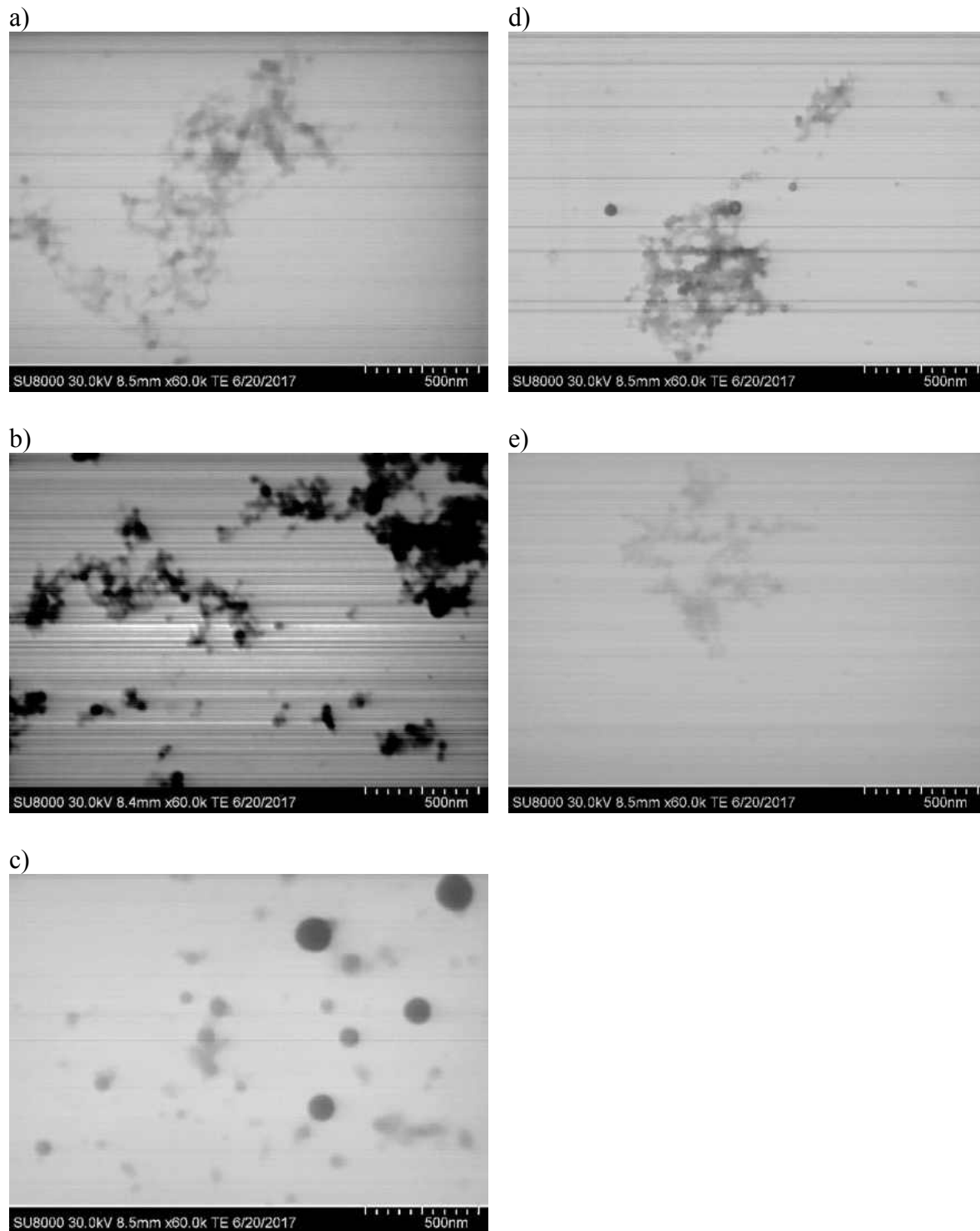


Figure H6. STEM images of the dried lignin fraction samples and the pre-eluate (magnification 60k): a) fraction 1, b) fraction 2; c) fraction 3; d) fraction 4; e) fraction 5.

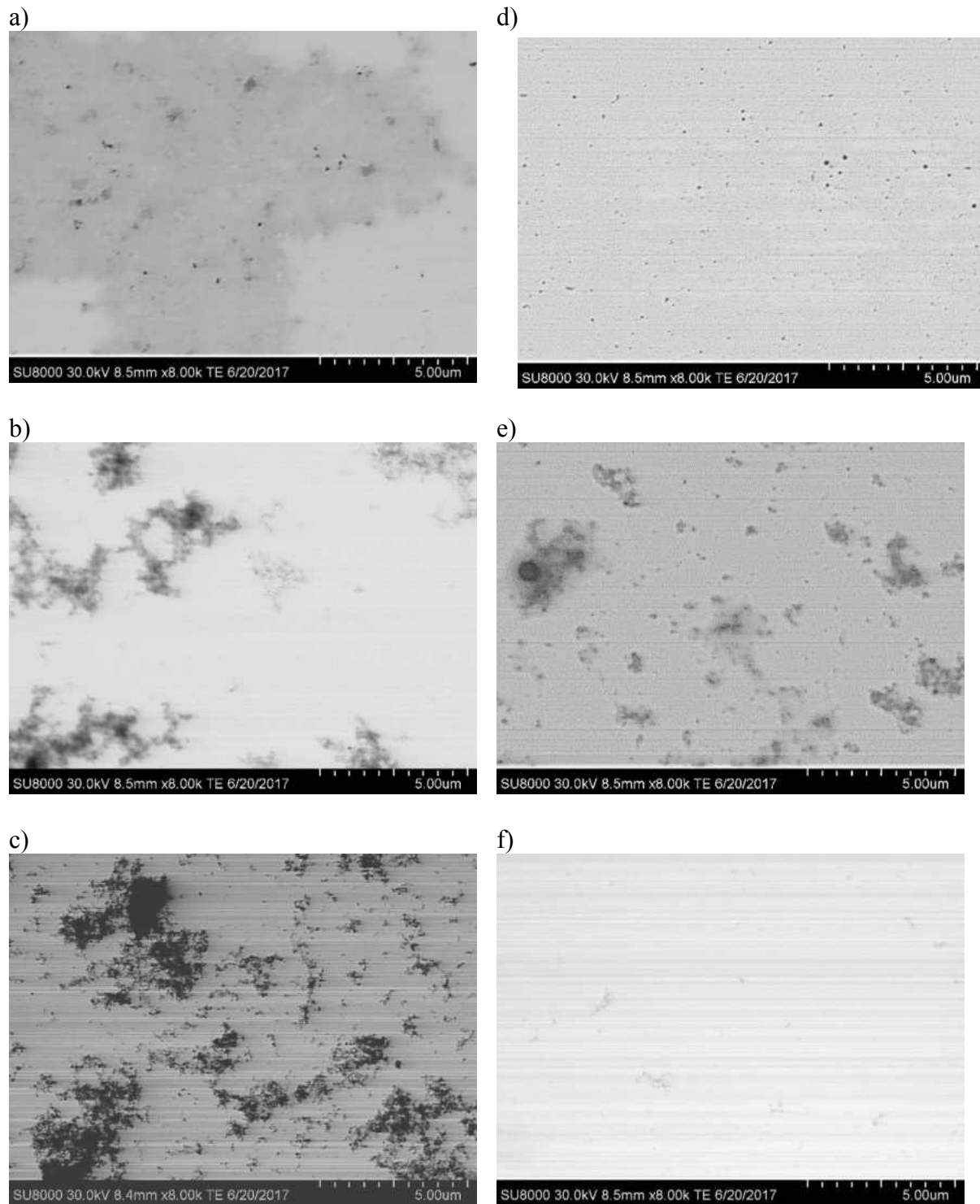


Figure H7. STEM images of the dried lignin fraction samples and the pre-eluate (magnification 8k): a) the pre-eluate; b) fraction 1, c) fraction 2; d) fraction 3; e) fraction 4; f) fraction 5.

Appendix I

Characterization of lignin fractions

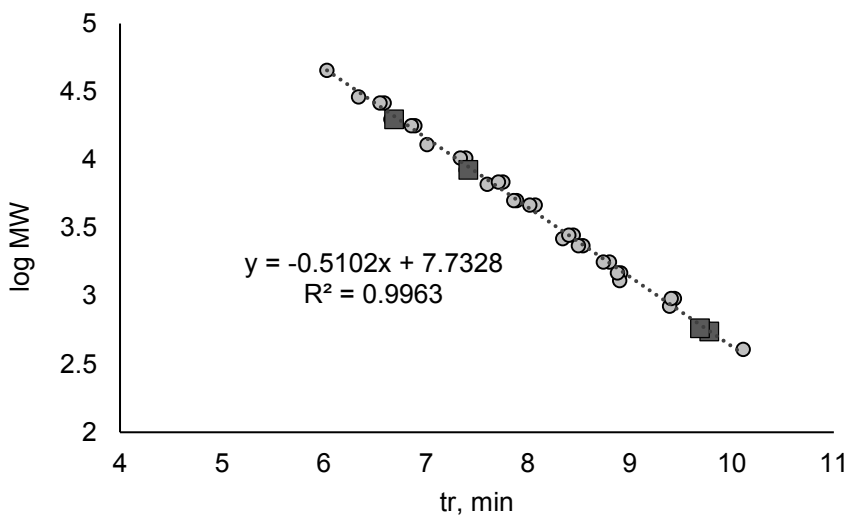


Figure I1. Log MW of PS standards plotted vs. t_r in analytical SEC utilizing analytical PLgel 1000 Å used for column calibration.

Appendix J

ESI mass spectra of PPG standards

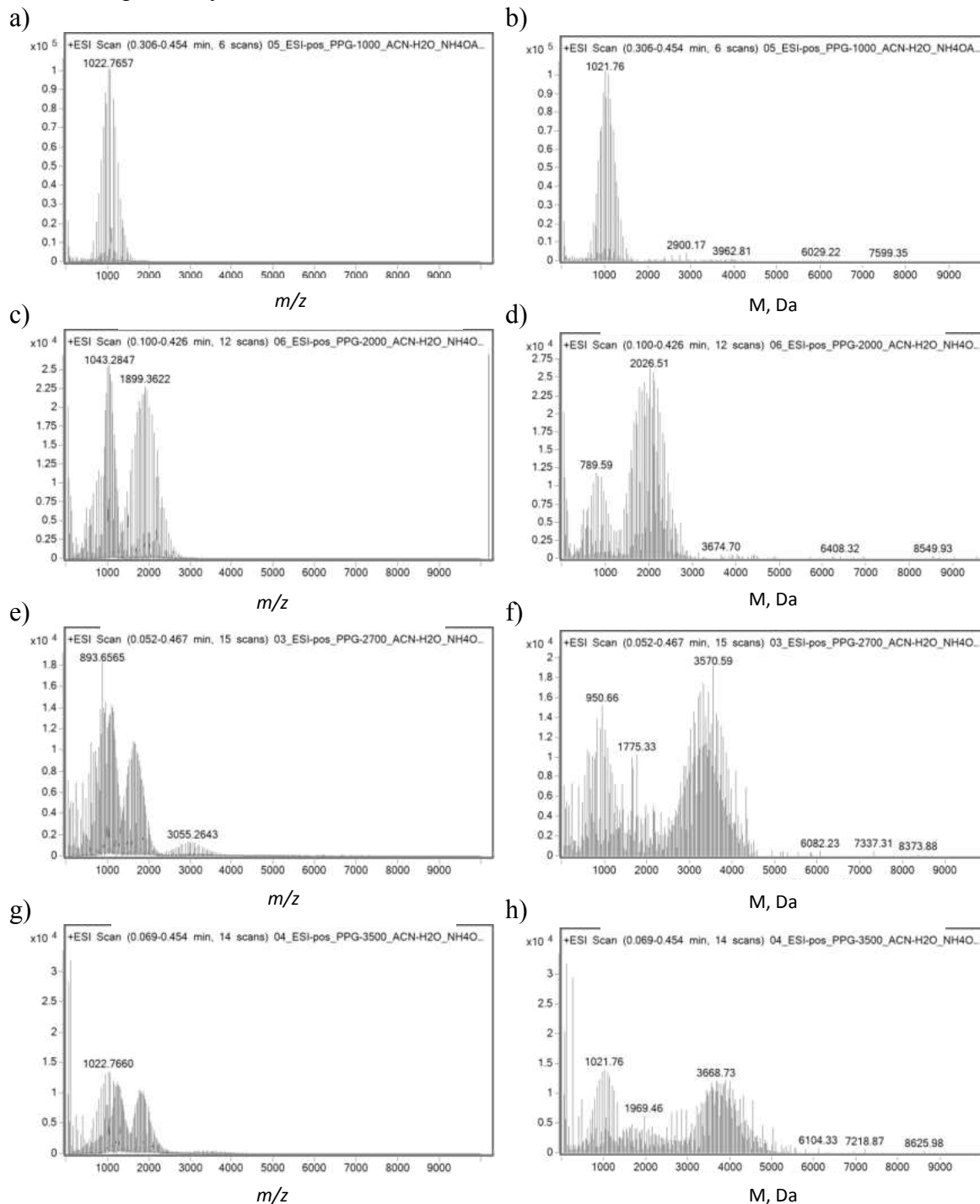


Figure J1. ESI mass spectra of PPG standards shown before and after deconvolution: PPG-1000 (a and b), PPG-2000 (c and d), PPG-2700 (e and f), PPG-3500 (g and h).

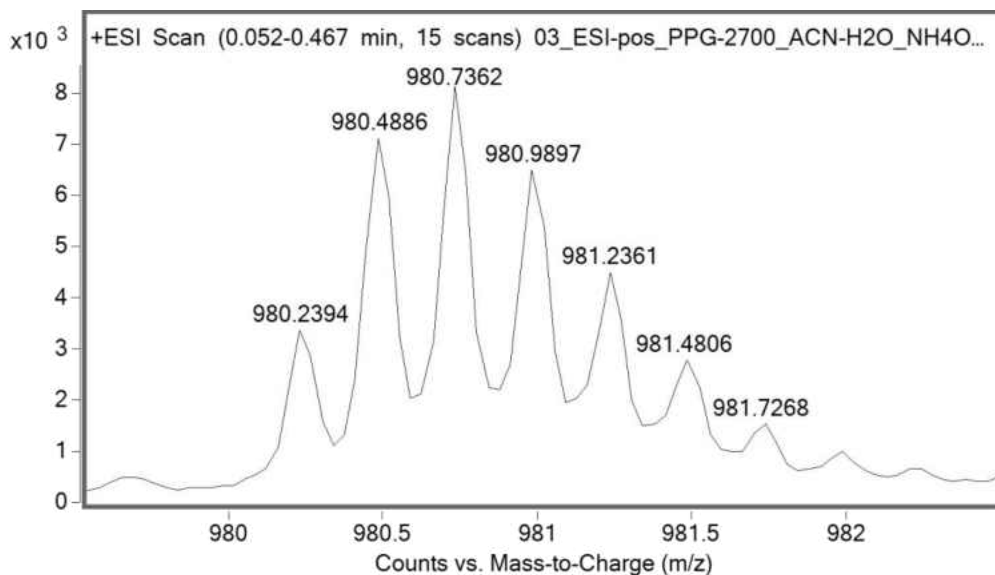


Figure J2. ESI mass spectra of PPG-2700. Features an ion carrying a charge of +4.

MW calculation based on the mass spectrum shown in Fig. H2 (more details on the method are provided in sections III.1.3 and III.2.5):

1) Determining the charge state

a) $980.9897 - 980.7362 = 0.2535$

$1 / 0.2535 = 3.94$

b) $980.7362 - 980.4886 = 0.2476$

$1 / 0.2476 = 4.03$

c) $980.4886 - 980.2394 = 0.2492$

$1 / 0.2492 = 4.01$

The analysis was performed with the positive mode ESI, thus the charge state was +4.

2) Calculating the MW considering that H^+ ions were the charge carriers

$$m/z \cdot z - [(atomic\ mass\ of\ hydrogen^1 - electron\ rest\ mass) \cdot z] = M, Da$$

$$980.7362 \cdot 4 - [(1.007825 - 0.000549) \cdot 4] = 3918.92 Da.$$

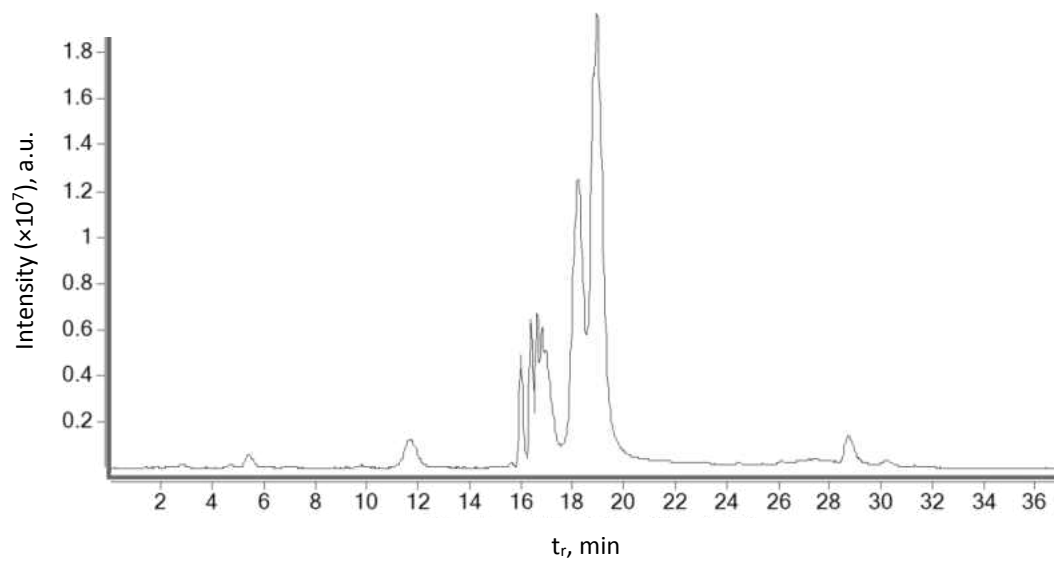


Figure J3. RP HPLC-ESI MS chromatogram of the narrow MW PEG standard mixture 3.

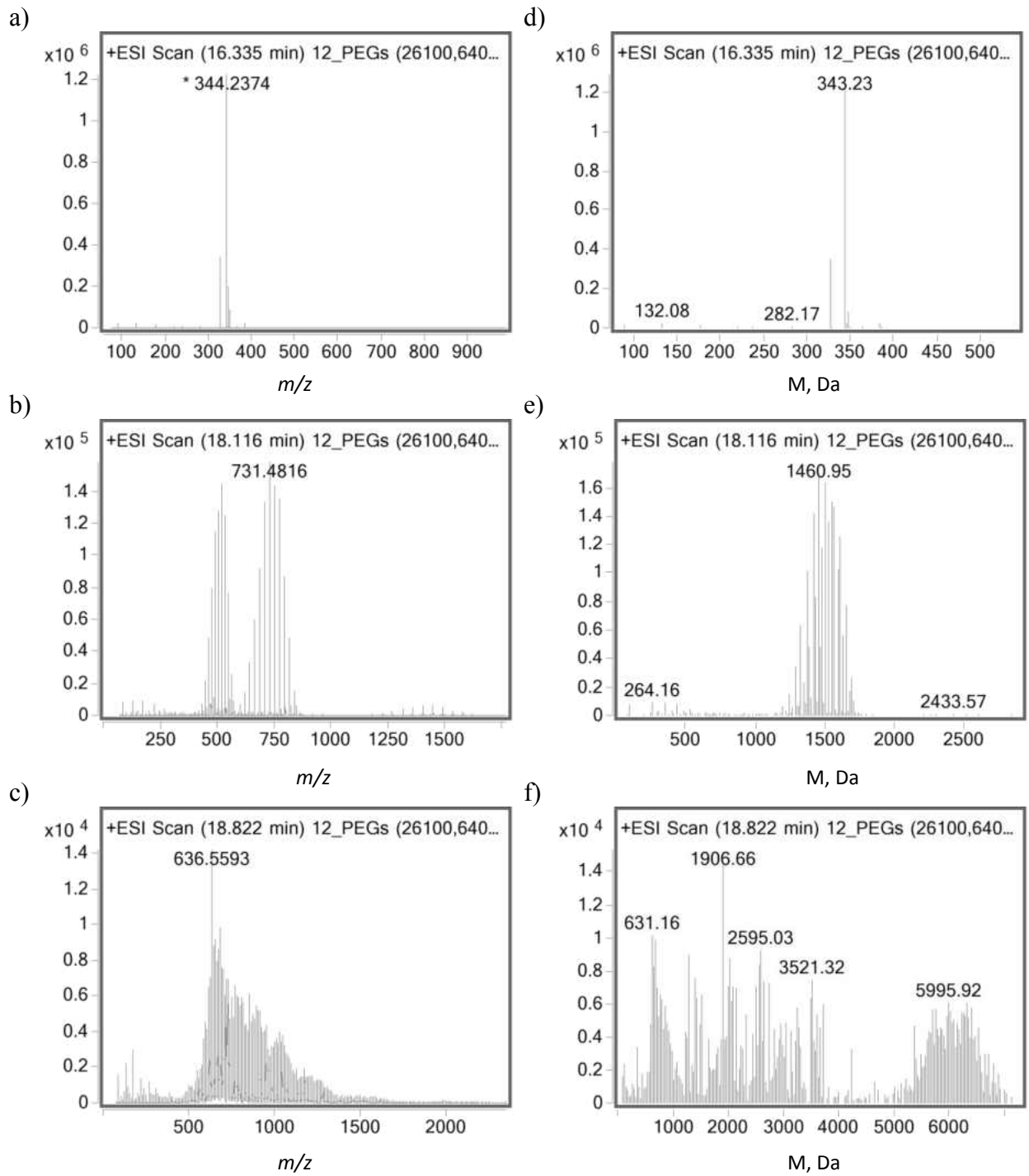


Figure J4. ESI mass spectra of PEG standards shown before and after deconvolution corresponding to the PEG standards with the M_n values of 269 Da (a, d), 1,380 Da (b, e) and 5,610 Da (c, f).

REFERENCES

1. Goring, D. A. I. Polymer properties of lignin and lignin derivatives. In *Lignins: Occurrence, Formation, Structure and Reactions*; Sarkanen, K. V., Ed.; Wiley Interscience, New York: 1971; pp 695-768.
2. Argyropoulos, D. S.; Menachem, S. B. Lignin. In *Biopolymers from Renewable Resources*; Kaplan, D. L., Ed.; Springer Verlag: Berlin Heidelberg, 1998; pp 292-322.
3. Chang, M. C. Harnessing energy from plant biomass. *Curr. Opin. Chem. Biol.* **2007**, *11* (6), 677-684.
4. Hatakka, A. Biodegradation of lignin. In *Lignin, Humic Substances and Coal*; Hofrichter, M.; Steinbuchel, A., Eds.; Wiley-VCH: Weinheim, 2001; Vol. 1, pp 129-180.
5. Brebu, M.; Vasile, C. Thermal degradation of lignin - a review. *Cell. Chem. Technol.* **2010**, *44*, 353-363.
6. Argyropoulos, D. S., Menachem., S. B. Lignin. In *Biopolymers From Renewable Resources*; Kaplan, D. L., Ed.; Springer Verlag: 1998; pp 292-322.
7. Hortling, B.; Turunen, E.; Kokkonen, P. Molar mass and size distribution of lignins. In *Handbook of Size Exclusion Chromatography and Related Techniques*; Wu, C. S., Ed.; Marcel Dekker: New York, 2004; pp 359-386.
8. Zakzeski, J.; Bruijninx, P. C.; Jongerius, A. L.; Weckhuysen, B. M. The catalytic valorization of lignin for the production of renewable chemicals. *Chem. Rev.* **2010**, *110* (6), 3552-3599.
9. Froass, P. M.; Ragauskas, A. J.; Jiang, J.-e. Chemical structure of residual lignin from kraft pulp. *J. Wood Chem. Technol.* **1996**, *16* (4), 347-365.

10. Kozliak, E. I.; Kubátová, A.; Artemyeva, A. A.; Nagel, E.; Zhang, C.; Rajappagowda, R. B.; Smirnova, A. L. Thermal liquefaction of lignin to aromatics: Efficiency, selectivity and product analysis. *ACS Sustain. Chem. Eng.* **2016**, *4* (10), 5106-5122.
11. Ragauskas, A. J.; Williams, C. K.; Davison, B. H.; Britovsek, G.; Cairney, J.; Eckert, C. A.; Frederick, W. J., Jr.; Hallett, J. P.; Leak, D. J.; Liotta, C. L.; Mielenz, J. R.; Murphy, R.; Templer, R.; Tschaplinski, T. The path forward for biofuels and biomaterials. *Science* **2006**, *311* (5760), 484-489.
12. Zhang, X.; Tu, M.; Paice, M. G. Routes to potential bioproducts from lignocellulosic biomass lignin and hemicelluloses. *Bioenergy Res.* **2011**, *4* (4), 246-257.
13. Gouveia, S.; Fernandez-Costas, C.; Sanroman, M. A.; Moldes, D. Enzymatic polymerisation and effect of fractionation of dissolved lignin from Eucalyptus globulus Kraft liquor. *Bioresour. Technol.* **2012**, *121*, 131-138.
14. Jääskeläinen, A. S.; Liitiä, T.; Mikkelsen, A.; Tamminen, T. Aqueous organic solvent fractionation as means to improve lignin homogeneity and purity. *Ind. Crops Prod.* **2017**, *103*, 51-58.
15. Li, M.-F.; Sun, S.-N.; Xu, F.; Sun, R.-C. Sequential solvent fractionation of heterogeneous bamboo organosolv lignin for value-added application. *Sep. Purif. Technol.* **2012**, *101*, 18-25.
16. Andrianova, A. A.; Yeudakimenka, N. A.; Lilak, S. L.; Kozliak, E. I.; Ugrinov, A.; Sibi, M. P.; Kubátová, A. Size exclusion chromatography of lignin: The mechanistic aspects and elimination of undesired secondary interactions. *J. Chromatogr., A* **2017**, *submitted*.
17. Baumberger, S.; Abaecherli, A.; Fasching, M.; Gellerstedt, G.; Gosselink, R.; Hortling, B.; Li, J.; Saake, B.; de Jong, E. Molar mass determination of lignins by size-exclusion chromatography: Towards standardisation of the method. *Holzforschung* **2007**, *61* (4), 459-468.

18. Huijgen, W. J. J.; Telysheva, G.; Arshanitsa, A.; Gosselink, R. J. A.; de Wild, P. J. Characteristics of wheat straw lignins from ethanol-based organosolv treatment. *Ind. Crops Prod.* **2014**, *59*, 85-95.
19. Gosselink, R. J. A.; Abächerli, A.; Semke, H.; Malherbe, R.; Käuper, P.; Nadif, A.; van Dam, J. E. G. Analytical protocols for characterisation of sulphur-free lignin. *Ind. Crops Prod.* **2004**, *19* (3), 271-281.
20. Luo, J.; Genco, J.; Cole, B.; Fort, R. Lignin recovered from the near-neutral hemicellulose extraction process as a precursor for carbon fiber. *Bioresources* **2011**, *6* (4), 4566-4593.
21. Kalliola, A.; Asikainen, M.; Talja, R.; Tamminen, T. Experiences of kraft lignin functionalization by enzymatic and chemical oxidation. *Bioresources* **2014**, *9* (4), 7336-7351.
22. Constant, S.; Wienk, H. L. J.; Frissen, A. E.; Peinder, P. d.; Boelens, R.; van Es, D. S.; Grisel, R. J. H.; Weckhuysen, B. M.; Huijgen, W. J. J.; Gosselink, R. J. A.; Bruijninx, P. C. A. New insights into the structure and composition of technical lignins: A comparative characterisation study. *Green Chem.* **2016**, *18* (9), 2651-2665.
23. Hu, Z.; Du, X.; Liu, J.; Chang, H.-m.; Jameel, H. Structural characterization of pine kraft lignin: BioChoice lignin vs Indulin AT. *J. Wood Chem. Technol.* **2016**, *36* (6), 432-446.
24. Wool, R. P. Lignin polymers and composites. In *Bio-Based Polymers and Composites*; Academic Press: Burlington, 2005; pp 551-598.
25. Sarkanen, V.; Ludwig, C. H. *Lignins: Occurrence, Formation, Structure and Reactions*; Wiley Interscience: New York, 1971; p 916.
26. Matron, J.; Marton, T. Molecular weight of kraft lignin. *Tappi* **1964**, *47* (8), 471-476.
27. Banoub, J.; Delmas, G. H., Jr.; Joly, N.; Mackenzie, G.; Cachet, N.; Benjelloun-Mlayah, B.; Delmas, M. A critique on the structural analysis of lignins and application of novel tandem

- mass spectrometric strategies to determine lignin sequencing. *J. Mass Spectrom.* **2015**, *50* (1), 5-48.
28. Uliyanchenko, E.; van der Wal, S.; Schoenmakers, P. J. Challenges in polymer analysis by liquid chromatography. *Polym. Chem.* **2012**, *3* (9), 2313-2335.
29. Lambrecht, M. A.; Rombouts, I.; Van Kelst, L.; Delcour, J. A. Impact of extraction and elution media on non-size effects in size exclusion chromatography of proteins. *J. Chromatogr., A* **2015**, *1415*, 100-107.
30. He, Y.; Hou, W.; Thompson, M.; Holoivics, H.; Hobson, T.; Jones, M. T. Size exclusion chromatography of polysaccharides with reverse phase liquid chromatography. *J. Chromatogr., A* **2014**, *1323*, 97-103.
31. Schure, M. R.; Moran, R. E. Size exclusion chromatography with superficially porous particles. *J. Chromatogr., A* **2017**, *1480*, 11-19.
32. Gidh, A. V.; Decker, S. R.; Vinzant, T. B.; Himmel, M. E.; Williford, C. Determination of lignin by size exclusion chromatography using multi angle laser light scattering. *J. Chromatogr., A* **2006**, *1114* (1), 102-110.
33. Gidh, A. V.; Decker, S. R.; Vinzant, T. B.; Himmel, M. E.; Williford, C. W. Fungal-induced redistribution of kraft lignin molecular weight by multi-angle laser light scattering. *Chem. Eng. Commun.* **2006**, *193* (12), 1546-1561.
34. Cathala, B.; Saake, B.; Faix, O.; Monties, B. Association behaviour of lignins and lignin model compounds studied by multidetector size-exclusion chromatography. *J. Chromatogr., A* **2003**, *1020* (2), 229-239.

35. Fredheima, G. E., Braatenb, S. M., Christensen, B. E. Molecular weight determination of lignosulfonates by size-exclusion chromatography and multi-angle laser light scattering. *J. Chromatogr., A* **2002**, *942*, 191-199.
36. Braaten, S. M.; Christensen, B. E.; Fredheim, G. E. Comparison of molecular weight and molecular weight distributions of softwood and hardwood lignosulfonates. *J. Wood Chem. Technol.* **2003**, *23* (2), 197-215.
37. Ringena, O.; Lebioda, S.; Lehnen, R.; Saake, B. Size-exclusion chromatography of technical lignins in dimethyl sulfoxide/water and dimethylacetamide. *J. Chromatogr., A* **2006**, *1102* (1-2), 154-163.
38. Contreras, S.; Gaspar, A. R.; Guerra, A.; Lucia, L. A.; Argyropoulos, D. S. Propensity of lignin to associate: Light scattering photometry study with native lignins. *Biomacromolecules* **2008**, *9* (12), 3362-3369.
39. Lange, H.; Rulli, F.; Crestini, C. Gel permeation chromatography in determining molecular weights of lignins: Critical aspects revisited for improved utility in the development of novel materials. *ACS Sustain. Chem. Eng.* **2016**, *4* (10), 5167-5180.
40. Kleen, M.; Ohra-aho, T.; Tamminen, T. On the interaction of HBT with pulp lignin during mediated laccase delignification - a study using fractionated pyrolysis-GC/MS. *J. Anal. Appl. Pyr.* **2003**, *70* (2), 589-600.
41. Del Río, J. C.; Gutiérrez, A.; Martínez, Á. T. Identifying acetylated lignin units in non-wood fibers using pyrolysis-gas chromatography/mass spectrometry. *Rapid Commun. Mass Spectrom.* **2004**, *18* (11), 1181-1185.
42. Ke, J.; Laskar, D. D.; Chen, S. Varied lignin disruption mechanisms for different biomass substrates in lower termite. *Renewable Energy* **2013**, *50*, 1060-1064.

43. Mullen, C. A.; Boateng, A. A. Catalytic pyrolysis-GC/MS of lignin from several sources. *Fuel Proc. Technol.* **2010**, *91*, 1446-1458.
44. Klingberg, A.; Odermatt, J.; Meier, D. Influence of parameters on pyrolysis-GC/MS of lignin in the presence of tetramethylammonium hydroxide. *J. Anal. Appl. Pyr.* **2005**, *74* (1-2), 104-109.
45. Kuroda, K.-i.; Izumi, A.; Mazumder, B. B.; Ohtani, Y.; Sameshima, K. Characterization of kenaf (*Hibiscus cannabinus*) lignin by pyrolysis-gas chromatography-mass spectrometry in the presence of tetramethylammonium hydroxide. *J. Anal. Appl. Pyr.* **2002**, *64*, 453-463.
46. Greenwood, P. F.; van Heemst, J. D. H.; Guthrie, E. A.; Hatcher, P. G. Laser micropyrolysis GC-MS of lignin. *J. Anal. Appl. Pyr.* **2002**, *62*, 365-373.
47. Britt, P. F.; Buchanan, A. C.; Evans, R. J.; Looker, M.; Nimlos, M. R. In *Investigation of the gas-phase pyrolysis of lignin model compounds by molecular beam mass spectrometry*, Fuel Chemistry Division Preprints, 2002; pp 395-397.
48. Del Río, J. C.; Gutiérrez, A.; Romero, J.; Martínez, M. J.; Martínez, A. T. Identification of residual lignin markers in eucalypt kraft pulps by Py-GC/MS. *J. Anal. Appl. Pyr.* **2001**, *58-59*, 425-439.
49. Hansen, B.; Kusch, P.; Schulze, M.; Kamm, B. Qualitative and quantitative analysis of lignin produced from beech wood by different conditions of the organosolv process. *J. Polym. Environ.* **2016**, 1-13.
50. Hu, J.; Shen, D.; Wu, S.; Zhang, H.; Xiao, R. Composition analysis of organosolv lignin and its catalytic solvolysis in supercritical alcohol. *Energy Fuels* **2014**, *28* (7), 4260-4266.

51. Kosyakov, D. S.; Ul'yanovskii, N. V.; Sorokina, E. A.; Gorbova, N. S. Optimization of sample preparation conditions in the study of lignin by MALDI mass spectrometry. *J. Anal. Chem.* **2014**, *69* (14), 1344-1350.
52. Richel, A.; Vanderghem, C.; Simon, M.; Wathelet, B.; Paquot, M. Evaluation of matrix-assisted laser desorption/ionization mass spectrometry for second-generation lignin analysis. *Anal. Chem. Insights* **2012**, *7*, 79-89.
53. Yoshioka, K.; Ando, D.; Watanabe, T. A comparative study of matrix- and nano-assisted laser desorption/ionisation time-of-flight mass spectrometry of isolated and synthetic lignin. *Phytochem. Anal.* **2012**, *23* (3), 248-253.
54. Song, Q.; Wang, F.; Cai, J.; Wang, Y.; Zhang, J.; Yu, W.; Xu, J. Lignin depolymerization (LDP) in alcohol over nickel-based catalysts via a fragmentation-hydrogenolysis process. *Energ. Environ. Sci.* **2013**, *6* (3), 994-1007.
55. Evtugin, D. V., Domingues, P., Amado, F. L., Pascoal Neto, C., Ferrer Correia, A. J. Electrospray ionization mass spectrometry as a tool for lignins molecular weight and structural characterisation. *Holzforschung* **1999**, *53*, 525-528.
56. Jacobs, A.; Dahlman, O. Absolute molar mass of lignins by size exclusion chromatography and MALDI-TOF mass spectroscopy. *Nord. Pulp Pap. Res. J.* **2000**, *15* (2), 120-127.
57. Bayerbach, R.; Nguyen, V. D.; Schurr, U.; Meier, D. Characterization of the water-insoluble fraction from fast pyrolysis liquids (pyrolytic lignin). *J. Anal. Appl. Pyr.* **2006**, *77* (2), 95-101.
58. Banoub, J. H.; Benjelloun-Mlayah, B.; Ziarelli, F.; Joly, N.; Delmas, M. Elucidation of the complex molecular structure of wheat straw lignin polymer by atmospheric pressure

photoionization quadrupole time-of-flight tandem mass spectrometry. *Rapid Commun. Mass Spectrom.* **2007**, *21* (17), 2867-2888.

59. Morreel, K.; Dima, O.; Kim, H.; Lu, F.; Niculaes, C.; Vanholme, R.; Dauwe, R.; Goeminne, G.; Inze, D.; Messens, E.; Ralph, J.; Boerjan, W. Mass spectrometry-based sequencing of lignin oligomers. *Plant Physiol.* **2010**, *153* (4), 1464-1478.

60. Raghuraman, A.; Tiwari, V.; Thakkar, J. N.; Gunnarsson, G. T.; Shukla, D.; Hindle, M.; Desai, U. R. Structural characterization of a serendipitously discovered bioactive macromolecule, lignin sulfate. *Biomacromolecules* **2005**, *6*, 2822-2832.

61. Banoub, J. H.; Delmas, M. Structural elucidation of the wheat straw lignin polymer by atmospheric pressure chemical ionization tandem mass spectrometry and matrix-assisted laser desorption/ionization time-of-flight mass spectrometry. *J. Mass Spectrom.* **2003**, *38* (8), 900-903.

62. Kiyota, E.; Mazzafera, P.; Sawaya, A. C. Analysis of soluble lignin in sugarcane by ultrahigh performance liquid chromatography-tandem mass spectrometry with a do-it-yourself oligomer database. *Anal. Chem.* **2012**, *84* (16), 7015-7020.

63. Morreel, K.; Kim, H.; Lu, F.; Dima, O.; Akiyama, T.; Vanholme, R.; Niculaes, C.; Goeminne, G.; Inzé, D.; Messens, E.; Ralph, J.; Boerjan, W. Mass spectrometry-based fragmentation as an identification tool in lignomics. *Anal. Chem.* **2010**, *82* (19), 8095-8105.

64. Kosyakov, D. S.; Ul'yanovskii, N. V.; Anikeenko, E. A.; Gorbova, N. S. Negative ion mode atmospheric pressure ionization methods in lignin mass spectrometry: A comparative study. *Rapid Commun. Mass Spectrom.* **2016**, *30* (19), 2099-2108.

65. D'Auria, M.; Emanuele, L.; Racioppi, R. FT-ICR-MS analysis of lignin. *Nat. Prod. Res.* **2012**, *26* (15), 1368-1374.

66. Evtuguin, D. V.; Amado, F. M. L. Application of electrospray ionization mass spectrometry to the elucidation of the primary structure of lignin. *Macromolecular Bioscience* **2003**, *3* (7), 339-343.
67. De Angelis, F. N., Rosario; Spreti, Nicoletta; Veri, Franca A new in vitro model of lignin biosynthesis. *Angew. Chem. Int. Ed.* **1999**, *38* (9), 1283-1285.
68. Munisamy, S. M.; Chambliss, C. K.; Becker, C. Direct infusion electrospray ionization-ion mobility high resolution mass spectrometry (DIESI-IM-HRMS) for rapid characterization of potential bioprocess streams. *J. Am. Soc. Mass Spectrom.* **2012**, *23* (7), 1250-1259.
69. Reale, S.; Di Tullio, A.; Spreti, N.; De Angelis, F. Mass spectrometry in the biosynthetic and structural investigation of lignins. *Mass Spectrom. Rev.* **2004**, *23*, 87-126.
70. Parker, C. E.; Warren, M. R.; Mocanu, V. Mass Spectrometry for Proteomics. In *Neuroproteomics*; Alzate, O., Ed.; CRC Press/Taylor & Francis: Boca Raton (FL), 2010.
71. Pinto, P. C.; Evtuguin, D. V.; Neto, C. P.; Silvestre, A. J. D.; Amado, F. M. L. Behavior of Eucalyptus Globulus lignin during kraft pulping. II. Analysis by NMR, ESI/MS, and GPC. *J. Wood Chem. Technol.* **2002**, *22* (2-3), 109-125.
72. Araujo, P.; Ferreira, M. S.; de Oliveira, D. N.; Pereira, L.; Sawaya, A. C.; Catharino, R. R.; Mazzafera, P. Mass spectrometry imaging: An expeditious and powerful technique for fast in situ lignin assessment in Eucalyptus. *Anal. Chem.* **2014**, *86* (7), 3415-3419.
73. Navarrete, P. P., A.; Pasch, H.; Delmotte, L. Study on lignin-glyoxal reaction by MALDI-TOF and CP-MAS ¹³C-NMR. *J. Adhes. Sci. Technol.* **2012**, *26* (8-9), 1069-1082.
74. Bocchini, P.; Galletti, G. C.; Seraglia, R.; Traldi, P.; Camarero, S.; Martinez, A. T. Matrix-assisted laser desorption/ionization mass spectrometry of natural and synthetic lignin. *Rapid Commun. Mass Spectrom.* **1996**, *10*, 1144-1147.

75. Awal, A.; Sain, M. Spectroscopic studies and evaluation of thermorheological properties of softwood and hardwood lignin. *J. Appl. Polym. Sci.* **2011**, *122* (2), 956-963.
76. Kleen, M. Surface lignin and extractives on hardwood RDH kraft pulp chemically characterized by ToF-SIMS. *Holzforschung* **2005**, *59* (5).
77. Hauptert, L. J.; Owen, B. C.; Marcum, C. L.; Jarrell, T. M.; Pulliam, C. J.; Amundson, L. M.; Narra, P.; Aqueel, M. S.; Parsell, T. H.; Abu-Omar, M. M.; Kenttämä, H. I. Characterization of model compounds of processed lignin and the lignome by using atmospheric pressure ionization tandem mass spectrometry. *Fuel* **2012**, *95*, 634-641.
78. Helander, M.; Theliander, H.; Lawoko, M.; Henriksson, G.; Zhang, L.; Lindström, M. E. Fractionation of technical lignin: Molecular mass and pH effects. *Bioresources* **2013**, *8* (2), 2270-2282.
79. Niemi, H.; Lahti, J.; Hatakka, H.; Kärki, S.; Rovio, S.; Kallioinen, M.; Mänttari, M.; Louhi-Kultanen, M. Fractionation of organic and inorganic compounds from black liquor by combining membrane separation and crystallization. *Chem. Eng. Technol.* **2011**, *34* (4), 593-598.
80. Wang, G.; Chen, H. Fractionation of alkali-extracted lignin from steam-exploded stalk by gradient acid precipitation. *Sep. Purif. Technol.* **2013**, *105*, 98-105.
81. García, A.; Spigno, G.; Labidi, J. Antioxidant and biocide behaviour of lignin fractions from apple tree pruning residues. *Ind. Crops Prod.* **2017**, *104*, 242-252.
82. Boeriu, C. G.; Fițigău, F. I.; Gosselink, R. J. A.; Frissen, A. E.; Stoutjesdijk, J.; Peter, F. Fractionation of five technical lignins by selective extraction in green solvents and characterisation of isolated fractions. *Ind. Crops Prod.* **2014**, *62*, 481-490.

83. Cui, C.; Sun, R.; Argyropoulos, D. S. Fractional precipitation of softwood kraft lignin: Isolation of narrow fractions common to a variety of lignins. *ACS Sustain. Chem. Eng.* **2014**, *2* (4), 959-968.
84. Duval, A.; Vilaplana, F.; Crestini, C.; Lawoko, M. Solvent screening for the fractionation of industrial kraft lignin. *Holzforschung* **2016**, *70* (1), 11-20.
85. Li, H.; McDonald, A. G. Fractionation and characterization of industrial lignins. *Ind. Crops Prod.* **2014**, *62*, 67-76.
86. Lovell, E. L.; Hibbert, H. Studies on lignin and related compounds. LII. New method for the fractionation of lignin and other polymers. *J. Am. Chem. Soc.* **1941**, *63* (8), 2070-2073.
87. Mörck, R.; Reimann, A.; Kringstad Knut, P., Fractionation of Kraft Lignin by Successive Extraction with Organic Solvents. III. Fractionation of Kraft Lignin from Birch. In *Holzforschung - International Journal of the Biology, Chemistry, Physics and Technology of Wood*, 1988; Vol. 42, p 111.
88. Ni, Y.; Hu, Q. Alcell® lignin solubility in ethanol–water mixtures. *J. Appl. Polym. Sci.* **1995**, *57* (12), 1441-1446.
89. Ropponen, J.; Räsänen, L.; Rovio, S.; Ohra-aho, T.; Liitiä, T.; Mikkonen, H.; van de Pas, D.; Tamminen, T. Solvent extraction as a means of preparing homogeneous lignin fractions. *Holzforschung* **2011**, *65* (4).
90. Sadeghifar, H.; Argyropoulos, D. S. Macroscopic behavior of kraft lignin fractions: Melt stability considerations for lignin–polyethylene blends. *ACS Sustain. Chem. Eng.* **2016**, *4* (10), 5160-5166.
91. Guo, G.; Li, S.; Wang, L.; Ren, S.; Fang, G. Separation and characterization of lignin from bio-ethanol production residue. *Bioresour. Technol.* **2013**, *135*, 738-741.

92. Xiao, L.; Xu, F.; Sun, R.-C. Chemical and structural characterization of lignins isolated from *Caragana sinica*. *Fibers and Polymers* **2011**, *12* (3), 316-323.
93. Dodd, A. P.; Kadla, J. F.; Straus, S. K. Characterization of fractions obtained from two industrial softwood kraft lignins. *ACS Sustain. Chem. Eng.* **2015**, *3* (1), 103-110.
94. Wang, S.; Wang, Y.; Cai, Q.; Wang, X.; Jin, H.; Luo, Z. Multi-step separation of monophenols and pyrolytic lignins from the water-insoluble phase of bio-oil. *Sep. Purif. Technol.* **2014**, *122*, 248-255.
95. Wang, G.; Chen, H. Fractionation and characterization of lignin from steam-exploded corn stalk by sequential dissolution in ethanol–water solvent. *Sep. Purif. Technol.* **2013**, *120*, 402-409.
96. Yuan, T.-Q.; He, J.; Xu, F.; Sun, R.-C. Fractionation and physico-chemical analysis of degraded lignins from the black liquor of *Eucalyptus pellita* KP-AQ pulping. *Polym. Degrad. Stab.* **2009**, *94* (7), 1142-1150.
97. Sun, R.; Tomkinson, J. Fractional separation and physico-chemical analysis of lignins from the black liquor of oil palm trunk fibre pulping. *Sep. Purif. Technol.* **2001**, *24* (3), 529-539.
98. Mussatto, S. I.; Fernandes, M.; Roberto, I. C. Lignin recovery from brewer's spent grain black liquor. *Carbohydr. Polym.* **2007**, *70* (2), 218-223.
99. Aleš, H.; Michal, J.; Lenka, D.; Alexandra, S.; Igor, Š. Thermal properties and size distribution of lignins precipitated with sulphuric acid. *Wood Res.* **2015**, *60* (3), 375-384.
100. Šurina, I.; Jablonský, M.; Ház, A.; Sladková, A.; Briškárová, A.; Kačík, F.; Šima, J. Characterization of non-wood lignin precipitated with sulphuric acid of various concentrations. *Bioresources* **2015**, *10* (1), 1408-1423.
101. Li, X.-H.; Wu, S.-B. Chemical structure and pyrolysis characteristics of the soda-alkali lignin fractions. *Bioresources* **2014**, *9* (4), 6277-6289.

102. Lourençon, T. V.; Hansel, F. A.; da Silva, T. A.; Ramos, L. P.; de Muniz, G. I. B.; Magalhães, W. L. E. Hardwood and softwood kraft lignins fractionation by simple sequential acid precipitation. *Sep. Purif. Technol.* **2015**, *154*, 82-88.
103. Gilarranz, M. A.; Rodriguez, F.; Oliet, M.; Revenga, J. A. Acid precipitation and purification of wheat straw lignin. *Sep. Sci. Technol.* **1998**, *33* (9), 1359-1377.
104. Liang, X.; Liu, J.; Fu, Y.; Chang, J. Influence of anti-solvents on lignin fractionation of eucalyptus globulus via green solvent system pretreatment. *Sep. Purif. Technol.* **2016**, *163*, 258-266.
105. Jiang, X.; Savithri, D.; Du, X.; Pawar, S.; Jameel, H.; Chang, H.-m.; Zhou, X. Fractionation and characterization of kraft lignin by sequential precipitation with various organic solvents. *ACS Sustain. Chem. Eng.* **2017**, *5* (1), 835-842.
106. Lange, H.; Schiffels, P.; Sette, M.; Sevastyanova, O.; Crestini, C. Fractional precipitation of wheat straw organosolv lignin: Macroscopic properties and structural insights. *ACS Sustain. Chem. Eng.* **2016**, *4* (10), 5136-5151.
107. Toledano, A.; García, A.; Mondragon, I.; Labidi, J. Lignin separation and fractionation by ultrafiltration. *Sep. Purif. Technol.* **2010**, *71* (1), 38-43.
108. Colyar, K. R.; Pellegrino, J.; Kadam, K. Fractionation of pre-hydrolysis products from lignocellulosic biomass by an ultrafiltration ceramic tubular membrane. *Sep. Sci. Technol.* **2008**, *43* (3), 447-476.
109. Jönsson, A.-S.; Nordin, A.-K.; Wallberg, O. Concentration and purification of lignin in hardwood kraft pulping liquor by ultrafiltration and nanofiltration. *Chem. Eng. Res. Des.* **2008**, *86* (11), 1271-1280.

110. Brodin, I.; Sjöholm, E.; Gellerstedt, G. Kraft lignin as feedstock for chemical products: The effects of membrane filtration. *Holzforschung* **2009**, *63* (3).
111. Norgren, M.; Lindström, B. Physico-chemical characterization of a fractionated kraft lignin. *Holzforschung* **2000**, *54* (5), 528-534.
112. Sevastyanova, O.; Helander, M.; Chowdhury, S.; Lange, H.; Wedin, H.; Zhang, L.; Ek, M.; Kadla, J. F.; Crestini, C.; Lindström, M. E. Tailoring the molecular and thermo-mechanical properties of kraft lignin by ultrafiltration. *J. Appl. Polym. Sci.* **2014**, *131* (18), 1-11.
113. Toledano, A.; Serrano, L.; Garcia, A.; Mondragon, I.; Labidi, J. Comparative study of lignin fractionation by ultrafiltration and selective precipitation. *Chem. Eng. J.* **2010**, *157* (1), 93-99.
114. Werhan, H.; Farshori, A.; Rudolf von Rohr, P. Separation of lignin oxidation products by organic solvent nanofiltration. *J. Membr. Sci.* **2012**, *423-424*, 404-412.
115. Wallberg, O.; Jönsson, A.-S.; Wimmerstedt, R. Ultrafiltration of kraft black liquor with a ceramic membrane. *Desalination* **2003**, *156* (1), 145-153.
116. Busse, N.; Fuchs, F.; Kraume, M.; Czermak, P. Treatment of enzyme-initiated delignification reaction mixtures with ceramic ultrafiltration membranes: Experimental investigations and modeling approach. *Sep. Sci. Technol.* **2016**, 1-20.
117. Zinovyev, G.; Sumerskii, I.; Korntner, P.; Sulaeva, I.; Rosenau, T.; Potthast, A. Molar mass-dependent profiles of functional groups and carbohydrates in kraft lignin. *J. Wood Chem. Technol.* **2016**, *37* (3), 171-183.
118. Miller-Chou, B. A.; Koenig, J. L. A review of polymer dissolution. *Prog. Polym. Sci.* **2003**, *28* (8), 1223-1270.

119. Ouano, A. C.; Carothers, J. A. Dissolution dynamics of some polymers: Solvent-polymer boundaries. *Polym. Eng. Sci.* **1980**, *20* (2), 160-166.
120. Kirk, T. K.; Brown, W.; Cowling, E. B. Preparative fractionation of lignin by gel-permeation chromatography. *Biopolymers* **1969**, *7* (2), 135-153.
121. Li, Z.; Gu, Y.; Gu, T. Mathematical modeling and scale-up of size-exclusion chromatography. *Biochem. Eng. J.* **1998**, *2* (2), 145-155.
122. Janson, J.-C. Process Scale Size Exclusion Chromatography. In *Process Scale Liquid Chromatography*; Wiley-VCH Verlag GmbH: 2007; pp 81-98.
123. Botaro, V. R.; Curvelo, A. A. Monodisperse lignin fractions as standards in size-exclusion analysis: comparison with polystyrene standards. *J. Chromatogr., A* **2009**, *1216* (18), 3802-3806.
124. Elbs, K. J. Uber dehydrodivanillin. *J. Prakt. Chem.* **1916**, *93*, 1-8.
125. Gaur, M.; Lohani, J.; Balakrishnan, V. R.; Raghunathan, P.; Eswaran, S. V. Dehydrodivanillin: Multi-dimensional NMR spectral studies, surface morphology and electrical characteristics of thin films. *Bull. Korean Chem. Soc.* **2009**, *30* (12), 2895-2898.
126. Kawai, S.; Okita, K.; Sugishita, K.; Tanaka, A.; Ohash, H. Simple method for synthesizing phenolic β -O-4 dilignols. *J. Wood Sci.* **1999**, *45* (5), 440-443.
127. Schumaker, J. E. Quantification of Lignin Hydroxyl-Containing Functional Groups via ^{31}P { ^1H } NMR Spectroscopy and Synthesis of Degradation Products. A thesis submitted to the graduate faculty of the University of North Dakota in partial fulfillment of the requirements for Master's degree, University of North Dakota, 2017.
128. Gaur, M.; Lohani, J.; Balakrishnan, V. R.; Raghunathan, P.; Eswaran, S. V. Dehydrodivanillin: Multi-dimensional NMR Spectral Studies, Surface Morphology and Electrical Characteristics of Thin Films. *Bulletin of the Korean Chemical Society* **2009**, *30* (12), 2895-2898.

129. Glasser, W. G.; Jain, R. K. Lignin derivatives. I. Alkanoates. *Holzforschung* **1993**, *47* (3), 225-233.
130. Young, R. J.; Lovell, P. A. *Introduction to Polymers*; Nelson Thornes: Cheltenham, UK, 2002.
131. Mori, S.; Barth, H. G. *Size Exclusion Chromatography*; Springer-Verlag: Berlin Heidelberg New York, 1999.
132. Sjöholm, E.; Gustafsson, K.; Colmsjö, A. Size exclusion chromatography of lignins using lithium chloride/N,N-dimethylacetamide as mobile phase. I. Dissolved and residual birch kraft lignins. *J. Liq. Chromatogr. Relat. Technol.* **1999**, *22* (11), 1663-1685.
133. Gosselink, R. J. A. Lignin as a renewable aromatic resource for the chemical industry. Ph.D. Dissertation, Wageningen University, Wageningen, NL, 2011.
134. Mattinen, M.-L.; Suortti, T.; Gosselink, R.; Argyropoulos, D. S.; Evtugin, D.; Suurnakki, A.; Jong, E.; Tamminen, T. Polymerization of different lignins by laccase. *Bioresources* **2008**, *3* (2), 549-565.
135. Mattinen, M. L.; Maijala, P.; Nousiainen, P.; Smeds, A.; Kontro, J.; Sipilä, J.; Tamminen, T.; Willför, S.; Viikari, L. Oxidation of lignans and lignin model compounds by laccase in aqueous solvent systems. *J. Mol. Catal. B: Enzym.* **2011**, *72* (3-4), 122-129.
136. Wallace, W. E.; Guttman, C. M., NIST Recommended Practice Guide. Molecular Mass Distribution Measurement by Mass Spectrometry. National Institute of Standards and Technology U.S. Department of Commerce: 2010.
137. Zakis, G. F. *Synthesis of Lignin Model Compounds*; Zinatne: Riga, 1980; p 183.

138. Popova, I. E.; Hall, C.; Kubátová, A. Determination of lignans in flaxseed using liquid chromatography with time-of-flight mass spectrometry. *J. Chromatogr., A* **2009**, *1216* (2), 217-229.
139. Strohalm, M.; Hassman, M.; Košata, B.; Kодиček, M. *mMass* data miner: an open source alternative for mass spectrometric data analysis. *Rapid Commun. Mass Spectrom.* **2008**, *22* (6), 905-908.
140. Sforza, S.; Galaverna, G.; Corradini, R.; Dossena, A.; Marchelli, R. ESI-mass spectrometry analysis of unsubstituted and disubstituted β -cyclodextrins: fragmentation mode and identification of the AB, AC, AD regioisomers. *J. Am. Soc. Mass Spectrom.* **2003**, *14* (2), 124-135.
141. Dongari, N.; Sauter, E. R.; Tande, B. M.; Kubátová, A. Determination of Celecoxib in human plasma using liquid chromatography with high resolution time of flight-mass spectrometry. *J. Chromatogr. B Analyt. Technol. Biomed. Life Sci.* **2014**, *955-956*, 86-92.
142. Hernandez, H.; Robinson, C. V. Determining the stoichiometry and interactions of macromolecular assemblies from mass spectrometry. *Nat Protoc* **2007**, *2* (3), 715-726.
143. Owen, B. C.; Hauptert, L. J.; Jarrell, T. M.; Marcum, C. L.; Parsell, T. H.; Abu-Omar, M. M.; Bozell, J. J.; Black, S. K.; Kenttamaa, H. I. High-performance liquid chromatography/high-resolution multiple stage tandem mass spectrometry using negative-ion-mode hydroxide-doped electrospray ionization for the characterization of lignin degradation products. *Anal. Chem.* **2012**, *84* (14), 6000-6007.
144. Voeller, K.; Bilek, H.; Kozliak, E.; Kubátová, A. Characterization of alkaline lignin and its degradation products using thermal desorption and pyrolysis methods. *ACS Sustain. Chem. Eng.* **2017**, *submitted*.

145. Voeller, K. M. Characterization of Kraft alkali lignin and products of its thermal degradation by fractional pyrolysis method. A thesis submitted to the graduate faculty of the University of North Dakota in partial fulfillment of the requirements for Master's degree, University of North Dakota, 2016.
146. Koshijima, T.; Watanabe, T. *Association Between Lignin and Carbohydrates in Wood and Other Plant Tissues*; Springer-Verlag Berlin Heidelberg: Berlin, 2003.
147. Erdman, J. Ueber die Concretionen in den Birnen. *Ann. Chem. Pharm.* **1866**, *138*, 1-19.
148. Tunc, M. S.; Lawoko, M.; van Heiningen, A. R. P. Understanding the limitations of removal of hemicelluloses during autohydrolysis of a mixture of southern hardwoods. *Bioresources* **2010**, *5* (1), 356-371.
149. Brzonova, I.; Kozliak, E. I.; Andrianova, A. A.; LaVallie, A.; Kubátová, A.; Ji, Y. Production of lignin based insoluble polymers (anionic hydrogels) by *C. versicolor*. *Scientific Reports* **2017**, *submitted*.
150. Brzonova, I. Biodegradation and biomodification of lignocellulose with a main focus on lignin. A dissertation submitted to the graduate faculty of the University of North Dakota in partial fulfillment of the requirements for the degree of doctor of philosophy, University of North Dakota, 2017.
151. Brzonova, I.; Asina, F.; Andrianova, A. A.; Kubátová, A.; Smoliakova, I. P.; Kozliak, E. I.; Ji, Y. Fungal biotransformation of insoluble kraft lignin into a water soluble polymer. *Ind. Eng. Chem. Res.* **2017**, *56* (21), 6103-6113.
152. Abbina, S.; Chidara, V. K.; Du, G. Ring-opening copolymerization of styrene oxide and cyclic anhydrides by using highly effective zinc amido-oxazolate catalysts. *ChemCatChem* **2017**, *9* (7), 1343-1348.